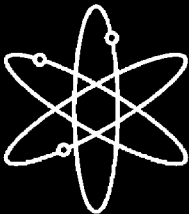
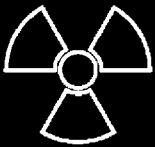


Integrated Chemical Effects Test Project: Test #4 Data Report



Los Alamos National Laboratory



**U.S. Nuclear Regulatory Commission
Office of Nuclear Regulatory Research
Washington, DC 20555-0001**



Integrated Chemical Effects Test Project: Test #4 Data Report

Manuscript Completed: November 2005
Date Published: November 2005

Principal Investigator: Jack Dallman

Prepared by
J. Dallman, B. Letellier, J. Garcia, J. Madrid, W. Roesch
Los Alamos National Laboratory
Los Alamos, NM 87545

D. Chen, K. Howe
University of New Mexico

L. Archuleta, F. Sciacca
OMICRON

B. P. Jain, NRC Project Manager

Prepared for
Division of Engineering Technology
Office of Nuclear Regulatory Research
U.S. Nuclear Regulatory Commission
Washington, DC 20555-0001



INTEGRATED CHEMICAL EFFECTS TEST PROJECT: TEST #4 DATA REPORT

ABSTRACT

A 30-day test was conducted in the Integrated Chemical Effects Test (ICET) project test apparatus. The test simulated the chemical environment present inside a pressurized water reactor containment water pool after a loss-of-coolant accident. The initial chemical environment contained 15.41 kg of boric acid, 8.47 kg of sodium hydroxide, 0.663 g of lithium hydroxide, and 212 mL of hydrochloric acid. An additional amount of sodium hydroxide (614 g) was added with the spray beginning at time zero and lasting until 30 minutes into the test. The test was conducted for 30 days at a constant temperature of 60°C (140°F). The materials tested within this environment included representative amounts of submerged and unsubmerged aluminum, copper, concrete, zinc, carbon steel, and insulation samples (80% calcium silicate and 20% fiberglass). Representative amounts of concrete dust and latent debris were also added to the test solution. Water was circulated through the bottom portion of the test chamber during the entire test to achieve representative flow rates over the submerged specimens. The test solution pH varied from 9.5 to 9.8 over the first two days, rose to 9.9 on Day 8, and then stayed between 9.7 and 9.9 for the remainder of the test. The test solution turbidity decreased to less than 3 NTU after 24 hours. The turbidity continued to decrease and averaged 0.5 NTU over the last three weeks of the test. Observations of the test solution indicated that no chemical byproducts were visible in the water and no precipitation occurred as samples cooled from test temperature to room temperature. The appearance of the submerged metallic coupons was largely unchanged throughout the test. Post-test examinations showed very little weight changes and only minimal visible deposits on some coupons. The unsubmerged coupons exhibited some streaking, but little or no weight changes. The bottom of the tank was filled with reddish-brown sediment, but no gel-like deposits were present. The test solution remained clearly Newtonian for the entire test. Aluminum was detectable in the solution for only the first 24 hours.

CONTENTS

ABSTRACT.....	i
EXECUTIVE SUMMARY	xi
ACKNOWLEDGMENTS	xiii
ACRONYMS AND ABBREVIATIONS	xiv
1 INTRODUCTION	1
1.1 Objective and Test Conditions.....	1
1.2 Information Presented in this Report	2
2 TEST PROCEDURES	3
2.1 Chemical Test Apparatus Functional Description	3
2.2 Pre-Test Preparation.....	4
2.2.1 Test Loop Cleaning.....	4
2.2.2 Test Coupons and Samples	5
2.2.3 Quality Assurance Program	9
2.2.4 Test Parameters.....	10
2.3 Test Operation.....	12
2.3.1 Description.....	12
2.3.2 Process Control	13
2.4 Analytical Methods.....	13
2.4.1 Data Compilation and Nomenclature.....	13
3 TEST RESULTS.....	20
3.1 General Observations.....	20
3.1.1 Control of Test Parameters	21
3.1.2 Hydrogen Generation.....	23
3.2 Water Samples	24
3.2.1 Wet Chemistry	24
3.2.2 Metal Ion Concentration	27
3.2.3 Optical/TEM Images from Filtered and Unfiltered Samples.....	32
3.3 Insulation.....	32
3.3.1 Deposits in Fiberglass Samples	32
3.3.2 Calcium Silicate Samples	74
3.4 Metallic and Concrete Coupons.....	81
3.4.1 Weights and Visual Descriptions.....	81
3.4.2 SEM Analyses.....	91
3.5 Sedimentation	92
3.6 Precipitates.....	99
3.7 Deposition Products	99
3.8 Gel Analysis.....	101
4 SUMMARY OF KEY OBSERVATIONS	102
REFERENCES	103

Appendices

Appendix A ESEM/EDS Data for Test #4 Day-5 Fiberglass in Low-Flow Zone

Appendix B ESEM Day-15 Fiberglass

- B1. ESEM/EDS Data for Test #4 Day-15 Fiberglass in Low-Flow Zones
- B2. ESEM/EDS Data for Test #4 Day-15 Fiberglass in High-Flow Zones

Appendix C ESEM Day-30 Fiberglass

- C1. ESEM/EDS Data for Test #4 Day-30 Fiberglass in Low-Flow Zones
- C2. ESEM/EDS Data for Test #4 Day-30 Fiberglass Inserted in Nylon Mesh in a Low-Flow Zone
- C3. ESEM Data for Test #4 Day-30 Low-Flow Fiberglass Samples in a Big Envelope
- C4. ESEM/EDS Data for Test #4 Day-30 Fiberglass in High-Flow Zones
- C5. ESEM/EDS Data for Test #4 Day-30 Fiberglass Inserted in Front of Header in a High-Flow Zone
- C6. ESEM/EDS Data for Test #4 Day-30 Drain Collar Fiberglass
- C7. ESEM/EDS Data for Test #4 Day-30 Birdcage Fiberglass

Appendix D ESEM/EDS Data for Test #4 Day-30 Low-Flow Cal-sil Samples

Appendix E ESEM and SEM/EDS Data for Test #4 Day-30 Deposition Products

Appendix F SEM Day-30 Coupons

- F1. SEM/EDS Data for Test #4 Day-30 Aluminum Coupons
- F2. SEM/EDS Data for Test #4 Day-30 Copper Coupons
- F3. SEM/EDS Data for Test #4 Day-30 Galvanized Steel Coupons
- F4. SEM/EDS Data for Test #4 Day-30 Steel Coupons

Appendix G SEM/EDS Data for Test #4 Day-30 Sediment

Appendix H TEM Data for Test #4 Solution Samples

Appendix I UV Absorbance Spectrum – Day-30 Solution Samples

Appendix J ICET Test #4: Pre-Test, Test, and Post-Test Project Instructions

FIGURES

Figure 2-1. Test loop process flow diagram.	4
Figure 2-2. Coupon rack configuration in the ICET tank. The blue line represents the surface of the test solution.	6
Figure 2-3. A typical loaded coupon rack in the ICET tank.	7
Figure 2-4. Fiberglass samples attached to a submerged coupon rack.	8
Figure 2-5. Solid pieces of cal-sil samples in SS mesh.	9
Figure 2-6. Cal-sil dust.	9
Figure 3-1. In-line pH measurements.	22
Figure 3-2. Bench-top pH meter results.	23
Figure 3-3. Hydrogen generation.	23
Figure 3-4. Day 1 turbidity results.	24
Figure 3-5. Daily turbidity results.	25
Figure 3-6. Test #4 TSS results.	26
Figure 3-7. Viscosity at 60°C and 23°C.	27
Figure 3-8. Aluminum concentration.	28
Figure 3-9. Calcium concentration.	28
Figure 3-10. Copper concentration.	29
Figure 3-11. Iron concentration.	29
Figure 3-12. Magnesium concentration.	30
Figure 3-13. Silica concentration.	30
Figure 3-14. Sodium concentration.	31
Figure 3-15. Zinc concentration.	31
Figure 3-16. Environmental SEM image magnified 80 times for a Test #4 Day 5 low-flow exterior fiberglass sample. (T4D5LFX1.jpg)	34
Figure 3-17. Environmental SEM image magnified 1000 times for a Test #4 Day 5 low-flow exterior fiberglass sample. (t4d5lx11.jpg)	35
Figure 3-18. Environmental SEM image magnified 500 times for a Test #4 Day 5 low-flow exterior fiberglass sample. (t4d5lx14.jpg)	35
Figure 3-19. Environmental SEM image magnified 1000 times for a Test #4 Day 5 low-flow exterior fiberglass sample. (t4d5lx12.jpg)	36
Figure 3-20. EDS counting spectrum for the film between the fibers shown in Figure 3-19. (t4d5lx13.jpg)	36
Figure 3-21. Environmental SEM image magnified 80 times for a Test #4 Day 5 low-flow interior fiberglass sample. (t4d5lfi5.jpg)	37
Figure 3-22. Environmental SEM image magnified 500 times for a Test #4 Day 5 low-flow interior fiberglass sample. (t4d5lfi7.jpg)	37
Figure 3-23. Environmental SEM image magnified 2000 times for a Test #4 Day 5 low-flow interior fiberglass sample. (t4d5lfi8.jpg)	38

Figure 3-24. Environmental SEM image magnified 1000 times for a Test #4 Day 5 low-flow interior fiberglass sample. (t4d5lfi9.jpg)..... 38

Figure 3-25. Environmental SEM image magnified 100 times for a Test #4 Day 15 exterior low-flow fiberglass sample. (t4d15lx1.jpg)..... 39

Figure 3-26. Annotated environmental SEM image magnified 100 times for a Test #4 Day 15 exterior low-flow fiberglass sample. (t4d15lx3.jpg) 40

Figure 3-27. EDS counting spectrum for the particulate deposit on fiberglass shown in Figure 3-26. (t4d15lx2.jpg) 40

Figure 3-28. Environmental SEM image magnified 500 times for a Test #4 Day 15 exterior low-flow fiberglass sample. (t4d15lx4.jpg)..... 41

Figure 3-29. Environmental SEM image magnified 100 times for a Test #4 Day 15 interior low-flow fiberglass sample. (t4d15li6.jpg) 41

Figure 3-30. Environmental SEM image magnified 500 times for a Test #4 Day 15 interior low-flow fiberglass sample. (t4d15li7.jpg) 42

Figure 3-31. Environmental SEM image magnified 100 times for a Test #4 Day 15 exterior high-flow fiberglass sample. (t4d15hx8.jpg)..... 43

Figure 3-32. Environmental SEM image magnified 400 times for a Test #4 Day 15 exterior high-flow fiberglass sample. (t4d15hx9.jpg)) 43

Figure 3-33. Environmental SEM image magnified 750 times for a Test #4 Day 15 exterior high-flow fiberglass sample. (t4d15hx7.jpg)..... 44

Figure 3-34. EDS counting spectrum for the spot on the film between the fibers shown in Figure 3-33. (t4d15hx6.jpg) 44

Figure 3-35. Environmental SEM image magnified 100 times for a Test #4 Day 15 interior high-flow fiberglass sample. (t4d15hi3.jpg) 45

Figure 3-36. Environmental SEM image magnified 800 times for a Test #4 Day 15 interior high-flow fiberglass sample. (t4d15hi2.jpg) 45

Figure 3-37. Environmental SEM image magnified 100 times for a Test #4 Day 30 exterior low-flow fiberglass sample. (t4d30lx1.jpg)..... 46

Figure 3-38. Environmental SEM image magnified 500 times for a Test #4 Day 30 exterior low-flow fiberglass sample. (t4d30lx2.jpg)..... 47

Figure 3-39. Environmental SEM image magnified 1000 times for a Test #4 Day 30 low-flow fiberglass sample. (t4d30lx5.jpg) 47

Figure 3-40. EDS counting spectrum for the spot of coating substance on the fiberglass shown in Figure 3-39. (t4d30lx4.jpg)..... 48

Figure 3-41. Environmental SEM image magnified 100 times for a Test #4 Day 30 interior low-flow fiberglass sample. (T4D30LI6.jpg) 48

Figure 3-42. Environmental SEM image magnified 500 times for a Test #4 Day 30 interior low-flow fiberglass sample. (t4d30li9.jpg) 49

Figure 3-43. EDS counting spectrum for the film on the fiberglass shown in Figure 3-42. (t4d30li8.jpg)..... 49

Figure 3-44. Environmental SEM image magnified 100 times for a Test #4 Day 30 nylon mesh submerged in low-flow area (inserted on Day 4). (t4d30nl1.jpg)..... 50

Figure 3-45. Environmental SEM image magnified 500 times for a Test #4 Day 30 nylon mesh submerged in low-flow area (inserted on Day 4). (t4d30nl2.jpg) 51

Figure 3-46. Environmental SEM image magnified 100 times for a Test #4 Day 30 exterior low-flow fiberglass sample contained in a nylon mesh (inserted on Day 4). (t4NLEx01.jpg)..... 51

Figure 3-47. Environmental SEM image magnified 500 times for a Test #4 Day 30 exterior low-flow fiberglass sample contained in a nylon mesh (inserted on Day 4). (t4nlex02.jpg)..... 52

Figure 3-48. Environmental SEM image magnified 100 times for a Test #4 Day 30 interior low-flow fiberglass sample contained in a nylon mesh (inserted on Day 4). (t4nlIn04.jpg) 52

Figure 3-49. Environmental SEM image magnified 500 times for a Test #4 Day 30 interior low-flow fiberglass sample contained in a nylon mesh (inserted on Day 4). (t4nlin05.jpg) 53

Figure 3-50. Environmental SEM image magnified 100 times for a Test #4 Day 30 exterior low-flow fiberglass sample in a big envelope. (t4evlx3.jpg). 54

Figure 3-51. Environmental SEM image magnified 500 times for a Test #4 Day 30 exterior low-flow fiberglass sample in a big envelope. (t4evlx2.jpg) 54

Figure 3-52. Environmental SEM image magnified 100 times for a Test #4 Day 30 interior low-flow fiberglass sample in a big envelope. (t4evli4.jpg)..... 55

Figure 3-53. Environmental SEM image magnified 500 times for a Test #4 Day 30 interior low-flow fiberglass sample in a big envelope. (t4evli7.jpg)..... 55

Figure 3-54. Environmental SEM image magnified 100 times for a Test #4 Day 30 exterior high-flow fiberglass sample. (T4HFEx01.jpg)..... 56

Figure 3-55. E Environmental SEM image magnified 500 times for a Test #4 Day 30 exterior high-flow fiberglass sample. (t4hfex07.jpg) 57

Figure 3-56. Environmental SEM image magnified 800 times for a Test #4 Day 30 exterior high-flow fiberglass sample. (t4hfex06.jpg) 57

Figure 3-57. EDS counting spectrum for the spot of film on the fiberglass shown in Figure 3-56. (t4hfex05.jpg)..... 58

Figure 3-58. Environmental SEM image magnified 100 times for a Test #4 Day 30 interior high-flow fiberglass sample. (t4hfin01.jpg)..... 58

Figure 3-59. Environmental SEM image magnified 500 times for a Test #4 Day 30 interior high-flow fiberglass sample. (t4hfin04.jpg)..... 59

Figure 3-60. Environmental SEM image magnified 100 times for a Test #4 Day 30 interior high-flow fiberglass sample. The sample was gently pre-rinsed with RO water. (T4Rnd01.jpg) 59

Figure 3-61. Environmental SEM image magnified 500 times for a Test #4 Day 30 interior high-flow fiberglass sample. The sample was gently pre-rinsed with RO water. (t4rnd05.jpg)..... 60

Figure 3-62: Environmental SEM image magnified 100 times for a Test #4 Day 30 exterior high-flow fiberglass sample in front of a header (inserted on Day 4). (t4d30hx1.jpg)..... 61

Figure 3-63: Environmental SEM image magnified 1000 times for a Test #4 Day 30 exterior high-flow fiberglass sample in front of a header (inserted on Day 4). (t4d30hx5.jpg)..... 61

Figure 3-64: EDS counting spectrum for the spot of coating substance on fiberglass shown in Figure 3-63. (t4d30hx4.jpg) 62

Figure 3-65: Environmental SEM image magnified 100 times for a Test #4 Day 30 interior high-flow fiberglass sample in front of a header (inserted on Day 4). (t4d30hi6.jpg) 62

Figure 3-66: Environmental SEM image magnified 500 times for a Test #4 Day 30 interior high-flow fiberglass sample in front of a header (inserted on Day 4). (t4d30hi9.jpg) 63

Figure 3-67: EDS counting spectrum for the spot of substance attached on fiberglass shown in Figure 3-66. (t4d30hi8.jpg)..... 63

Figure 3-68: Environmental SEM image magnified 1000 times for a Test #4 Day 30 interior high-flow fiberglass sample in front of a header (inserted on Day 4). (t4d30hi1.jpg)..... 64

Figure 3-69: Environmental SEM image magnified 100 times for a Test #4 Day 30 exterior fiberglass sample on the drain collar (away from the drain screen). (t4dcox05.jpg)..... 65

Figure 3-70: Environmental SEM image magnified 500 times for a Test #4 Day 30 exterior fiberglass sample on the drain collar (away from the drain screen). (t4dcox02.jpg)..... 65

Figure 3-71: Environmental SEM image magnified 1000 times for a Test #4 Day 30 exterior fiberglass sample on the drain collar (away from the drain screen). (t4dcox03.jpg)..... 66

Figure 3-72: EDS counting spectrum for the large mass of particulate deposits on fiberglass shown in Figure 3-71. (t4dcox04.jpg)..... 66

Figure 3-73: Environmental SEM image magnified 100 times for a Test #4 Day 30 interior fiberglass sample on the drain collar. (t4dcin11.jpg)..... 67

Figure 3-74: Environmental SEM image magnified 500 times for a Test #4 Day 30 interior fiberglass sample on the drain collar. (t4dcin12.jpg)..... 67

Figure 3-75: Environmental SEM image magnified 500 times for a Test #4 Day 30 interior fiberglass sample on the drain collar. (t4dcin15.jpg)..... 68

Figure 3-76: Environmental SEM image magnified 100 times for a Test #4 Day 30 exterior fiberglass sample on the drain collar (next to the drain screen). (t4dcix06.jpg)..... 68

Figure 3-77: Environmental SEM image magnified 500 times for a Test #4 Day 30 exterior fiberglass sample on the drain collar (next to the drain screen). (t4dcix07.jpg)..... 69

Figure 3-78: Environmental SEM image magnified 1000 times for a Test #4 Day 30 exterior fiberglass sample on the drain collar (next to the drain screen). (t4dcix08.jpg)..... 69

Figure 3-79: EDS counting spectrum for the large mass of particulate deposits on fiberglass shown in Figure 3-78. (t4dcix09.jpg)..... 70

Figure 3-80: Environmental SEM image magnified 100 times for a Test #4 Day 30 exterior fiberglass sample within the birdcage. (T4D30BX1.jpg)..... 71

Figure 3-81: Environmental SEM image magnified 500 times for a Test #4 Day 30 exterior fiberglass sample within the birdcage. (T4D30bx2.jpg) 71

Figure 3-82: Annotated environmental SEM image magnified 500 times for a Test #4 Day 30 exterior fiberglass sample within the birdcage. (t4d30bx4.jpg)..... 72

Figure 3-83: EDS counting spectrum for the particulate deposits on fiberglass shown in Figure 3-82. (T4D30bx3.jpg) 72

Figure 3-84: Environmental SEM image magnified 100 times for a Test #4 Day 30 interior fiberglass sample within the birdcage. (t4d30bi5.jpg)..... 73

Figure 3-85: Environmental SEM image magnified 500 times for a Test #4 Day 30 interior fiberglass sample within the birdcage. (t4d30bi7.jpg)..... 73

Figure 3-86: Environmental SEM image magnified 100 times for a Test #4 Day 30 low-flow exterior raw cal-sil sample. (T4RCX01.jpg) 75

Figure 3-87: Environmental SEM image magnified 500 times for a Test #4 Day 30 low-flow exterior raw cal-sil sample. (t4rcex02.jpg)..... 75

Figure 3-88: EDS counting spectrum for the whole image shown in Figure 3-87. (t4rcex03.jpg)..... 76

Figure 3-89: Environmental SEM image magnified 100 times for a Test #4 Day 30 low-flow interior raw cal-sil sample. (t4rcin04.jpg)..... 76

Figure 3-90: Environmental SEM image magnified 500 times for a Test #4 Day 30 low-flow interior raw cal-sil sample. (t4rcin05.jpg)..... 77

Figure 3-91: EDS counting spectrum for the whole image shown in Figure 3-90. (t4rcin06.jpg) 77

Figure 3-92: Environmental SEM image magnified 100 times for a Test #4 Day 30 low-flow exterior baked cal-sil sample. (T4BCX07.jpg)..... 78

Figure 3-93: Environmental SEM image magnified 500 times for a Test #4 Day 30 low-flow exterior baked cal-sil sample. (t4bcex08.jpg) 78

Figure 3-94: EDS counting spectrum for the whole image shown in Figure 3-93. (t4bcex09.jpg)..... 79

Figure 3-95: Environmental SEM image magnified 100 times for a Test #4 Day 30 low-flow interior baked cal-sil sample. (T4BCIN10.jpg)..... 79

Figure 3-96: Environmental SEM image magnified 500 times for a Test #4 Day 30 low-flow interior baked cal-sil sample. (t4bcin11.jpg)..... 80

Figure 3-97: EDS counting spectrum for the whole image shown in Figure 3-95. (t4bcin12.jpg)..... 80

Figure 3-98: Al-237 submerged, pre-test (left) and post-test (right). 81

Figure 3-99: Al-238 submerged, pre-test (left) and post-test (right). 82

Figure 3-100: Al-239 submerged, pre-test (left) and post-test (right). 82

Figure 3-101: GS-130 submerged, pre-test (left) and post-test (right). 82

Figure 3-102: GS-132 submerged, pre-test (left) and post-test (right). 83

Figure 3-103: GS-134 submerged, pre-test (left) and post-test (right). 83

Figure 3-104: IOZ-233 submerged, pre-test (left) and post-test (right). 84

Figure 3-105: IOZ-234 submerged, pre-test (left) and post-test (right). 84

Figure 3-106: CU-548 submerged, pre-test (left) and post-test (right). 84

Figure 3-107: CU-572 submerged, pre-test (left) and post-test (right). 85

Figure 3-108: US-17 submerged, pre-test (left) and post-test (right). 85

Figure 3-109: Conc-004 submerged, pre-test (left) and post-test (right). 85

Figure 3-110: AI-003 unsubmerged, pre-test (left) and post-test (right). 87

Figure 3-111: AI-229 unsubmerged, pre-test (left) and post-test (right). 87

Figure 3-112: GS-33 unsubmerged, pre-test (left) and post-test (right). 88

Figure 3-113: GS-91 unsubmerged, pre-test (left) and post-test (right). 88

Figure 3-114: CU-536 unsubmerged, pre-test (left) and post-test (right). 89

Figure 3-115: CU-584 unsubmerged, pre-test (left) and post-test (right). 89

Figure 3-116: IOZ-263 unsubmerged, pre-test (left) and post-test (left). 89

Figure 3-117: IOZ-275 unsubmerged, pre-test (left) and post-test (right). 90

Figure 3-118: US-16 unsubmerged, pre-test (left) and post-test (right). 90

Figure 3-119. Sediment removed from the tank. 93

Figure 3-120. Sediment on the tank bottom. 94

Figure 3-121. Drain collar surrounded by sediment on the tank bottom. 94

Figure 3-122. Drain collar and drain screen removed from the tank. 95

Figure 3-123. Birdcage and cal-sil baskets after draining of the tank. 95

Figure 3-124: SEM image magnified 100 times for a Test #4 Day 30 sediment sample at the bottom of the tank. (T4D30SEDMT026.bmp) 96

Figure 3-125: SEM image magnified 500 times for a Test #4 Day 30 sediment sample at the bottom of the tank. (T4D30SEDMT027.bmp) 96

Figure 3-126: Annotated SEM image magnified 500 times for a Test #4 Day 30 sediment sample at the bottom of the tank. (T4D30SEDMT027.bmp) 97

Figure 3-127: EDS counting spectrum for the white snow like deposits (EDS1) shown in Figure 3-126. (T4D30SEDMT16.jpg) 97

Figure 3-128: EDS counting spectrum for the dark deposits (EDS2) shown in Figure 3-126. (T4D30SEDMT17.jpg) 98

Figure 3-129: XRD result of the possible matching crystalline substances in Test #4 Day 30 sediment. 98

Figure 3-130: SEM image magnified 1000 times for a Test #4 Day 30 fine powder on the submerged rack. (T4D30RackPowder030.bmp) 100

Figure 3-131: EDS counting spectrum for the particles (whole image) shown in Figure 3-130. (T4D30Rackpowder18.jpg) 100

TABLES

Table 1-1. Test Series Parameters.....	2
Table 2-1. Quantity of Each Coupon Type in Test #4.....	5
Table 2-2. Material Quantity/Sump Water Volume Ratios for the ICET Tests	11
Table 3-1. ICP Results for Selected Elements	27
Table 3-2: Weight Data for Submerged Coupons.....	86
Table 3-3: Weight Data for Unsubmerged Coupons	90
Table 3-4: Mean Gain/Loss Data for All Submerged Coupons (g).....	91
Table 3-5: Mean Gain/Loss Data for All Unsubmerged Coupons (g).....	91
Table 3-6. Dry Mass Composition of Test #4 Day 30 Sediment by XRF Analysis	99

INTEGRATED CHEMICAL EFFECTS TEST PROJECT: TEST #4 DATA REPORT

EXECUTIVE SUMMARY

The U.S. Nuclear Regulatory Commission (NRC) Office of Nuclear Regulatory Research has developed a comprehensive research program to support resolution of Generic Safety Issue (GSI)-191. GSI-191 addresses the potential for debris accumulation on pressurized water reactor (PWR) sump screens, with the consequent loss of net-positive-suction-head margin in the emergency core-cooling system (ECCS) pump. Among the GSI-191 research program tasks is the experimental investigation of chemical effects that may exacerbate sump-screen clogging.

The Integrated Chemical Effects Test (ICET) project represents a joint effort by the U.S. NRC and the nuclear utility industry, undertaken through the Memorandum of Understanding on Cooperative Nuclear Safety between NRC and Electric Power Research Institute (EPRI), Addendum on Integral Chemical Effects Testing for PWR ECCS Recirculation. The ICET project simulates the chemical environment present inside a containment water pool after a loss-of-coolant accident (LOCA) and monitors the chemical system for an extended time to identify the presence, composition, and physical characteristics of chemical products that form during the test. The ICET test series is being conducted by Los Alamos National Laboratory at the University of New Mexico, with the assistance of professors and students in the civil engineering department.

This report describes the ICET experimental apparatus and surveys the principal findings of Test #4. This interim data report summarizes both primary and representative findings that were available at the time the report was prepared. The NRC and the nuclear power industry may conduct additional analyses to enhance the understandings obtained from this test.

All of the ICET tests were conducted in an environment that simulates expected containment pool conditions during recirculation. The initial chemical environment contains 2800 mg/L of boron, 100 mg/L of hydrochloric acid, 0.7 mg/L of lithium hydroxide. The tests are conducted for 30 days at a constant temperature of 60°C (140°F). The materials tested within this environment include representative amounts of submerged and unsubmerged aluminum, copper, concrete, zinc, carbon steel, and insulation samples. Representative amounts of concrete dust and latent debris are also added to the test solution. Tests consist of an initial 4-hour spray phase to simulate containment spray interaction with the unsubmerged samples. Water is circulated through the bottom portion of the test chamber during the entire test to achieve representative flow rates over the submerged specimens.

ICET Test #4 was conducted using sodium hydroxide to control pH, with a target pH of 10. Insulation samples consisted of scaled amounts of NUKON™ fiberglass and calcium silicate (cal-sil) material. In addition, the test apparatus contained 373 metal coupon samples and 1 concrete sample. Process control consisted of monitoring online measurements of recirculation flow rate, test solution temperature, and pH. Flow rate and temperature were controlled to maintain the desired values of 25 gpm and 140°F. Daily water samples were obtained for

measurements of pH, turbidity, total suspended solids, kinematic viscosity, and shear-dependent viscosity and for analytical laboratory evaluations of the chemical elements present. In addition, microscopic evaluations were conducted on water sample filtrates, fiberglass, cal-sil, coupons, and sediment.

Before time zero, 15.14 kg of boric acid, 0.663 g of lithium hydroxide, 8.47 kg of sodium hydroxide, and 212 mL of 12.29 N hydrochloric acid were dissolved into the ICET tank. The measured pH was 9.5, which was the expected value obtained from analytical predictions. An additional 614 g of sodium hydroxide were added through the spray line for the first 30 minutes of the test. The pH rose to a value of 9.8 at the end of the spray cycle.

The test ran for 30 days, and all conditions were maintained within the accepted flow and temperature ranges, with two exceptions. On Day 11, a power outage occurred which caused a recirculation pump trip. Recirculation flow was re-established 2 hours and 15 minutes later. During that time, the maximum solution temperature rose to 62.4°C, which is 0.4°C above the target maximum. The maximum temperature was above 62.0°C for approximately one hour.

Observations of the test solution indicated similar behavior of the solution at both room temperature and test temperature. After the initial cloudiness caused by the cal-sil dust had cleared up, no chemical byproducts were visible in the water and no precipitation occurred as samples cooled from test temperature to room temperature.

Analyses of the test solution revealed aluminum in the solution, but only for the first 24 hours and at trace amounts. Calcium, silica, and sodium were prevalent in the solution.

Examinations of fiberglass taken from the test apparatus revealed chemical products and a film that spanned individual fibers. Some coating was also observed on individual fibers. The amounts of these deposits did not increase significantly from Day 5 until Day 30. The coating was likely formed by chemical precipitation. In addition to films and coatings, samples in high-flow regions had significant amounts of particulate deposits that were likely physically attached.

Daily measurements of the constant-shear kinematic viscosity of the test solution revealed an approximately constant value at both test temperature and room temperature. Shear-dependent viscosity measurements indicated that the test solution was representative of a Newtonian fluid.

The ICET series is being conducted under an approved quality assurance (QA) program, and QA procedures and project instructions were reviewed and approved by the project sponsors. Analytical laboratory results are generated under a quality control program approved by the Environmental Protection Agency, and other laboratory analyses were performed using standard practices, as referenced in the body of this report.

ACKNOWLEDGMENTS

The principal authors of this report gratefully acknowledge the assistance of the following persons, without whom successful completion of the fourth Integrated Chemical Effects Test could not have been accomplished. Mr. John Gisclon, representing the Electric Power Research Institute, contributed much practical, timely advice on preparation of the QA experimental project instructions and the preparation of calcium silicate. Mr. Michael Niehaus from Sandia National Laboratories provided a characterization of time-dependent strain-rate viscosity measurements for the circulating solution. Mr. Luke Bartlein, of Los Alamos National Laboratory's Nuclear Design and Risk Analysis group (D-5), provided timely tagging of all test pictures and analytical images. Mr. Jim Young, of group PS-1, provided valuable reviews and inputs to QA documentation and practices. The authors also express their gratitude for the contributions and continued participation of numerous NRC staff members who reviewed the project instructions and preliminary data to ensure relevance to plant safety, high-quality defensible results, and timely execution of this test. Dr. Alicia Aragon of Sandia National Laboratories provided a very thorough review of the report and many helpful suggestions.

The authors acknowledge Ms. Eileen Patterson of IM-1, Los Alamos National Laboratory, and Ms. Katsura Fujiike of OMICRON, for their editing support.

ACRONYMS AND ABBREVIATIONS

Al	Aluminum
Au	Gold
cal-sil	calcium silicate
CPVC	Chlorinated Polyvinyl Chloride
CS	Coated steel
Cu	Copper
DAS	Data Acquisition System
DHR	Decay Heat Removal
ECCS	Emergency Core-Cooling System
EDS	Energy-Dispersive Spectroscopy
EPA	Environmental Protection Agency
ESEM	Environmental Scanning Electron Microscopy
F	Filtered
GS	Galvanized Steel
GSI	Generic Safety Issue
HCl	Hydrochloric Acid
HI	High-flow Interior Fiberglass Sample
HX	High-flow Exterior Fiberglass Sample
ICET	Integrated Chemical Effects Tests
ICP	Inductively Coupled Plasma
ICP-AES	Inductively Coupled Plasma – Atomic Emission Spectroscopy
IOZ	Inorganic Zinc
LANL	Los Alamos National Laboratory
LI	Low-flow Interior Fiberglass Sample
LiOH	Lithium Hydroxide
LOCA	Loss-of-Coolant Accident
LX	Low-flow Exterior Fiberglass Sample
NIST	National Institute of Standards and Technology
NRC	Nuclear Regulatory Commission
NTU	Nephelometric Turbidity Unit
P	Phosphorous
Pd	Palladium
PI	Project Instruction

PVC	Polyvinyl Chloride
PWR	Pressurized Water Reactor
QA	Quality Assurance
RO	Reverse Osmosis
SEM	Scanning Electron Microscopy
SS	Stainless Steel
TEM	Transmissive Electron Microscopy
TOC	Total Organic Carbon
TSP	Trisodium Phosphate
TSS	Total Suspended Solids
U	Unfiltered
UNM	University of New Mexico
US	Uncoated steel
WD	Working Distance
XRD	X-Ray Diffraction
XRF	X-Ray Fluorescence

1 INTRODUCTION

The Integrated Chemical Effects Test (ICET) project represents a joint effort by the United States Nuclear Regulatory Commission (NRC) and the nuclear utility industry to simulate the chemical environment present inside a containment water pool after a loss-of-coolant accident (LOCA) and to monitor the chemical system for an extended time to identify the presence, composition, and physical characteristics of chemical products that may form. The ICET series is being conducted by Los Alamos National Laboratory (LANL) at the University of New Mexico (UNM), with the assistance of professors and students in the civil engineering department.

1.1. Objective and Test Conditions

Containment buildings of pressurized water reactors (PWRs) are designed to accommodate the energy release following a postulated accident. They also permit recirculation of reactor coolant and emergency-core-cooling-system (ECCS) water to the decay heat removal (DHR) heat exchangers. The water collected in the sump from the reactor coolant system, the safety injection system, and the containment spray system is recirculated to the reactor core to remove residual heat. The sump contains a screen to protect system structures and components in the containment spray and ECCS flow paths from the effects of debris that could be transported to the sump. Concerns have been raised that fibrous insulation material could form a mat on the screen, obstructing flow, and that chemical reaction products such as gelatinous or crystalline precipitants could migrate to the screen, causing further blockage and increased head losses across the debris bed. Another potential adverse chemical effect includes increased bulk fluid viscosity that could also increase head losses through a debris bed.

The primary objectives for the ICET series are (1) to determine, characterize, and quantify chemical reaction products that may develop in the containment sump under a representative post-LOCA environment and (2) to determine and quantify any gelatinous material that could be produced during the post-LOCA recirculation phase.

The ICET series was conceived as a limited-scope suite of five different 30-day tests with different constituents. The conditions selected for each test are shown in Table 1-1. As shown in this table, Test #4 of the ICET series was to be operated at a high pH (~10) and included substantial quantities of calcium silicate insulation material as well as fiberglass. All tests in the series included metal coupons whose surface areas were scaled to those in representative PWR containment and sump systems. A complete rationale for the selection of these test conditions is provided in Ref. 1.

Table 1-1. Test Series Parameters

Run	Temp (°C)	TSP Na ₃ PO ₄ ·12H ₂ O	NaOH	pH	Boron (mg/L)	Note
1	60	N/A	Yes	10	2800	100% fiberglass insulation test. High pH, NaOH concentration as required by pH
2	60	Yes	N/A	7	2800	100% fiberglass insulation test. Low pH, TSP concentration as required by pH.
3	60	Yes	N/A	7	2800	80% calcium silicate/20% fiberglass insulation test. Low pH, TSP concentration as required by pH
4	60	N/A	Yes	10	2800	80% calcium silicate/20% fiberglass insulation test. High pH, NaOH concentration, as required by pH.
5	60	TBD	TBD	TBD	TBD	Confirmatory test; one of the above four tests will be repeated.

The ICET apparatus consists of a large stainless-steel (SS) tank with heating elements, spray nozzles, and associated recirculation pump and piping to simulate the post-LOCA chemical environment. Samples of structural metals, concrete, and insulation debris are scaled in proportion to their relative surface areas found in containment and in proportion to a maximum test dilution volume of 250 gal. of circulating fluid. Representative chemical additives, temperature, and material combinations are established in each test; the system is then monitored while corrosion and fluid circulation occur for a duration comparable to the ECCS recirculation mission time.

1.2. Information Presented in This Report

This report surveys the principal findings of ICET Test #4. As an interim data report, this exposition summarizes both primary and representative findings, but it cannot be considered comprehensive. For example, only a small selection of photographs out of several hundred is presented here. In addition, this report presents observations and data without in-depth analyses or interpretations. However, trends and typical behaviors are noted where appropriate. Section 2 of this report reviews the test procedures followed for Test #4. Analytical techniques used in evaluating test results are also briefly reviewed in Section 2. Section 3 presents key test results for Test #4, including representative and noteworthy results of water sampling, insulation samples (cal-sil and fiberglass), metallic and concrete coupon samples, tank sediment, corrosion products, and gel. The results for Test #4 are presented in both graphical and narrative form. Section 4 presents a summary of key observations for Test #4. This report also includes several appendices that capture additional Test #4 images and information. The data presented in the appendices are largely qualitative, consisting primarily of environmental scanning electron microscopy

(ESEM), scanning electron microscopy (SEM), transmissive electron microscopy (TEM) micrographs, and energy-dispersive spectroscopy (EDS) spectra.

2 TEST PROCEDURES

The functional description and physical attributes of the ICET apparatus were presented in detail in the ICET Test #1 report (Ref. 2). The experimental apparatus is briefly described below, followed by a review of the test operation and analytical techniques used to evaluate the test results.

2.1 Chemical Test Apparatus Functional Description

The test apparatus was designed to meet the functional requirements of the Project Test Plan (Ref. 1). Functional aspects of the test apparatus are as follows:

1. The central component of the system is a test tank. The test apparatus was designed to prevent solids from settling in the test piping.
2. The test tank can maintain both a liquid and vapor environment, as would be expected in post-LOCA containment.
3. The test loop controls the liquid temperature at 140°F ($\pm 5^\circ\text{F}$).
4. The system circulates water at flow rates that simulate spray flow rates per unit area of containment cross section.
5. The test tank provides for water flow over submerged test coupons that is representative of containment pool fluid velocities expected at plants.
6. Piping and related isolation valves are provided such that a section of piping can be isolated without interrupting the test.
7. The pump discharge line is split in two, one branch directing the spray header in the tank's vapor space and the other returning to the liquid side of the tank. Each branch is provided with an isolation valve, and the spray line includes a flow meter.
8. The recirculation piping includes a flow meter.
9. The pump circulation flow rate is controlled at the pump discharge to be within $\pm 5\%$ of the flow required to simulate fluid velocities in the tank. Flow is controlled manually.
10. The tank accommodates a rack of immersed sample coupons, including the potential reaction constituents identified in the test plan.

11. The tank also accommodates six racks of sample coupons that are exposed to a spray of liquid that simulates the chemistry of a containment spray system. Provision is made for these racks to be visually inspected.
12. The coupon racks provide sufficient space between the test coupons to preclude galvanic interactions among the coupons. The different metallic test coupons are also electrically isolated from each other and the test stand to prevent galvanic effects resulting from metal-to-metal contact between specimens or between the test tank and the specimens.
13. The fluid volumes and sample surface areas are based on scaling considerations that relate the test conditions to actual plant conditions.
14. All components of the test loop are made of corrosion-resistant material (for example, SS for metallic components).

The as-built test loop consists of a test tank, a recirculation pump, 2 flow meters, 10 isolation valves, and pipes that connect the major components, as shown schematically in Figure 2-1. P, T, and pH represent pressure, temperature, and pH probes, respectively.

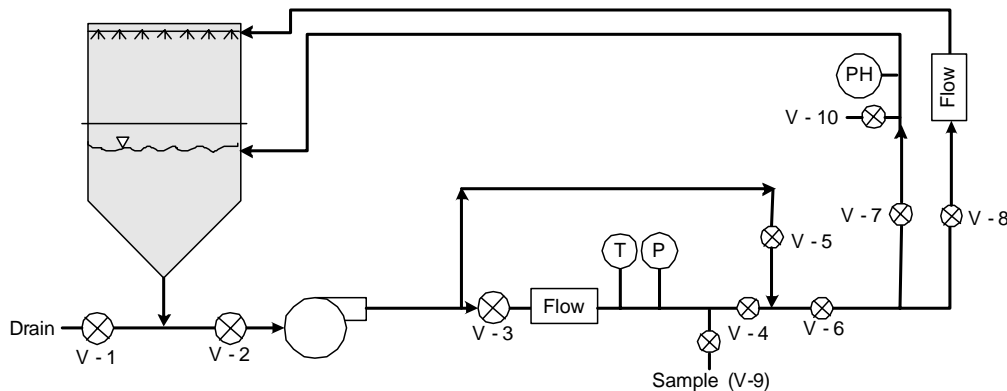


Figure 2-1. Test loop process flow diagram.

2.2 Pre-Test Preparation

2.2.1. Test Loop Cleaning

In preparation for Test #4, the experiment test loop was thoroughly cleaned to remove all Test #3 deposits and residues. In addition to visual inspections, the test apparatus was flushed and cleaned per the written direction given in the pre-test operations project instruction (PI) (Ref. 3). The system was flushed with ammonium hydroxide, followed by ethanol, and then nitric acid until it was visually clean and the water conductivity was $<50 \mu\text{S}/\text{cm}$.

2.2.2. Test Coupons and Samples

Each ICET experiment exposes metallic and concrete coupons to anticipated post-LOCA environments. Each coupon is approximately 12 in. square. The metallic coupons are approximately 1/16 in. thick, except for the inorganic-coated steel coupons, which are approximately 3/32 in. thick. The concrete coupons (one per test) are approximately 1-1/2 in. thick. Insulation materials are also exposed. For Test #4, fiberglass insulation samples and calcium silicate samples were included in the test. As with previous tests, Test #4 subjected seven racks of coupons to the specified environment, with one being submerged in the test tank and the remaining six being held in the tank's gas/vapor space. The Test #4 coupons of each type were as shown in Table 2-1.

Table 2-1. Quantity of Each Coupon Type in Test #4

Material	No. of Coupons
Coated Steel (CS)	77
Aluminum (Al)	59
Galvanized Steel (GS)	134
Copper (Cu)	100
Uncoated Steel (US)	3
Concrete	1

Note: Inorganic zinc (IOZ) coated steel and CS are the same coupon type.

The arrangement of the coupon racks in the test tank is schematically illustrated in Figure 2-2. The figure shows a side view of the ICET tank, with the ends of the seven CPVC racks illustrated. The normal water level is indicated by the blue line in the figure. Rack #1 is the only submerged rack, and it sits on angle iron. It is centered in the tank so that flow from the two headers reaches it equally. Racks #2–#4 are positioned above the water line, supported by angle iron in the tank. Racks #5–#7 are positioned at a higher level, also supported by angle iron. Racks #2–#7 are exposed to spray. In the figure, north is to the right, and south is to the left. Directions are used only to identify such things as rack locations and sediment locations.

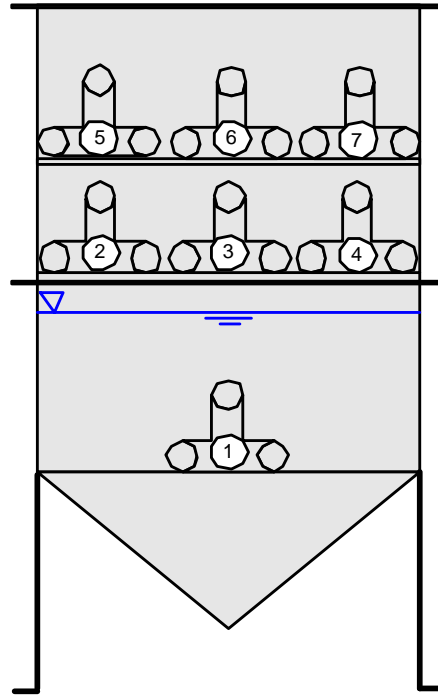


Figure 2-2. Coupon rack configuration in the ICET tank. The blue line represents the surface of the test solution.

Figure 2-3 shows the configuration of a typical unsubmerged coupon rack loaded with metal coupons in the ICET tank. The loading pattern of the racks was nearly identical, varying by only one or two coupons. Shown in the figure from left to right, the coupons are arranged as follows: 4 Cu, 4 Al, 4 inorganic zinc (IOZ), 7 GS, 4 Cu, 3 Al, 4 IOZ, 7 GS, 4 Cu, 3 Al, 4 IOZ, and 7 GS.



Figure 2-3. A typical loaded coupon rack in the ICET tank.

Several fiberglass samples were placed in the ICET tank. Samples were either submerged or held above the water level. The unsubmerged fiberglass samples were positioned so they would be exposed to sprays. The fiberglass samples were contained in SS wire mesh that allowed water flow while confining the fiberglass material. Both loosely packed and more tightly packed samples were used. In addition, some submerged fiberglass samples were located where they would be exposed to relatively high-flow conditions (in front of the flow header, attached to the submerged coupon rack), and others were located in quiescent regions of the tank (behind the flow header). Figure 2-4 shows what the so-called “sacrificial” fiberglass samples look like in wire mesh pouches attached to the submerged coupon rack (rack 1 in Figure 2-2). Each pouch contains approximately 5 g of fiberglass. Those samples were attached with SS wire; removed from the tank on Days 5, 15, and 30; and examined. As shown in the figure, bigger insulation bags were wrapped around the sacrificial specimens during the test. See Subsection 2.4.1.1 for descriptions of other fiberglass samples.



Figure 2-4. Fiberglass samples attached to a submerged coupon rack.

Several cal-sil insulation samples were also placed in the ICET tank. Samples were either submerged or held above the water level. The unsubmerged cal-sil samples were positioned so they would be exposed to sprays. As with the fiberglass samples, all of the cal-sil samples (except for the dust) were contained in SS wire mesh that allowed water flow while confining the cal-sil material. In addition to solid pieces of cal-sil, cal-sil dust (approximately 43.5 lb) was placed in the tank solution before the test began. Both types of samples are shown in Figures 2-5 and 2-6.



Figure 2-5. Solid pieces of cal-sil samples in SS mesh.

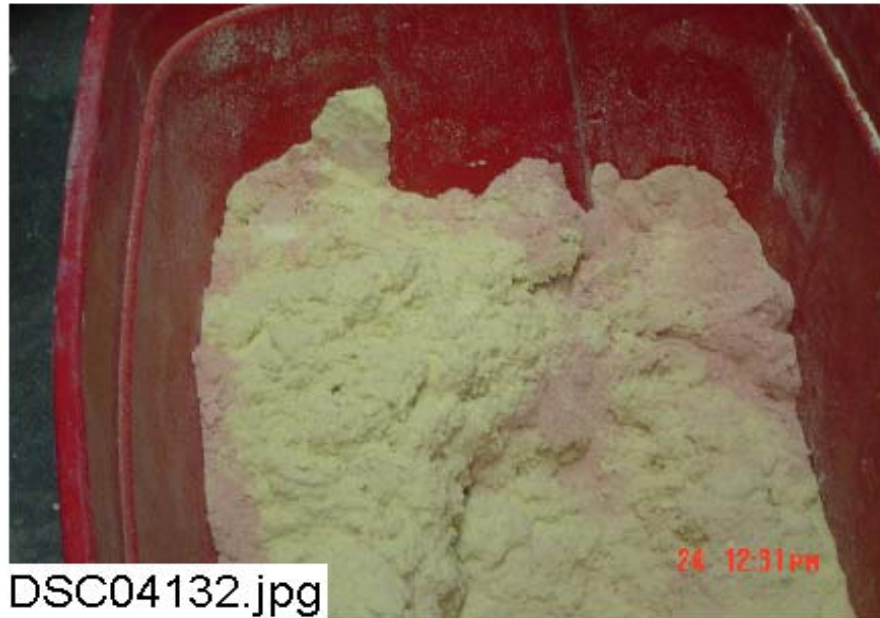


Figure 2-6. Cal-sil dust.

2.2.3. Quality Assurance Program

A project QA manual was developed to satisfy the contractual requirements that apply to the ICET project. Specifically, those requirements were to provide credible results by maintaining an appropriate level of QA in the areas of test loop design, sampling,

chemicals, operation, and analysis. These requirements were summarized in the contract requirement that QA was to be consistent with the intent of the appropriate sections of 10CFR50, Appendix B.

The 18 criteria of 10CFR50, Appendix B, were addressed separately in the QA manual, and the extents to which they apply to the ICET project were delineated. A resultant set of QA procedures was developed. In addition, project-specific instructions were written to address specific operational topics that required detailed step-by-step guidance. PIs generally applicable to all tests were written for the following topics and were followed for Test #4:

- Data Acquisition System (DAS)
- Coupon Receipt, Preparation, Inspection, and Storage
- DAS Alarm Response
- Chemical Sampling and Analysis
- TEM Examination of Test Samples
- SEM Characterization of Test Samples
- Viscosity Measurements

Project instructions specific to Test #4 were written for the following:

- Pre-Test Operations
- Test Operations, Test #4 (cal-sil, fiberglass, and NaOH at pH 10)
- Post-Test Operations

The pre-test, test, and post-test operations PIs that were used in Test #4 are included in Appendix J.

2.2.4. Test Parameters

ICET test parameters were selected based on literature surveys and the results of surveys of United States nuclear power plants. Quantities of test materials were selected to preserve the scaling of representative ratios between material surface areas and total cooling-water volumes. Chemical additives also simulate the post-LOCA sump environment. The Project Test Plan (Ref. 1) is the basis for the following information in this section.

The materials included in the tests are zinc, aluminum, copper, carbon steel, concrete, and insulation materials such as fiberglass and calcium silicate. The amounts of each material are given in Table 2-2 in the form of ratios (material surface area to water volume), with three exceptions: concrete dust, which is presented as a ratio of mass to water volume, and fiberglass and calcium silicate, which are presented as a ratio of insulation volume to water volume. Also shown in the table are the percentages of material that are submerged and unsubmerged in the test chamber.

Table 2-2. Material Quantity/Sump Water Volume Ratios for the ICET Tests

Material	Value of Ratio for the Test (ratio units)	Percentage of Material Submerged (%)	Percentage of Material Unsubmerged (%)
Zinc in Galvanized Steel	8.0 (ft ² /ft ³)	5	95
Inorganic Zinc Primer Coating (non-top coated)	4.6 (ft ² /ft ³)	4	96
Inorganic Zinc Primer Coating (top coated)	0.0 (ft ² /ft ³)	–	–
Aluminum	3.5 (ft ² /ft ³)	5	95
Copper (including Cu-Ni alloys)	6.0 (ft ² /ft ³)	25	75
Carbon Steel	0.15 (ft ² /ft ³)	34	66
Concrete (surface)	0.045 (ft ² /ft ³)	34	66
Concrete (particulate)	0.0014 (lbm/ft ³)	100	0
Insulation Material (fiberglass or calcium silicate)	0.137 (ft ³ /ft ³)	75	25

The physical and chemical parameters that are critical for defining the tank environment and that have a significant effect on sump-flow blockage potential and gel formation have been identified in Reference 1. These physical and chemical parameters are summarized as follows:

Physical Parameters

• Water volume in the test tank	949 L	250 gal.
• Circulation flow	0–200 L/min	0–50 gpm
• Spray flow	0–20 L/min	0–5 gpm
• Sump temperature	60°C	140°F

Chemistry Parameters

• H ₃ BO ₃ concentration	2800 mg/L as boron
• Na ₃ PO ₄ ·12H ₂ O concentration	As required to reach pH 7 in the simulated sump fluid
• NaOH concentration	As required to reach pH 10 in the simulated sump fluid
• HCl concentration	100 mg/L
• LiOH concentration	0.7 mg/L as Li

The parameters planned for each ICET test run are described in Table 1-1.

2.3 Test Operation

2.3.1. Description

Preparation of ICET Test #4 (Run #4 in Table 1-1) began with 239 gal. of reverse osmosis (RO) water heated to 65°C. (Adding the metal coupons and insulation samples reduces the water temperature by approximately 5°C, so the water was heated initially to 65°C.) With 25 gpm circulating through the loop, the predetermined quantities of boric acid (15.41 kg), sodium hydroxide (8.47 kg), lithium hydroxide (0.66 g), and hydrochloric acid (212 mL) were added and dissolved in the ICET tank solution. The chemicals were added with 10 gallons of RO water. After the chemicals were added and observed to be well mixed, a baseline grab sample and measurements of the test solution were taken. Then the premeasured latent debris and concrete dust were added to the tank solution. After the solution circulated for 10 minutes, the pump was stopped and the coupon racks and insulation samples were put into the tank (see Section 2.2.2).

The test commenced with initiation of the tank sprays (3.5 gpm). For the first 30 minutes, one gallon of RO water containing 614 g of sodium hydroxide was metered into the spray. The sprays were terminated after 4 hours. The test ran for 30 days, with one 2-hour, 15-minute interruption due to a power outage, which occurred on Day 11.

The experiment commenced at 2:30 p.m. on Tuesday, May 24, 2005, and it ended on June 23, 2005. During the test, grab samples were taken daily for wet chemistry and inductively coupled plasma – atomic emission spectroscopy (ICP-AES) analyses. Water loss due to water sample removals and evaporation was made up with RO water. Water samples, insulation, and metal coupons were analyzed after the test. Sampling and analyses were conducted in accordance with approved project instructions (Refs. 3, 4, and 5).

2.3.2. Process Control

During the test, critical process control parameters were monitored to ensure that the test conditions met the functional test requirements. Recirculation flow rate and temperature were controlled throughout the test. The solution pH was initially targeted to reach the prescribed value of 10 after the spray phase ended. The predetermined amounts of chemicals were added, and pH was not controlled.

Recirculation flow in the test loop was controlled by adjusting the pump speed. Fine tuning was achieved by manually adjusting a valve located downstream of the recirculation pump. In-line flow meters were used to measure the flow rate in the recirculation line and the spray line.

Titanium-jacketed immersion electric heaters controlled the water temperature. The heaters were thermostatically controlled to automatically maintain the desired temperature.

2.4 Analytical Methods

Data collected during Test #4 included the in-line measurements of temperature, pH, and loop flow rate. During the daily water grab sample analysis, bench-top measurements were obtained for temperature, pH, turbidity, total suspended solids (TSS), and kinematic viscosity. The concentration of hydrogen in the tank atmosphere was also measured and could be used as an indicator of chemical reactions taking place. Water, fiberglass, and metal coupon samples were taken to other laboratory locations for additional analyses. These analyses included strain-rate viscosity, ESEM, SEM, EDS, TEM, ICP-AES, x-ray fluorescence (XRF), and x-ray diffraction (XRD). EDS provided a semi-quantitative elemental analysis after calibration of the instrument's x-ray signal using an internal element standard. Descriptions of the principles of operation and limitations of these analytical methods were provided in the Test #1 report (Ref. 2).

2.4.1. Data Compilation and Nomenclature

This section provides a brief guide to assist the reader in interpreting the ICET Test #4 information and data presented in the following sections and in the appendices. Standardized nomenclature is defined first to clarify the origin of samples that are described in the data sets. The appendices are listed, and a description is provided of how they were compiled.

2.4.1.1. Nomenclature

Many spatially unique but physically similar sample types were collected in ICET Test #4. To ensure that consistent interpretations and comparisons of data sets are made, it is imperative that a standardized nomenclature be adopted when referring to each sample type. Many different qualitative descriptions of these samples might be equally suitable, but different adjectives convey different connotations to each observer. Therefore, the following definitions establish the convention used in this report when

making generic references to sample type. Every effort should be made to adhere to this standard when interpreting the data so that all future audiences will have a common understanding of sample origins from the ICET series.

- White Precipitate** The behavior of test solution at test temperature and upon cooling is observed during testing. Precipitates and their prominence indicate chemical interactions occurring in the solution. White precipitate formed in Test #1 water solution samples drawn from the test loop. Upon cooling below the test temperature, Test #1 daily water samples extracted from the tank formed a visible white material that is referred to as a precipitate. This precipitate was absent in Test #4 water samples. Test #1 had a high pH of about 9.5, and the pH for Test #4 was about 9.8. It is unclear what caused precipitates to form in Test #1 but not in Test #4.
- Latent Debris** Commercial power plant containments gradually accumulate dust, dirt, and fibrous lint that are generically referred to as latent debris. This classification distinguishes resident material from debris generated during an accident scenario. At the beginning of Test #4, measured quantities of crushed concrete and soil were added to simulate the latent debris present in containment. These materials were examined via SEM/EDS to establish a baseline composition for comparison with sediment samples (see “Sediment” below).
- Sediment** Surrogate latent debris particulates and fugitive fiberglass fragments that were initially suspended in water at the beginning of Test #4 gradually settled to the bottom of the tank. In addition, a large amount of cal-sil dust was added to the tank solution. Most of that dust ended up on the tank bottom. A deep layer of sediment formed, which was 8-in. deep in some places at the end of the test. At the conclusion of the test, the sediment was recovered as completely as possible.
- Powder** At the conclusion of Test #4, fine particulate deposits were found on the submerged CPVC coupon rack. They were referred to as powder and examined by SEM/EDS. These deposits are also referred to as deposition products (see Appendix E).
- Fiberglass** One of the principal debris types introduced to Test #4 was shredded fiberglass insulation. This debris was bundled in 3-in.-thick bags (or blankets) of fiberglass confined in SS mesh to prevent ingestion through the pump and to better control the placement of debris in various flow regimes. Fiberglass samples are designated by their placement in high-flow and low-flow areas of the tank. Fiberglass in the “big envelope” sat on the tank bottom in a low-flow area of the tank. Additional 4-in.-square envelopes of

fiberglass were also prepared for extraction during the course of the test. These samples are referred to as “sacrificial” samples. One sample, called the “birdcage,” was constructed so that the fiberglass within was loose and not compacted. The birdcage fiberglass sat on the tank bottom and was removed on Day 30. Some amount of fiber, especially short-fiber fragments, escaped the mesh bags and was deposited in other locations within the tank. This material is referred to as “fugitive” fiberglass. Two additional fiberglass samples were added after the test began and the water clarity improved. A sacrificial sample was placed directly in front of one of the flow headers (high-flow area) on Day 2. Another sacrificial sample enclosed in nylon mesh was placed in a low-flow area on Day 3.

- Cal-sil The insulation samples used in Test #4 were 80% cal-sil by volume. That amount was divided into 4 size categories, in pieces that were roughly cubes. Of the total cal-sil, 14% was over 3 in., 19% was 1–3 in., 5% was less than 1 in., and 62% was “dust.” The dust consisted of cal-sil pieces that were ground into a fine powder. With the exception of the dust, the cal-sil pieces were contained within SS mesh and apportioned into submerged and unsubmerged samples. The dust was put into the tank solution before the test started, and it became the primary constituent of the sediment.
- Drain Screen A 12-in.-tall screen made of coarse SS mesh (1/8-in. holes) wrapped into a 2-in.-diam cylinder was inserted into the outlet drain at the bottom of the tank to protect the pump from ingesting large debris items. Two inches of the screen were inserted into the tank outlet to provide a solid base and stability. A 6-in.-tall drain collar was installed around the drain screen. This drain collar was a cylinder of fiberglass held in SS mesh. The drain collar was exposed to higher-velocity water flow than other samples in the tank. However, when the sediment built up around the drain collar, it was only exposed to water flow down through the drain screen. The drain collar fiberglass was examined as a separate debris location to identify any apparent differences with other sample locations.
- Gelatinous Material This term generically refers to any observed sample constituent with amorphous, hydrated, or noncrystalline physical characteristics. When Test #4 was shut down, there was no evidence of gel-like precipitates in the tank or piping.
- Water Sample Daily water samples were extracted from the ICET tank for elemental concentration analyses. After the sample line was properly flushed, some of this water was extracted directly from

the tap. An equal amount of water was also generally collected through a micropore filter. Thus, daily water samples were designated as filtered (F) and unfiltered (U), and a corresponding filter paper exists in the sample archive for each daily sample that was collected.

- High-Volume Filter** If white precipitates are observed in the tests, larger quantities of test solution are periodically extracted for filtration to determine whether suspended chemical products are present in the test liquid under in situ conditions. The intent of this exercise is to maintain the liquid temperature while forcing the liquid through a micropore filter under vacuum. Because the precipitates were not present in Test #4, these high-volume filter samples were not obtained.
- Filter Paper** Many different samples of tank solution were fractionated by micropore filtration into a liquid supernate and a solid filtrate that existed at the time and temperature conditions of the filtering process. These samples included (1) daily water samples filtered during extraction, (2) daily water samples filtered after cooling to room temperature, and (3) high-volume water samples.
- Chemical Deposits** Sacrificial fiberglass samples that were extracted at Day 5, Day 15, and Day 30 showed evidence of chemical products forming on and between fiber strands. These products are referred to as “deposits,” although the exact physical mechanism of formation is not well understood. The physical appearance suggests growth, agglomeration, or crystallization on and around the fiber strands over time rather than capture or impaction of particles from the bulk solution. This observation is supported by the fact that the small sacrificial fiberglass samples were located in a region of lower-velocity water flow (i.e., in the interior of larger blankets).
- Concrete Sample** Several chips of concrete (1/4–3/4 in. diam) were broken from the primary slab of submerged concrete and introduced to the tank in a small SS envelope at the start of the test. Examinations of these chips were conducted to determine if concrete surfaces provide a preferential site for gel formation.

Although these terms have been defined, the reader may note minor inconsistencies in the caption labels used in this document. The caption labels use the same descriptions that were applied in laboratory notebooks to improve traceability of the data.

2.4.1.2. Usage

The 10 appendices listed below are provided to present data collected for the sample types and analysis methods listed below. In addition, an appendix is provided with pertinent Test #4 project instructions.

- Appendix A ESEM/EDS Data for Test #4 Day-5 Fiberglass in Low-Flow Zone
- Appendix B ESEM Day-15 Fiberglass
- Appendix C ESEM Day-30 Fiberglass
- Appendix D ESEM/EDS Data for Test #4 Day-30 Low-Flow Cal-sil Samples
- Appendix E ESEM and SEM/EDS Data for Test #4 Day-30 Deposition Products
- Appendix F SEM Day-30 Coupons
- Appendix G SEM/EDS Data for Test #4 Day-30 Sediment
- Appendix H TEM Data for Test #4 Solution Samples
- Appendix I UV Absorbance Spectrum – Day-30 Solution Samples
- Appendix J ICET Test #4: Pre-Test, Test, and Post-Test Project Instructions

These data are largely qualitative in nature, consisting primarily of ESEM, SEM, TEM micrographs, and EDS spectra. Each appendix represents a separate session of laboratory work that can be traced to a batch of samples that were processed in chronological order. This organizational scheme preserves the connection with laboratory notebooks and timelines that naturally developed during operation; however, in a few cases, results for a given sample type may be mixed across two or more appendices because of the order in which the individual samples were analyzed.

ESEM analyses were added to the ICET diagnostic suite for the first time during Test #2 as a means of examining hydrated chemical products. This equipment operates as an electron microscope, but it does not require a high-vacuum condition in the sample chamber. Thus, a sample need only be thoroughly drained of free water content before examination rather than fully desiccated, making the ESEM ideal for examinations of biological and environmental specimens. The complementary EDS capability that is often found with equipment of this type is not presently functional at UNM, so duplicate examinations are often performed on the same ICET sample using ESEM to obtain images of hydrated structural details and SEM/EDS to obtain representative elemental compositions. Throughout the report, ESEM analyses are also indicated by the descriptions of “hydrated” and “low-vacuum” findings.

Transcriptions of the logbooks are provided for each appendix to better document commonalities that existed among the samples at the time of analysis. Interpretation and understanding of the images and their accompanying EDS spectra will be greatly improved by frequent reference to the logbook sample descriptions and sequences. Typically, a relatively large quantity of a test sample was delivered for SEM or TEM

analysis, and then several small sub-samples of each item were examined. Note that each sub-sample was assigned a sequential reference number during the laboratory session. These reference numbers have been cited in the figure captions whenever possible to preserve the connection between the micrographs and the notebook descriptions. Electronic file names have also been stamped on the images to permit retrieval of the original data files that are archived elsewhere. Individual data sets for a given sample item have been collated into a typical sequence of (1) visual image, (2) EDS spectra, and (3) semi-quantitative mass composition.

For most of the EDS spectra, semi-quantitative mass compositions are also presented. These results are obtained from a commercial algorithm that decomposes the spectra into the separate contributions of each element. Several caveats should be considered when interpreting the numeric compositions thus obtained; however, despite these caveats, semi-quantitative EDS analysis offers a natural complement to micrographic examination as a survey technique for identifying trends in composition.

1. The spectral deconvolution algorithm is based on a library of unique signatures of each element that were obtained for pure samples using a standard beam setting that may not identically match the conditions applied for the test item.
2. The operator must select a limited number of elements to be used in the proportional mass balance. These candidates are chosen from among the peaks that are observed in the spectrum; however, the composition percentages can vary, depending on which elements are included in the list. In a few cases, two or more alternative compositions have been generated by selecting a different set of elements from the same spectrum to illustrate the sensitivity of this technique to operator input.
3. The spectral unfolding algorithm is a statistical technique having a precision that depends on the relative quality of the data in each peak. Compositions with high R^2 correlation coefficients and total-mass normalization factors closer to unity represent the more-reliable estimates. The precision obtained in the fit depends on the duration of the scan and the number of counts received in each energy bin.
4. All sub-samples examined in the SEM microprobe facility are coated with a thin layer of either carbon or gold/palladium alloy to prevent the sub-samples from accumulating a charge from the impinging electron beam. Spectral peaks visible for gold (Au) and palladium (Pd) are not indigenous to the samples.
5. The EDS spectral analysis software contains a peak-recognition algorithm and an automated cursor that scans across the spectrum to locate each peak. An accompanying library of elemental energy signatures is also provided to suggest what constituents might be contributing to a given energy bin, but the operator must judge what label to assign to the spectral image. It is possible that some peaks near closely neighboring elements have been mislabeled in these images. However, every effort was made to choose from candidate elements that were most likely to be present in the test material. In a few cases, the spectral peaks were not labeled by the SEM operator. These spectra should be viewed as

corroborating evidence for similar samples that are definitively labeled. Careful comparisons of the energy scales in combination with a library of electron-scattering energies can also be used to infer the origin of the more-prominent peaks that are present in unlabeled spectra.

6. Unless an obvious spatial heterogeneity is being examined, the exact location of an EDS spectrum is not always relevant because the operator chooses arbitrary sites that are visually judged to be representative. It is not possible to sample a surface comprehensively on a microscopic basis and compute average compositions. In many cases, two or three replicate spectra are provided for this purpose, but SEM/EDS is most effective as a survey diagnostic.
7. EDS analysis is not particularly sensitive to the presence of boron for several reasons: (a) boron has a low atomic mass that does not interact well with electrons in the beam, (b) the emission lines are very close to those of carbon, and (c) the beam-port material has a high absorption cross section for these emission energies. Therefore, the correction factors used in the semi-quantitative composition analysis are quite large, as are the uncertainties in the estimated percentage of total composition for this element. There may be spectra presented in the appendices in which the lowest energy peaks are labeled as either B (boron) and/or C (carbon).

EDS locations were chosen manually at regions of specific interest. In many cases, multiple spectra were collected from a single sample and an annotated image is provided to identify the specific location. These annotated images are not generally noted in the laboratory logbook entries, but they are provided in proper sequence within the appendices.

Appendix H presents TEM data for water samples extracted from the ICET solution at Day 4, Day 15, and Day 30. The purpose of this examination was to determine whether the physical structure of any suspended products exhibits crystalline or amorphous characteristics. These data are also qualitative in nature, consisting generally of a set of high-resolution micrographs followed by companion electron diffraction images. The TEM sample holder consists of a carbon grid that is “lacey,” or filamentary, in nature. This grid is visible as a relatively large-scale structure in the background of most images. Surface tension in a droplet of liquid suspends the particulates of interest across the grid so that the electron beam can illuminate the sample through the holes without interference from a substrate. Crystalline material will exhibit diffraction patterns unique to the molecular arrangement. Amorphous material that is diffuse or disorganized in structure will not exhibit regular diffraction patterns that can be identified.

Water samples submitted for TEM analysis are not temperature controlled because the temperature cannot be maintained during the examination.

In a few cases, data file names that were noted by the operator in the laboratory log were not successfully saved in electronic form. These cases are noted in the transcribed log sheets, but the corresponding images are unavailable and therefore cannot be presented in the data sequence.

3 TEST RESULTS

This section describes the results obtained from Test #4. An overview is first presented in the form of general observations. This overview is followed by more-detailed information organized by the type of samples/data collected. Data and photographs are provided here for the (1) water samples, (2) insulation [NUKON™ fiberglass samples and cal-sil materials] (3) metallic and concrete samples, (4) sediment, and (5) deposition products.

3.1 General Observations

These observations are taken from the project daily log book. They were meant to capture observations of the test solution and/or test samples during the daily sampling activities.

Four hours after the test began, the solution was very murky and the cal-sil had not completely settled. The color of the tank solution was a yellowish-brown.

On Day 1, there was no observed sedimentation on the coupon racks or insulation holders. Also, the solution was clear with no observed presence of suspended particles. Most of the cal-sil had settled to the bottom of the tank.

On Day 3, a very thin round 2-in. diameter white deposit was observed on the submerged insulation holder on the north side of the tank. Five gallons of RO make-up water were added to the system into the tank outlet pipe, upstream of the recirculation pump. The turbidity before water addition was approximately 1.5 NTU and after the water addition, it was 9.8 NTU.

On Day 4, a collection of white particles was observed on the submerged insulation holder and the mesh birdcage on the north side of the tank.

On Day 8, 5 gallons of RO make-up water were added to the tank through the top using the recycle funnel. The flow remained steady at 25 gpm throughout this process. The water clarity declined slightly after RO water addition and turbidity was 3.0 NTU one hour after the water was added. This is greater than the 0.8 NTU value that was measured just before RO water addition.

On Day 11, a power outage took place. The recirculation pump was stopped for 2 hours and 15 minutes. Also, the maximum solution temperature rose to 62.4°C, which is 0.4°C above the target maximum. The maximum temperature was above 62.0°C for approximately 1 hour.

On Day 13, fiber-like material was observed to be deposited on some of the submerged coupons. Also on that day, 6 gallons of RO make-up water were added to the tank through the recycle funnel at the top of the tank. The flow remained steady throughout this process. The turbidity prior to water addition was 0.6 NTU; 1 hour after RO water addition, the turbidity was 1.6 NTU.

On Day 14, a high-flow sacrificial fiberglass sample was removed from the tank. This caused a disturbance in the tank and the solution became visibly more turbid. The fiberglass fibers that were first observed on Day 13 were no longer present.

On Day 16, small fibers similar to those observed previously were present on some submerged coupons.

On Day 17, 5 gallons of RO make-up water were added to the tank through the top using the recycle funnel. The flow remained steady at 25 gpm throughout this process. The water clarity declined slightly after RO water addition and turbidity was measured to be 0.9 NTU 30 minutes after the water was added.

On Day 22, 5 gallons of RO make-up water were added to the tank through the top of the recycle funnel. The flow remained unchanged during the process. The water clarity declined slightly after RO water addition and turbidity was measured to be 0.7 NTU thirty minutes after the water was added.

On Day 24, one of the three redundant thermocouples in the tank failed. The test solution temperature was subsequently recorded with the two remaining thermocouples.

On Day 27, 5 gallons of RO make-up water were added to the tank through the top using the recycle funnel. The flow remained steady at 25 gpm throughout this process. The water clarity declined slightly after RO water addition and turbidity was measured to be 0.6 NTU 30 minutes after the water was added.

Excluding Day zero, tank clarity and color remained constant throughout the test even with the addition of make-up RO water. The color was similar to weak, iced tea. No corrosion products were observed on the submerged coupons. A total of 31 gallons of make-up water were added to the system, and the system volume at the end of the test was 247 gallons.

3.1.1. Control of Test Parameters

Recirculation flow rate: Neglecting the power outage on Day 11, the average recirculation flow rate was 94.4 L/min (24.9 gpm). The recorded recirculation flow rate had a standard deviation of 0.04 L/min with a range of 93.9 to 95.8 L/min (24.8 to 25.3 gpm) excluding the spray cycle.

Temperature: Temperature is recorded at three submerged locations in the ICET tank. On Day 24, one of the three thermocouples failed. To reset the high temperature alarm, a thermocouple that measures room temperature replaced the bad thermocouple within the data acquisition system (DAS). Neglecting the deactivated thermocouple, the average recorded temperatures at the two locations were 60.8°C and 60.7°C (141.5°F and 141.2°F). The standard deviation in temperature recorded was within $\pm 0.26^\circ\text{C}$ ($\pm 0.46^\circ\text{F}$), with a maximum range of 58.1°C to 62.4°C (136.3 F to 144.4 F). The minimum

temperature occurred during the addition of make-up water. The maximum temperature occurred during the power outage.

pH: Before time zero, 15.14 kg of boric acid, 8.47 kg of sodium hydroxide, 212 ml of 12.24 N hydrochloric acid solution, and 0.663 g of lithium hydroxide were dissolved into the ICET tank solution. The measured bench-top pH was 9.5. During the addition of the sodium hydroxide solution during the first 30 minutes, the pH rose to 9.8 and remained at that value through the spray cycle. The pH declined for the first 2 days to a value of 9.6, which was the predicted value for a solution in complete equilibrium with the atmosphere. After the second day the pH began to rise to a high value of 9.9 on Day 8. The pH varied between 9.7 and 9.9 from Day 9 to the end of the test. This can be seen in Figures 3-1 and 3-2.

The in-line pH probe produced the data in Figure 3-1. At four hours, the in-line pH measurement was 9.9 and at Day 30, it was 9.8. The bench-top pH measurements, which are calibrated daily, are presented in Figure 3-2. At 4 hours, the bench-top pH measurement was 9.8 and at Day 30, it was also 9.8.

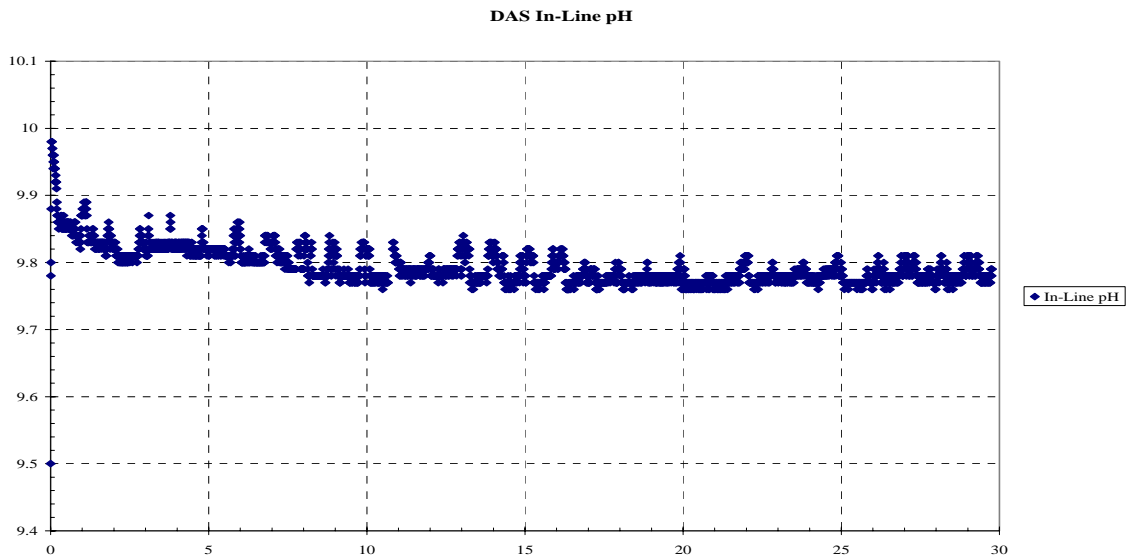


Figure 3-1. In-line pH measurements.

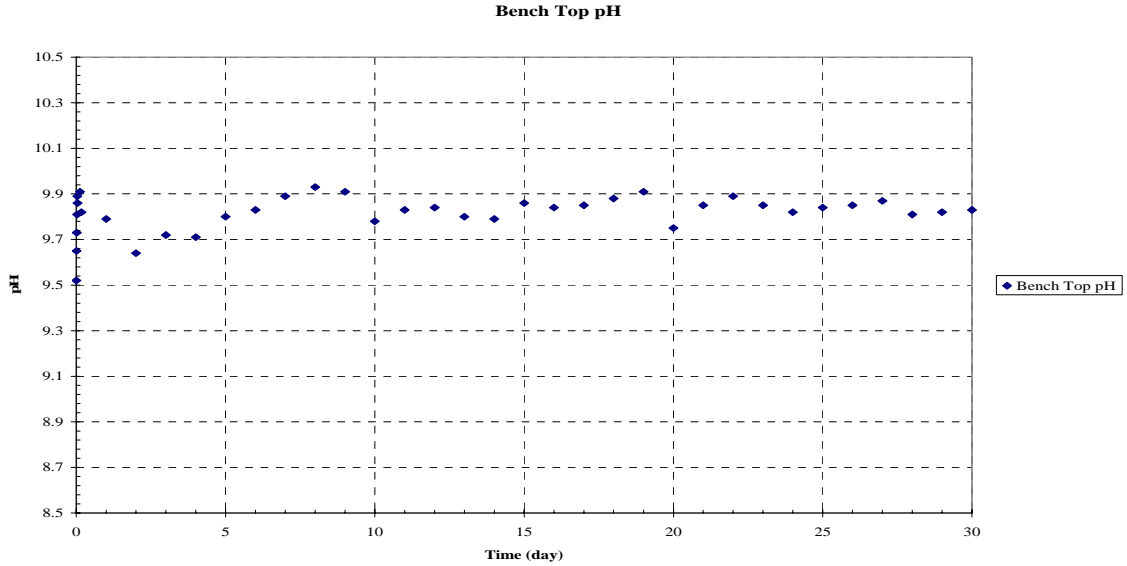


Figure 3-2. Bench-top pH meter results.

3.1.2. Hydrogen Generation

Hydrogen remained at or below 0.05 percent for the duration of the test as shown in Figure 3-3. All of the measured values are well below the hydrogen safety action threshold of 0.4 percent.

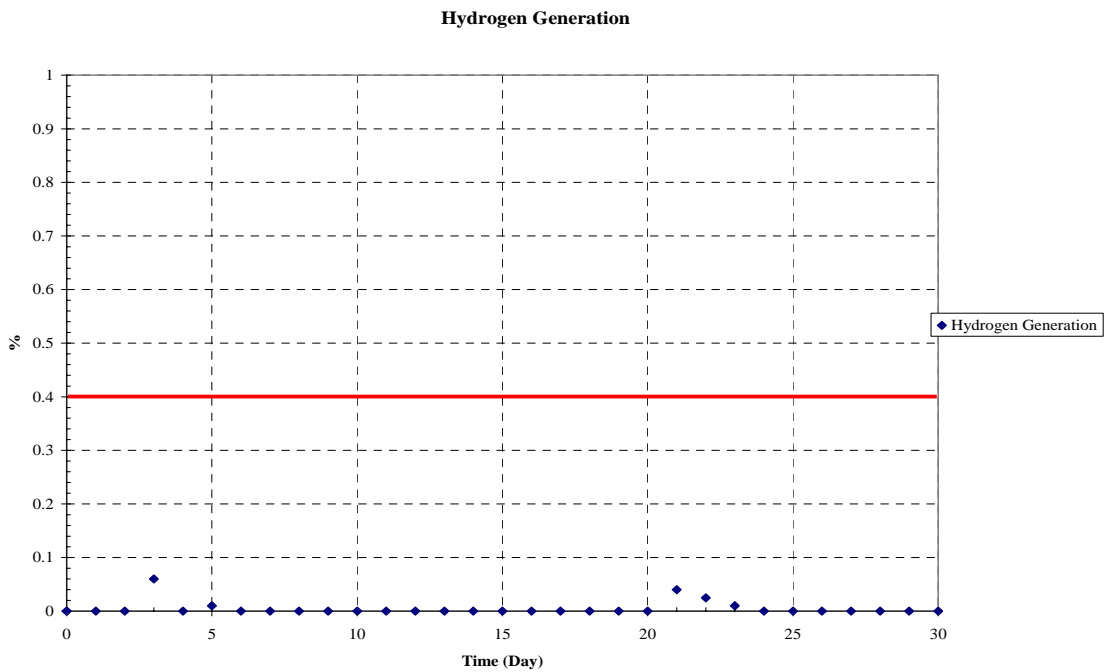


Figure 3-3. Hydrogen generation.

3.2 Water Samples

3.2.1. Wet Chemistry

Wet chemistry analyses included turbidity, TSS, and kinematic viscosity.

Turbidity: The baseline turbidity values, which were taken after the latent debris and concrete dust were added, for the 23°C and 60°C water samples were 1.3 NTU and 0.9 NTU. After the addition of cal-sil, the tank solution became very cloudy. Upon the addition of the chemicals through the spray line, particulates were suspended in solution and the solution became even more cloudier.

Due to the cloudy nature of the water in the tank after the recirculation pump was turned on, turbidity values were measured at 60°C over the initial 4-hour spray phase which were in addition to regular daily monitoring. Figure 3-4 shows the turbidity during this time period. The x-axis on the graph represents the time in hours after the spray nozzles were turned on. As can be seen, the turbidity gradually decreased from 129 NTU at the time-zero point to 36 NTU at the 4-hour point.

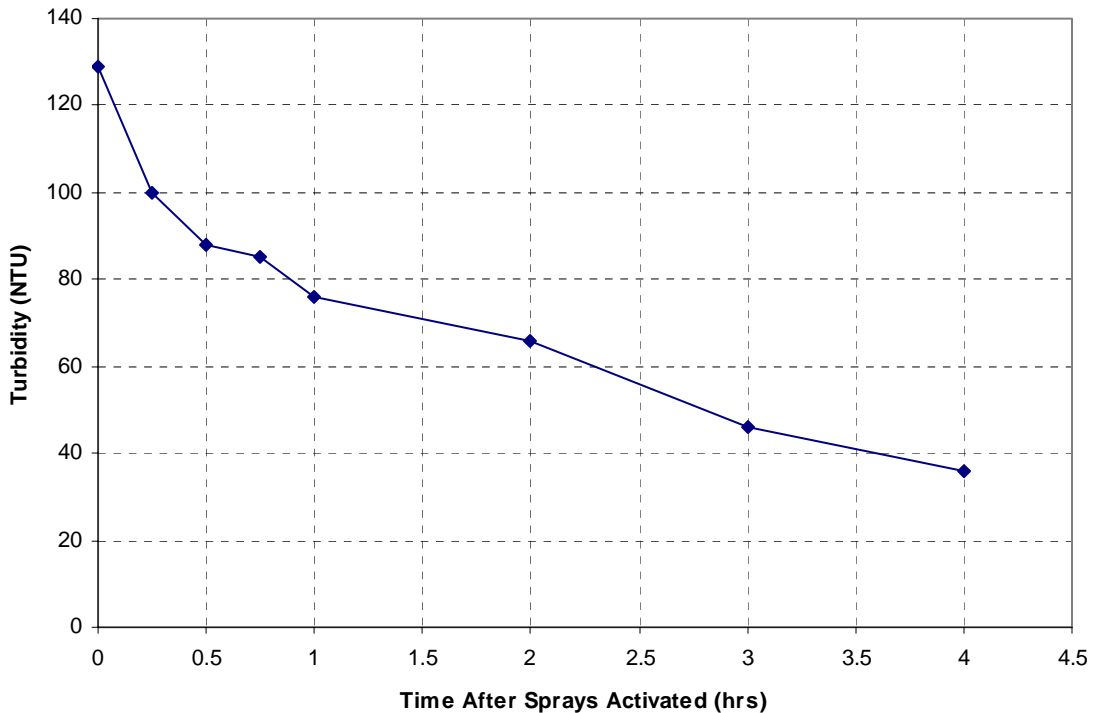


Figure 3-4. Day 1 turbidity results.

Figure 3-5 contains the daily turbidity values at 23°C and 60°C throughout the test. The trend of each curve exhibits an initial spike at the beginning of the spray cycle, followed by a sharp decline during the first four hours of the test. The turbidity results continued to decline and remained low from Day 1 until Day 30. During the last three weeks of

testing, the turbidity values for the 23°C and 60°C samples averaged 0.54 NTU and 0.56 NTU, respectively.

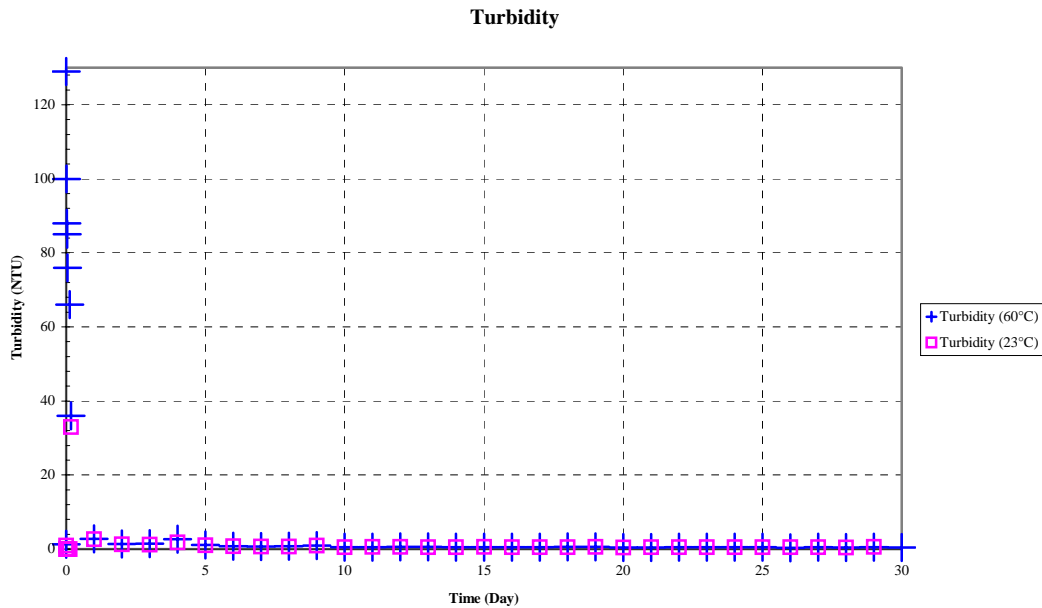


Figure 3-5. Daily turbidity results.

Total Suspended Solids: Total suspended solids (TSS) are measured by running a volume of approximately 500 mL through an in-line filter directly at the sample tap. The selected equipment assures that TSS measurements are not affected by temperature-dependent or time-dependent precipitation reactions that may occur once the process solution is removed from the tank. Figure 3-6 presents Test #4 TSS data as the experiment progressed. The baseline TSS measurement, taken prior to time zero, was 29.4 mg/L. Further TSS measurements were taken throughout the spray cycle. At the start of the spray cycle, the TSS measurement was at its highest value of 128.7 mg/L. At four hours, the TSS measurement had dropped to 68.0 mg/L. Following the spray cycle and beginning at 24 hours, the TSS measurements were performed daily. After 24 hours, TSS measurements varied approximately 16 mg/L over the 30-day test period, from a low of 28.8 mg/L to a high of 44.8 mg/L.

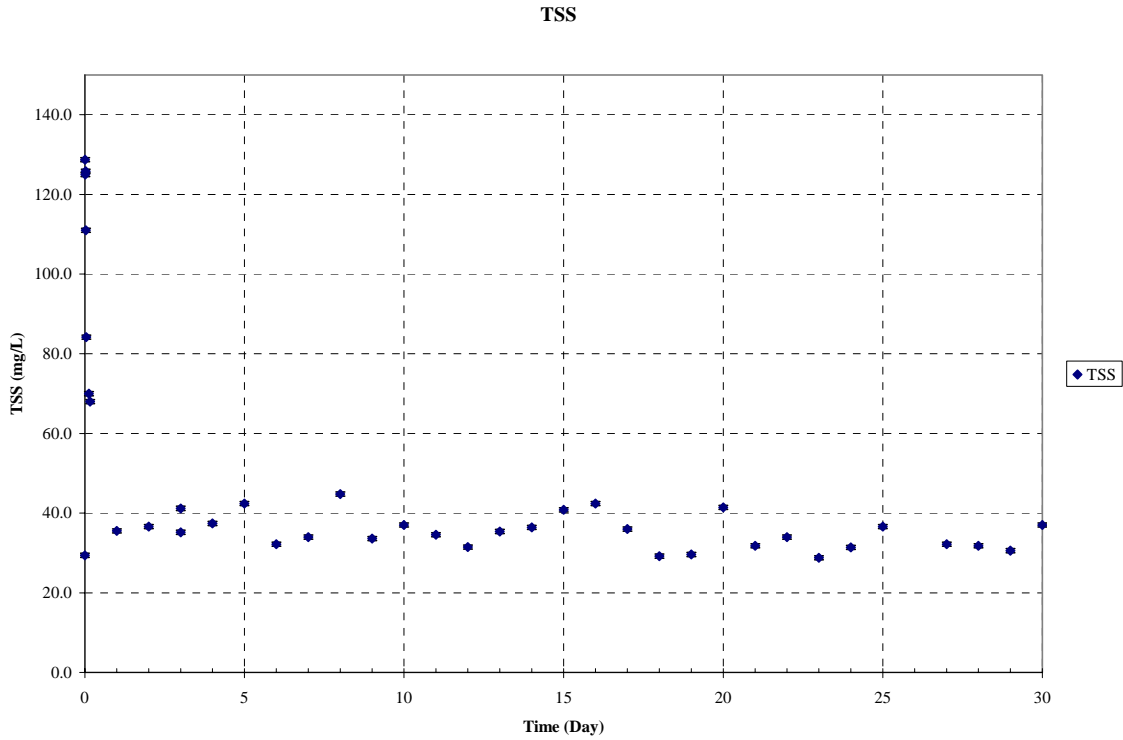


Figure 3-6. Test #4 TSS results.

Kinematic Viscosity: Kinematic viscosity was measured with a Cannon-Fenske capillary viscometer. Viscosity was measured on unfiltered samples, each at a temperature of $60^{\circ}\text{C} \pm 1.0^{\circ}\text{C}$ ($140^{\circ}\text{F} \pm 1.8^{\circ}\text{F}$) and $23^{\circ}\text{C} \pm 2.0^{\circ}\text{C}$ ($73.4^{\circ}\text{F} \pm 3.6^{\circ}\text{F}$). Viscosity of water is highly sensitive to temperature, and the allowed temperature range results in a variation of viscosity of 2.9 percent between 59°C (138.2°F) and 61°C (141.8°F), and a 9.3 percent variation between 21°C (69.8°F) and 25°C (77.0°F). For this reason, temperature was measured to 0.1°C accuracy with a NIST-traceable thermometer for all viscosity measurements, and the measured viscosity values were corrected to a common temperature to facilitate comparisons. The corrected temperatures were 60.0°C (140°F) and 23.0°C (73.4°F). The measured viscosity is shown in Figure 3-7. The values were steady throughout the test.

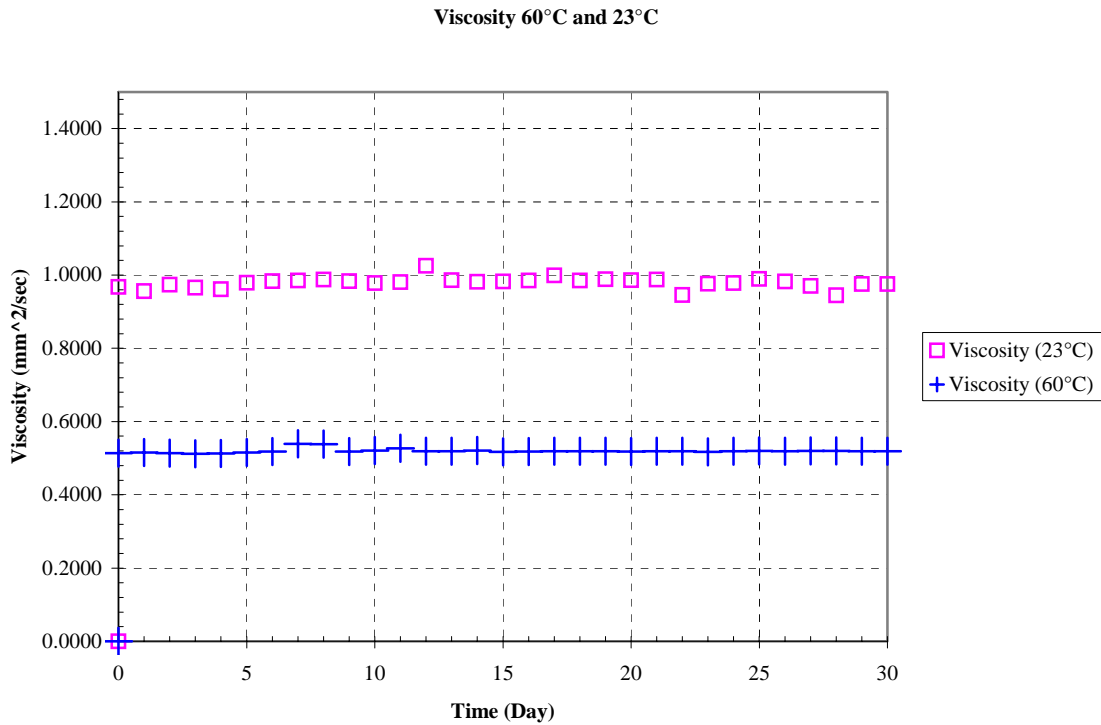


Figure 3-7. Viscosity at 60°C and 23°C.

3.2.2. Metal Ion Concentration

ICP results for Test #4 are displayed in Figures 3-8 through 3-15, which are daily sample results. Table 3-1 contains ICP results for elements that were analyzed on Days 1, 17, and 30. Table 3-1 shows the chloride, boron, lead, lithium, and potassium concentrations. An examination of the figures reveals that aluminum, copper, iron, magnesium, and zinc were present in trace amounts, below 1 mg/L. It also can be seen that calcium, silica, and magnesium are present in higher concentrations.

Table 3-1. ICP Results for Selected Elements

Sample Time	Unfiltered Samples				
	Chloride	Boron	Lead	Lithium	Potassium
	mg/L				
Baseline	83.5	2880	0.02	0.19	7.7
4 Hours	87.7	2830	0.02	0.23	46.9
Day 1	88.9	2880	0.02	0.22	52.0
Day 17	93.3	2860	0.02	0.29	67.1
Day 30	91.0	3390	0.02	0.26	39.9

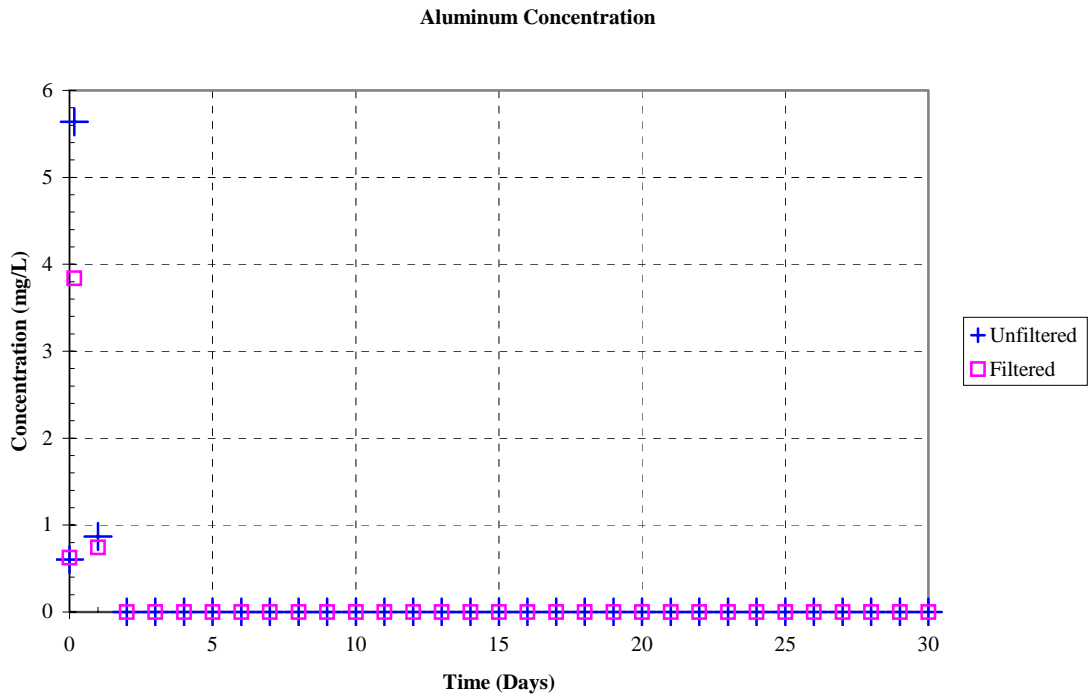


Figure 3-8. Aluminum concentration.

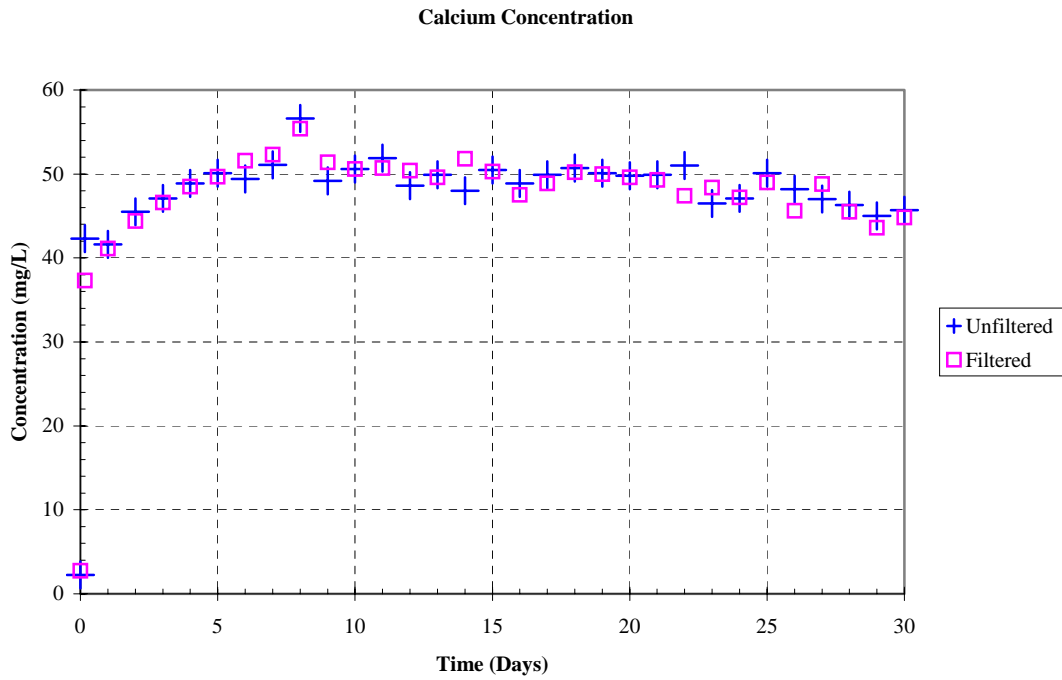


Figure 3-9. Calcium concentration.

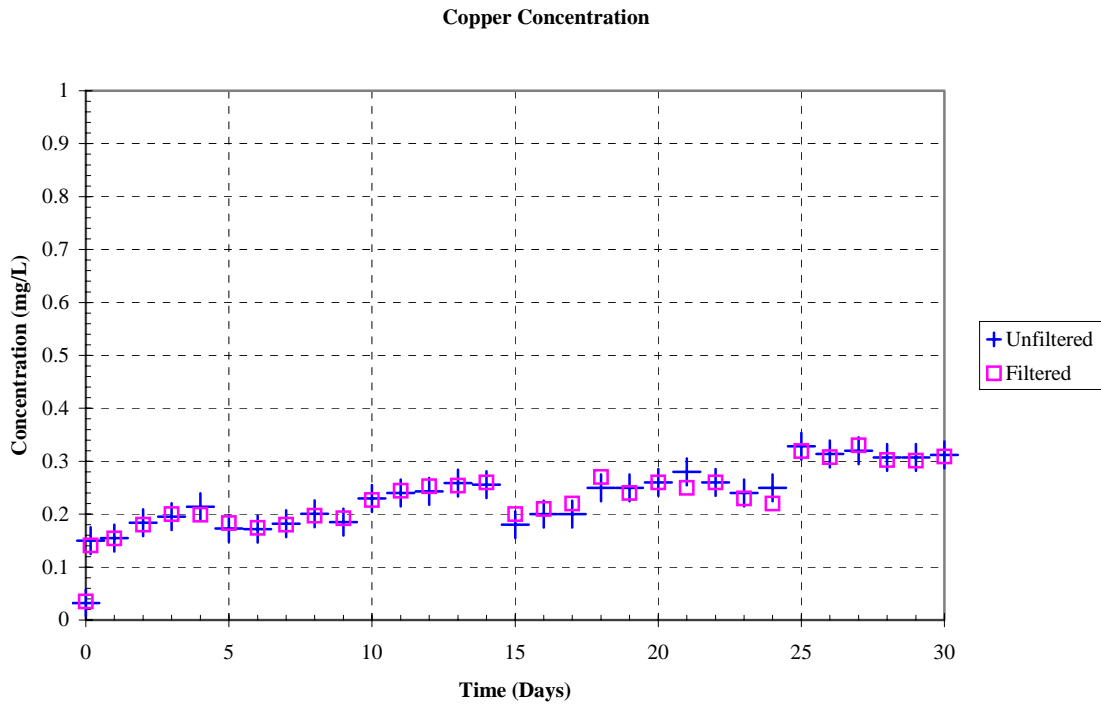


Figure 3-10. Copper concentration.

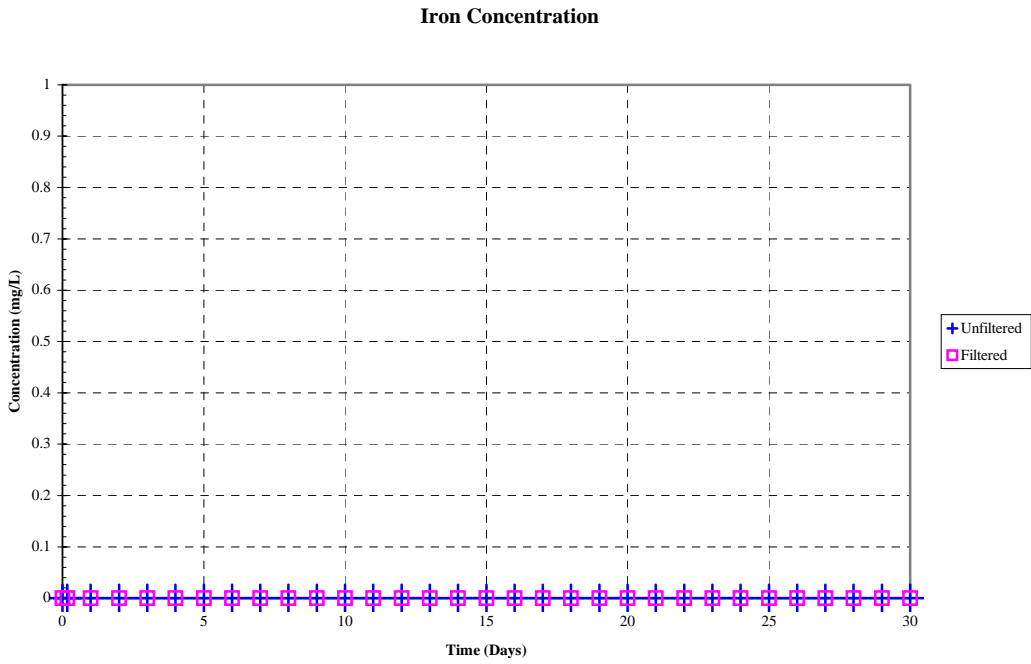


Figure 3-11. Iron concentration.

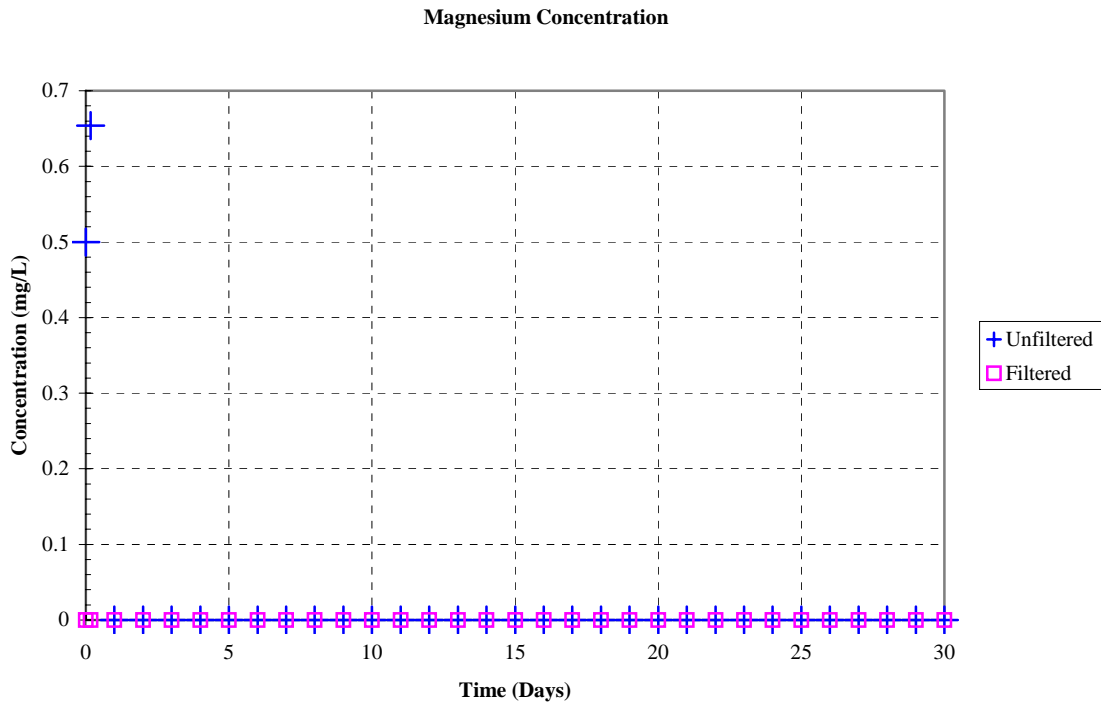


Figure 3-12. Magnesium concentration.

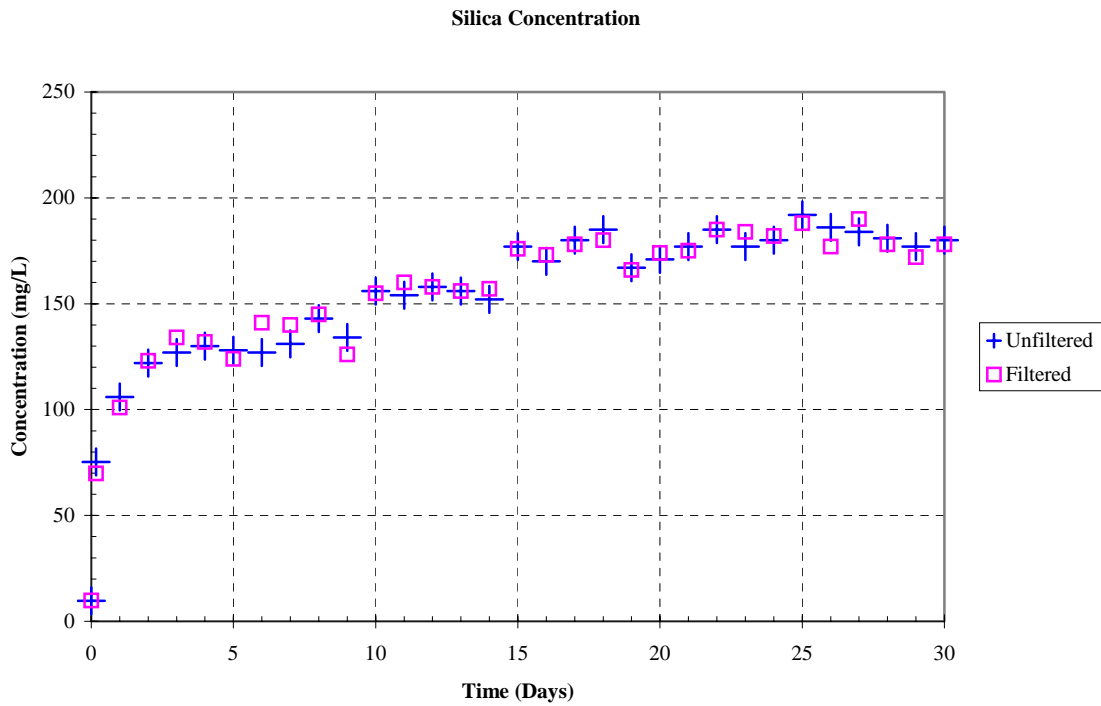


Figure 3-13. Silica concentration.

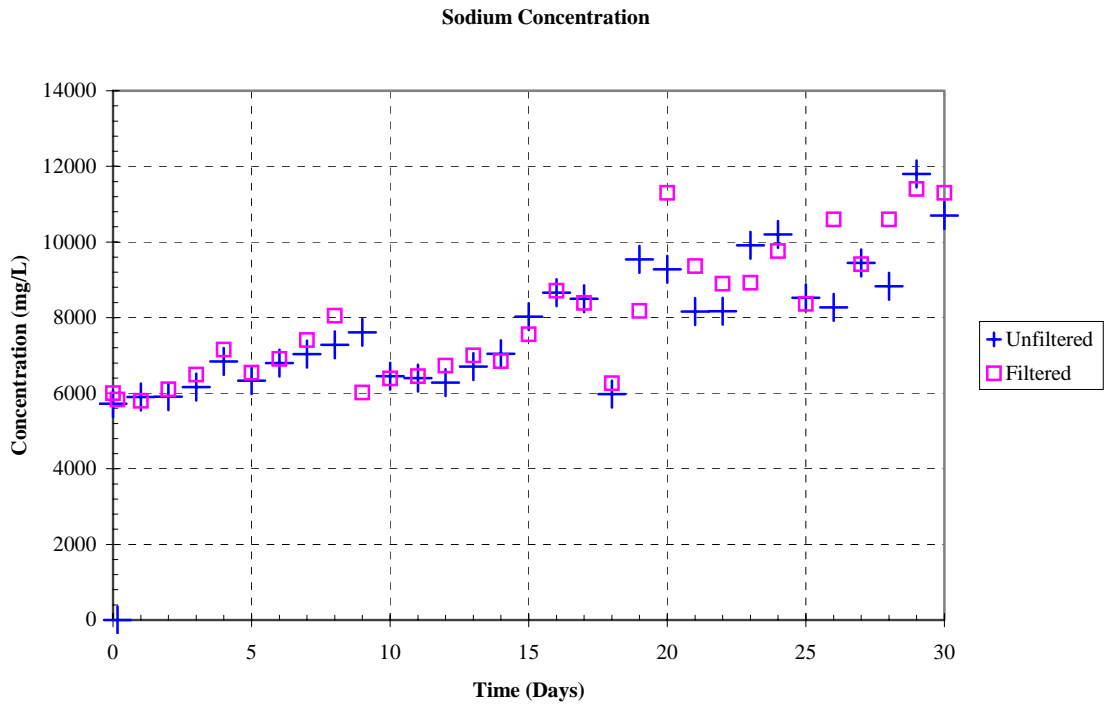


Figure 3-14. Sodium concentration.

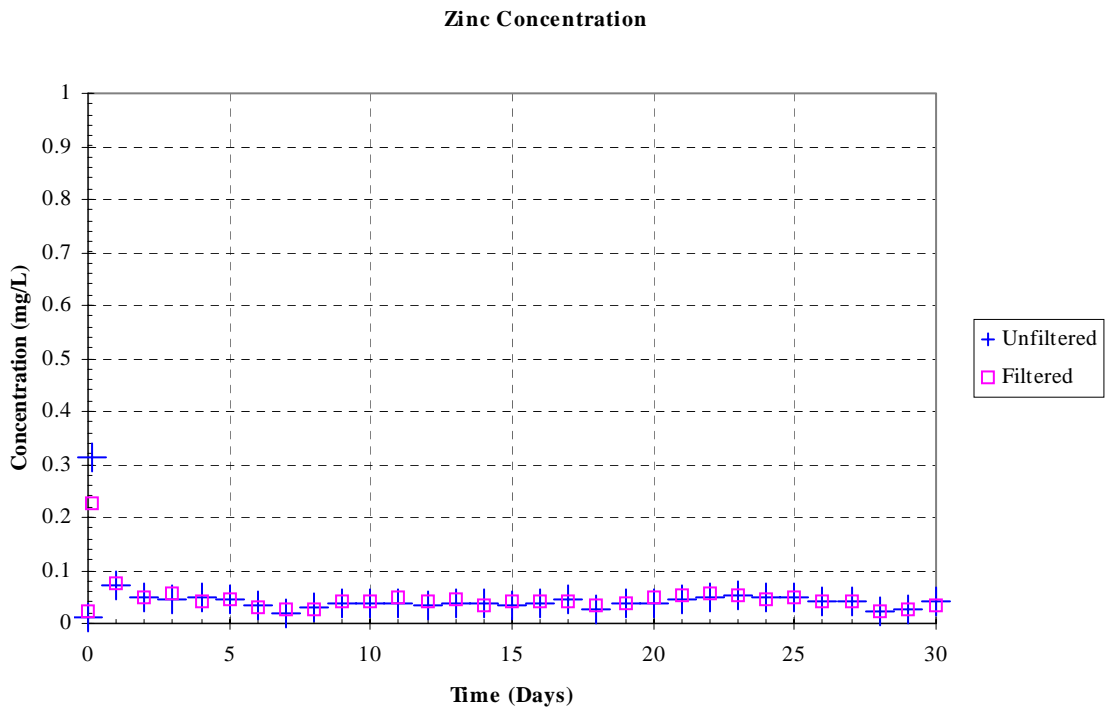


Figure 3-15. Zinc concentration.

3.2.3. Optical/TEM Images from Filtered and Unfiltered Samples

TEM/EDS and diffraction pattern analyses were performed for Test #4 Day 4, Day 15, and Day 30 unfiltered solution samples. The unfiltered solution samples were extracted from the tank directly. The results showed no significant diffraction pattern, due to the amorphous nature of the samples. In addition, no significant presence of colloidal particles was observed. Appendix H contains the TEM data.

3.3 Insulation

Test #4 was the second ICET test that included cal-sil insulation in addition to NUKON™ fiberglass samples. The fiberglass samples received thorough investigations, with samples removed from the tank on Day 5, Day 15, and Day 30. The cal-sil was analyzed based on its Day 30 character. In addition, analyses were performed on the raw cal-sil, both baked and not baked.

3.3.1 Deposits in Fiberglass Samples

The fiberglass samples were contained in SS mesh bags to minimize migration of the fiberglass throughout the tank and piping. Small mesh envelopes, approximately 4 in. square, containing approximately 5 g of fiber, were pulled out of the tank periodically for SEM examination. These sample envelopes were placed in a range of water flow conditions, but none experienced direct water flow through the fiberglass. All were thoroughly immersed in the test solution until they were recovered from the tank.

Fiberglass samples that were examined with SEM after they had been exposed in the test solution for several days exhibited deposits throughout the fiber matrix. Those would be either chemically originated and/or physically retained or attached. Because there was no significant water flow directly through the fiber, the migration of particles into the fiberglass interior is likely insignificant. Therefore, the deposits found in the interior of the fiberglass samples were likely chemically originated, i.e., formed through precipitation. However, particulate deposits may have been physically retained or attached on the fiberglass exterior.

To understand the formation of the film deposits, control experiments were performed by gently rinsing the interior fiberglass samples with several drops of RO water before ESEM analysis. The results show that after being rinsed with RO water, the film deposits disappeared from the fiberglass samples. This fact suggests that the film is actually soluble, which is consistent with the explanation that the film was formed by chemical precipitation during the drying process of fiberglass. In other words, although the ESEM analysis maintains samples in a moister state than conventional SEM, the partial drying that took place during ESEM analysis was sufficient for some chemicals to precipitate and form the film deposits that were observed. Sections 3.3.1.6 and 3.3.1.7 contain results from rinsed fiberglass samples.

There were four fiberglass locations in the tank that were examined in this test, including in a low-flow area, a high-flow area, the birdcage, and the drain collar. (See Subsection 2.4.1.1 for descriptions of the fiberglass samples.) Both the exterior and the interior of the fiberglass samples from each location were examined. Subsections 3.3.1.1 through 3.3.1.10 give the ESEM/SEM/EDS results according to the location of the fiberglass samples in the tank and when the sample was removed from the tank. The different samples include Day 5 low-flow, Day 15 low-flow, Day 15 high-flow, Day 30 low-flow, Day 30 low-flow in nylon mesh, Day 30 low-flow in big envelope, Day 30 high-flow, Day 30 high-flow in front of header, Day 30 drain collar, and Day 30 birdcage. The corresponding figures are Figures 3-16 through 3-85. Additional micrographs of fiberglass samples are presented in Appendices A, B, and C.

In general, particulate deposits were found only on the exterior of the fiberglass. This result suggests that almost all of the particulate deposits were physically retained or attached on the fiberglass exterior. The amount of particulate deposits increases from Day 15 low- and high-flow to the Day 30 high-flow samples. Further increases in particulate deposits were observed in the Day 30 big envelope low-flow sample, with even more on the birdcage sample, and the most on the drain collar sample. EDS shows that these particulate deposits contain significant amount of Si and Ca, suggesting they are from cal-sil debris. In contrast, the interior of fiberglass samples at different locations was relatively clean. Only film deposits were observed. There was no significant trend with respect to the location and the time. The film deposits were primarily composed of O, Na, Ca, C, Mg, Al, and possibly Si. These deposits are likely formed by chemical precipitation during the dehydration process of the samples. Control experiments were performed by gently rinsing the fiberglass interior samples with RO water, followed by ESEM analysis. The film deposits disappeared after this preparation technique. These results suggest that the film is soluble, which is consistent with the explanation that the film was formed by chemical precipitation.

Results also show that the mesh material, i.e., stainless steel or nylon did not significantly affect the deposits on fiberglass. In addition, the Day 30 high-flow fiberglass (in front of the header and placed in the tank on Day 2) sample exterior had much less particulate deposits attached/retained than the other high-flow sample exterior that was placed in the tank on Day 0. That was due to the settling of suspended particles in the test solution during the first two days.

3.3.1.1 Day 4 Low-Flow Fiberglass Samples

Since there was no significant water flowing through the fiberglass samples during the test, the migration of particulate deposits from the solution into the fiberglass interior is insignificant. Based on the ESEM results, some deposits were found after 5 days of the test on both the exterior and the interior of the low-flow fiberglass samples. In these deposits, a few particulates were found on the fiberglass exterior only (see Figure 3-17). However, most of the deposits were formed continuously like a film among glass fibers and coatings on the fibers. Therefore, these deposits are likely of chemical origin instead of being physically attached/retained. EDS results indicated that the film was composed of C, O, Na, Ca, Mg, Al, and possibly Si. Comparing the amount of the film on the

fiberglass revealed no significant difference between the interior and exterior samples. Again, this fact may be explained by the likely chemical origin of the deposits, since chemical precipitation would occur to a similar degree on both the exterior and the interior fiberglass samples if the concentrations were similar. Figures 3-16 through 3-24 show the Day 4 low-flow fiberglass results.

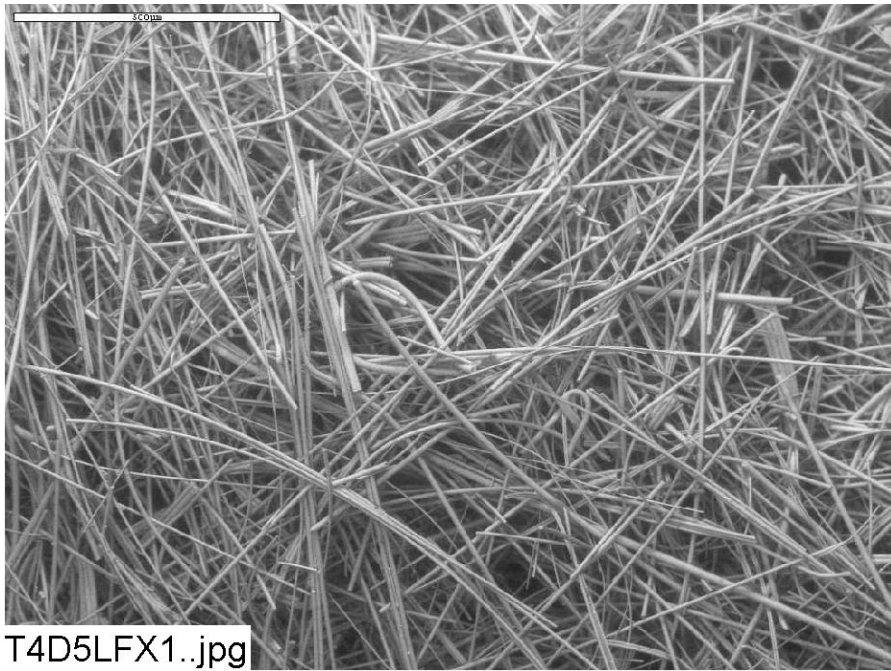


Figure 3-16. Environmental SEM image magnified 80 times for a Test #4 Day 5 low-flow exterior fiberglass sample. (T4D5LFX1.jpg)

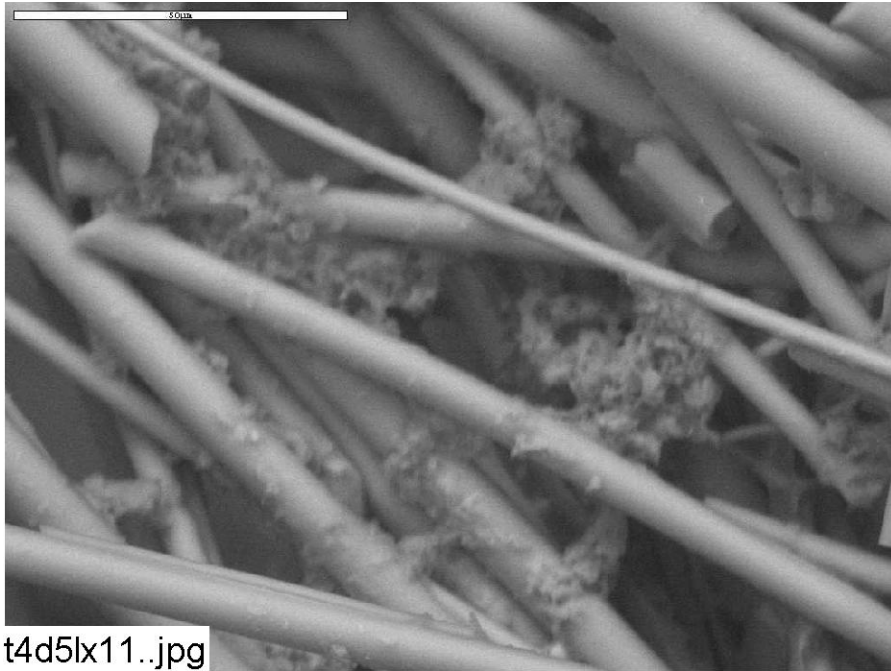


Figure 3-17. Environmental SEM image magnified 1000 times for a Test #4 Day 5 low-flow exterior fiberglass sample. (t4d5lx11.jpg)

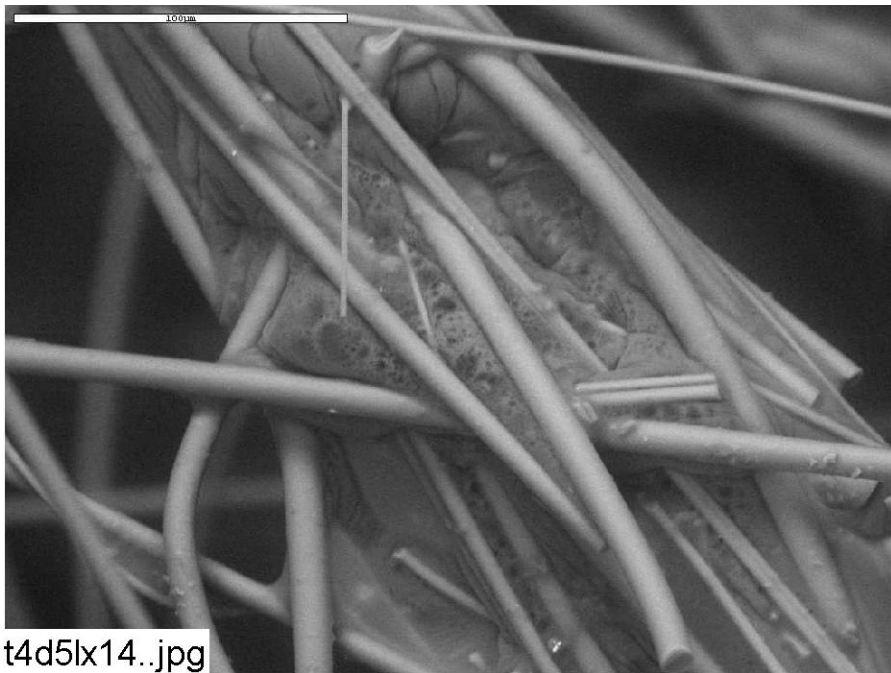


Figure 3-18. Environmental SEM image magnified 500 times for a Test #4 Day 5 low-flow exterior fiberglass sample. (t4d5lx14.jpg)

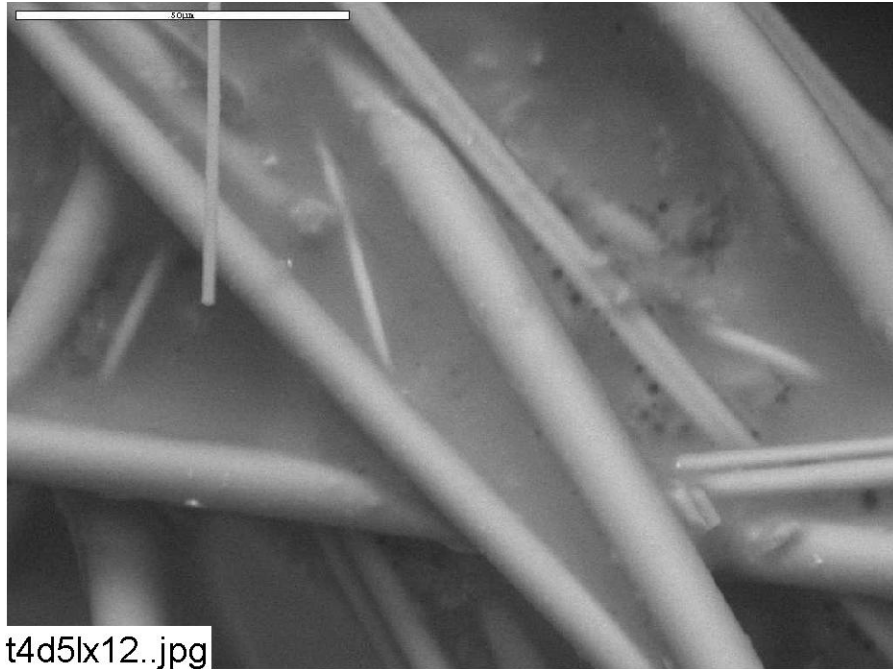


Figure 3-19. Environmental SEM image magnified 1000 times for a Test #4 Day 5 low-flow exterior fiberglass sample. (t4d5lx12.jpg)

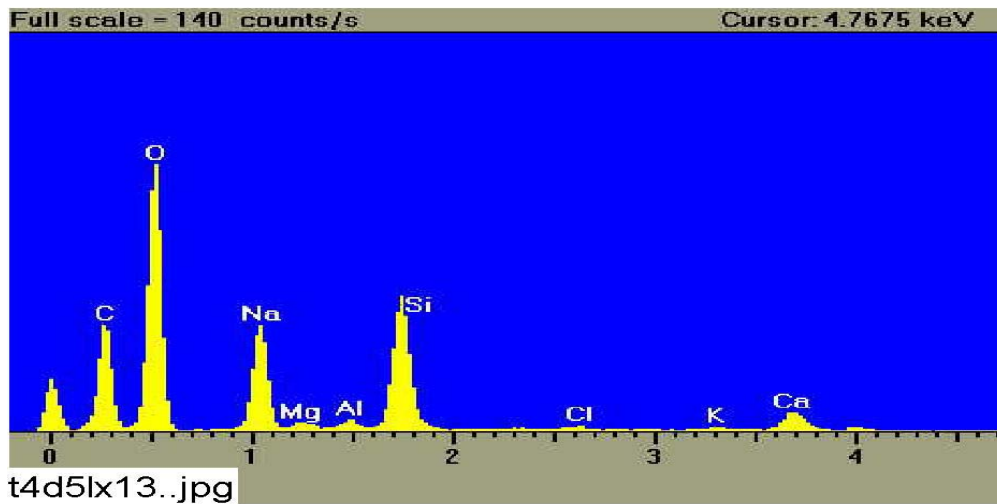


Figure 3-20. EDS counting spectrum for the film between the fibers shown in Figure 3-19. (t4d5lx13.jpg)

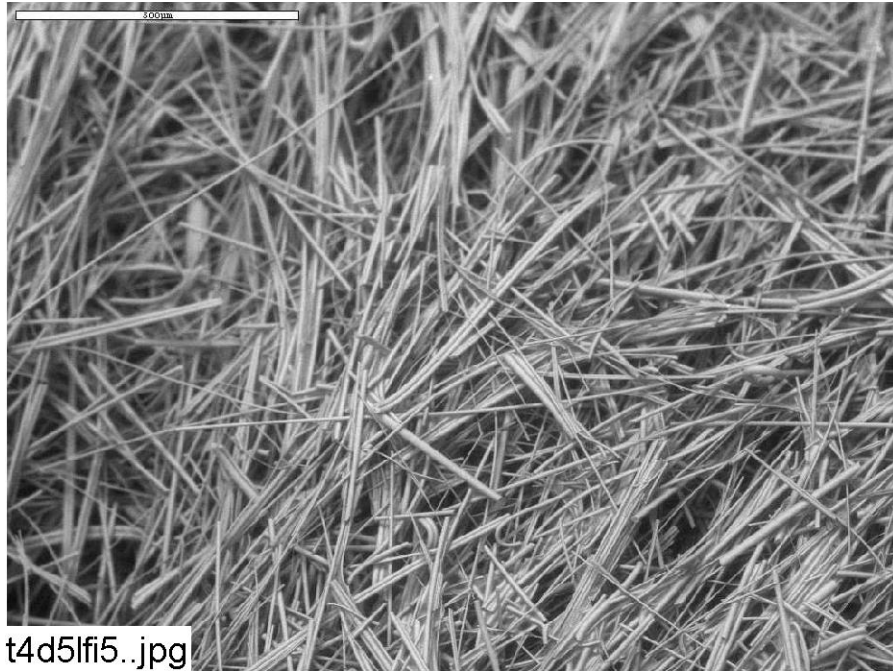


Figure 3-21. Environmental SEM image magnified 80 times for a Test #4 Day 5 low-flow interior fiberglass sample. (t4d5lf15.jpg)

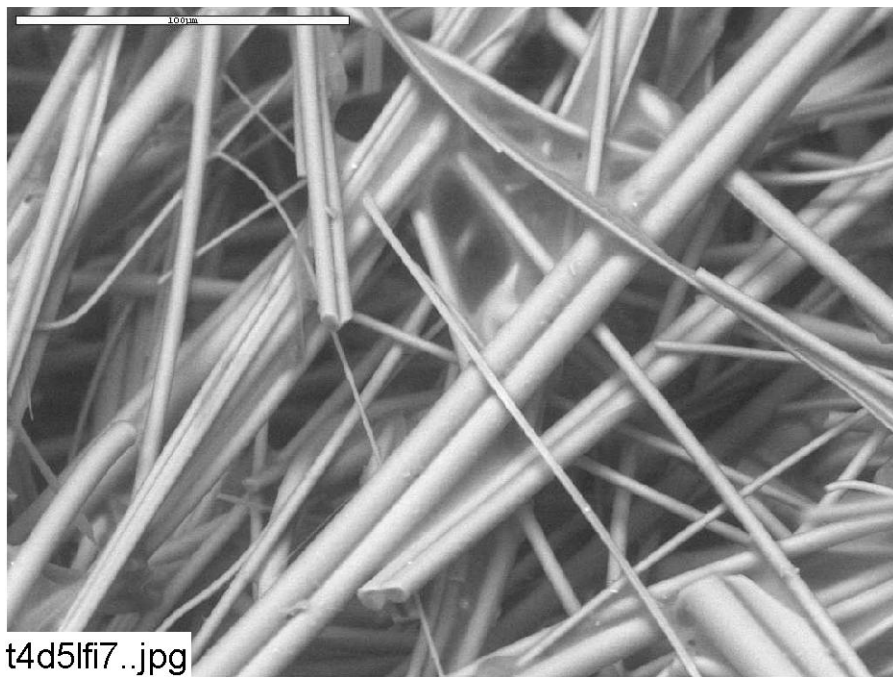


Figure 3-22. Environmental SEM image magnified 500 times for a Test #4 Day 5 low-flow interior fiberglass sample. (t4d5lf17.jpg)

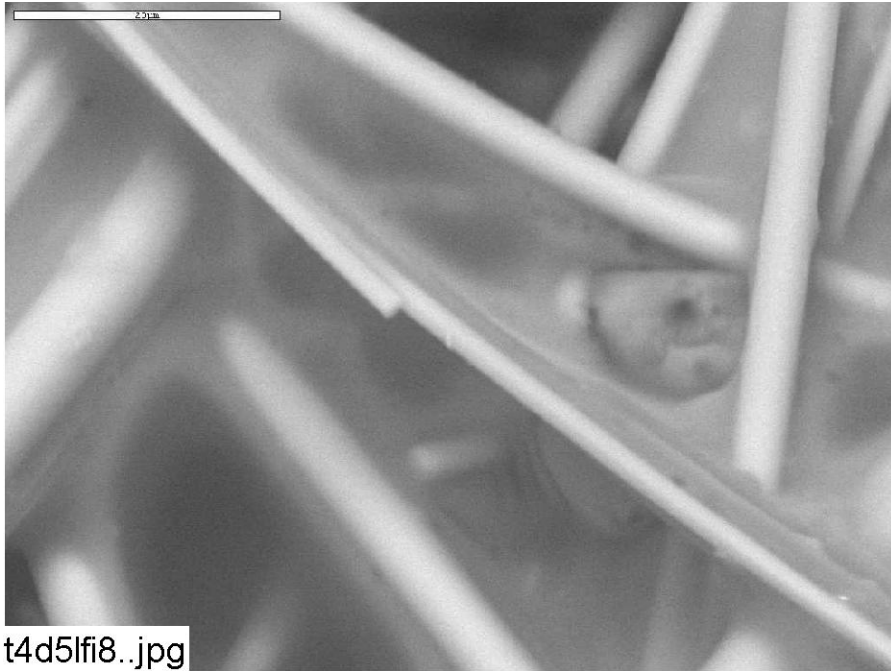


Figure 3-23. Environmental SEM image magnified 2000 times for a Test #4 Day 5 low-flow interior fiberglass sample. (t4d5lf18.jpg)

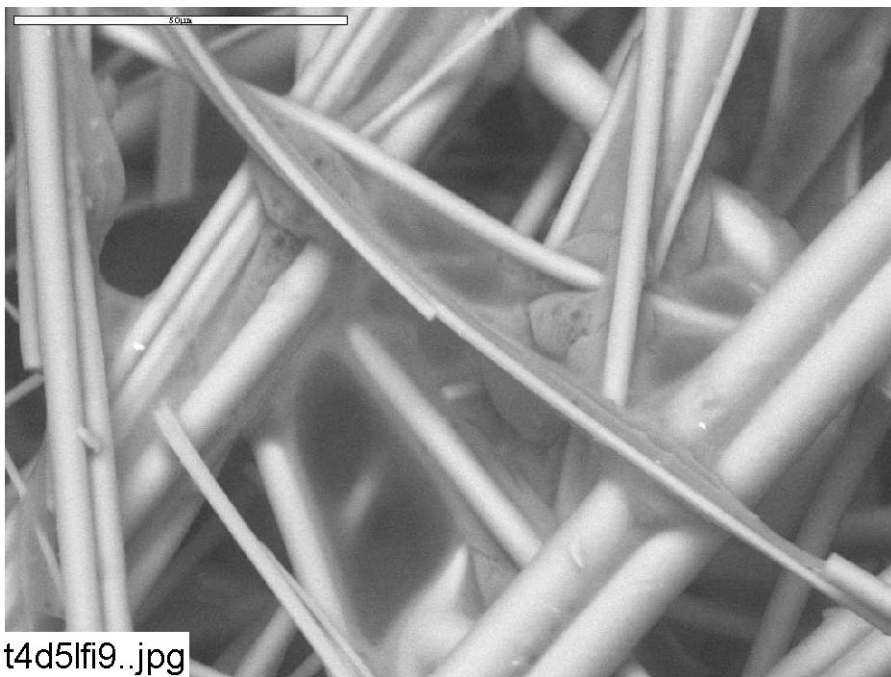


Figure 3-24. Environmental SEM image magnified 1000 times for a Test #4 Day 5 low-flow interior fiberglass sample. (t4d5lf19.jpg)

3.3.1.2 Day 15 Low-Flow Fiberglass Samples

Similar to the Day 5 samples, a few particulate deposits were found on the fiberglass exterior. EDS analysis shows that the particulate deposits were mainly composed of O, Na, Ca, Al, Mg, B, C, K, and possibly Si. However, the film deposits were prevalent on both the exterior and the interior fiberglass samples. There was no significant increase in the amount of deposits on Day 15 samples compared to Day 5 samples. Comparing the amount of the film deposits on the exterior and the interior Day 15 low-flow fiberglass samples, the difference was insignificant. Figures 3-25 through 3-30 show the Day 15 low-flow fiberglass results.

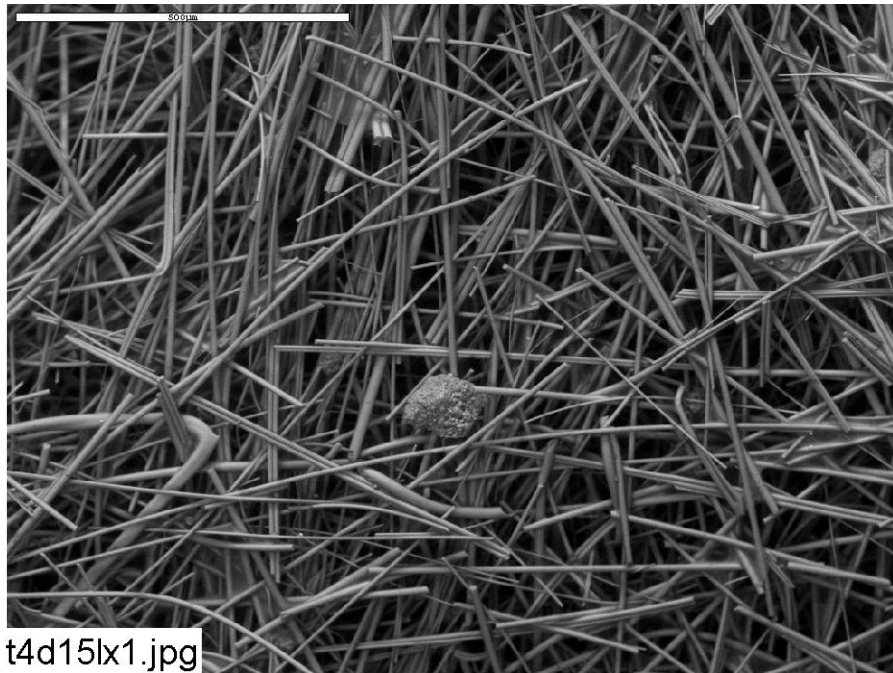


Figure 3-25. Environmental SEM image magnified 100 times for a Test #4 Day 15 exterior low-flow fiberglass sample. (t4d15lx1.jpg)

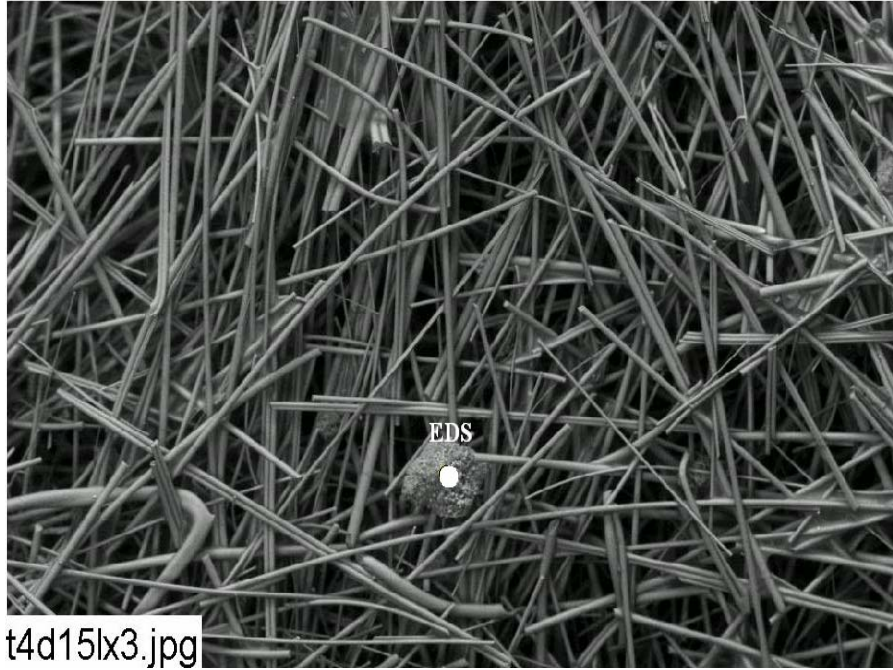


Figure 3-26. Annotated environmental SEM image magnified 100 times for a Test #4 Day 15 exterior low-flow fiberglass sample. (t4d15lx3.jpg)

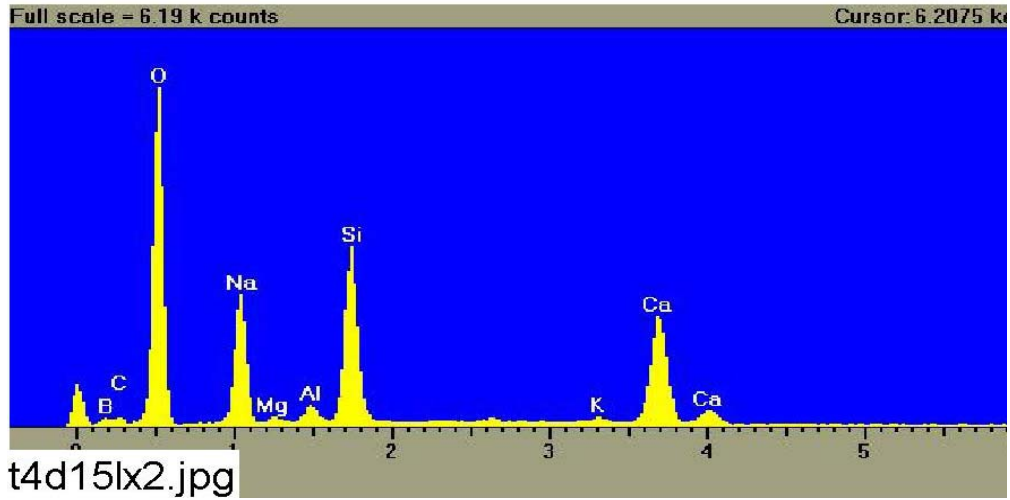


Figure 3-27. EDS counting spectrum for the particulate deposit on fiberglass shown in Figure 3-26. (t4d15lx2.jpg)

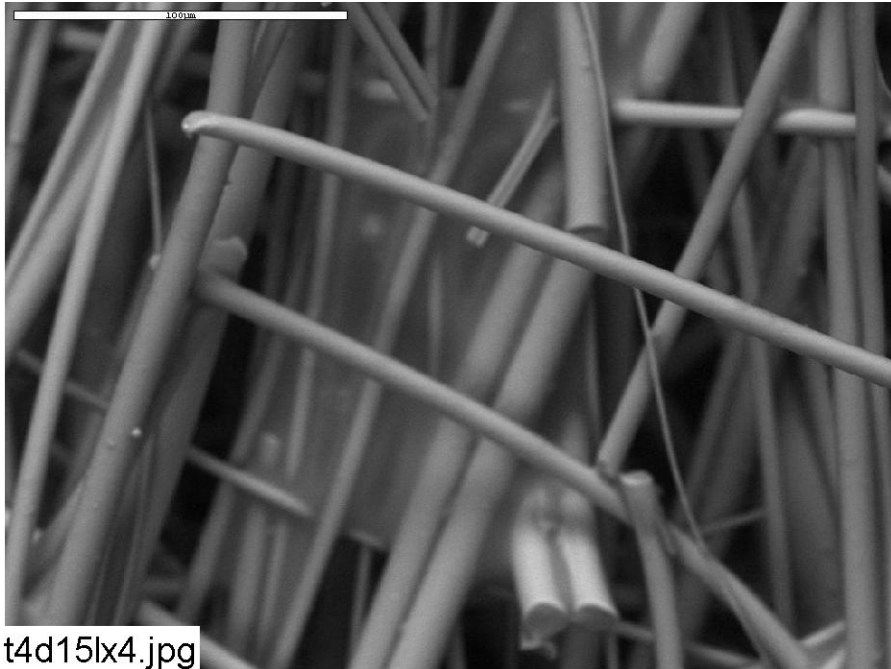


Figure 3-28. Environmental SEM image magnified 500 times for a Test #4 Day 15 exterior low-flow fiberglass sample. (t4d15lx4.jpg)

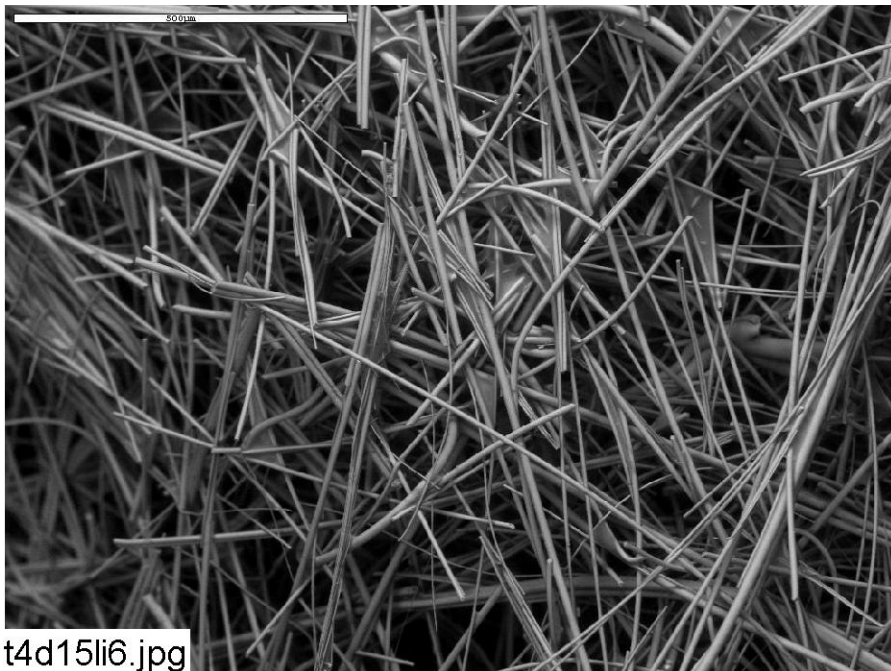


Figure 3-29. Environmental SEM image magnified 100 times for a Test #4 Day 15 interior low-flow fiberglass sample. (t4d15li6.jpg)

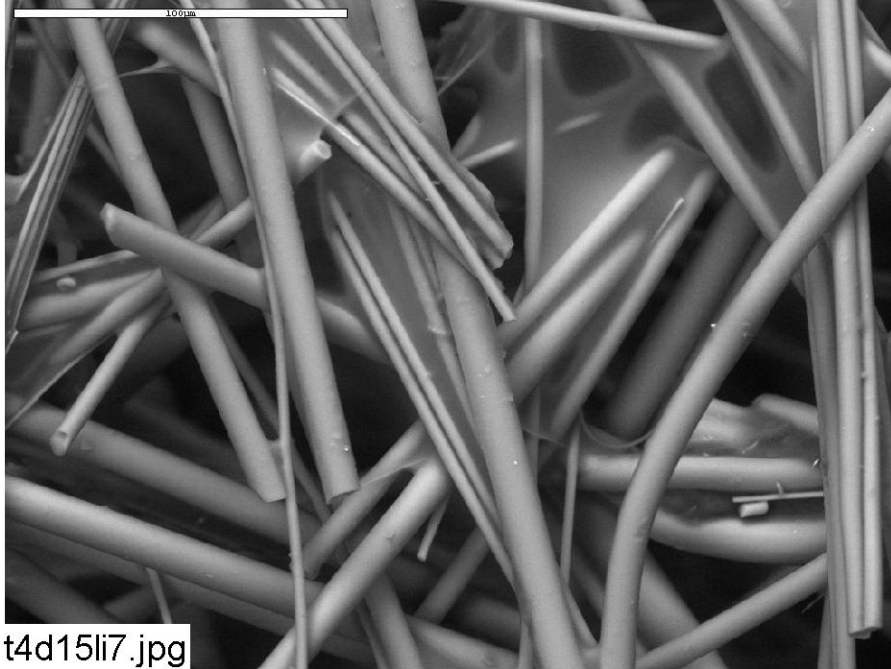


Figure 3-30. Environmental SEM image magnified 500 times for a Test #4 Day 15 interior low-flow fiberglass sample. (t4d15li7.jpg)

3.3.1.3 Day 15 High-Flow Fiberglass Samples

No significant difference was found between Day 15 high-flow and low-flow fiberglass samples. The film deposits were prevalent on both the exterior and interior fiberglass samples. Consistently, EDS analysis indicates that the film was composed of O, Na, Ca, C, Mg, Al, K, and possibly Si. There was no significant difference regarding the amount of the film deposits between the exterior and the interior fiberglass samples, suggesting the likely chemical origin of the film. In addition, no particulate deposits were observed on either the exterior or interior fiberglass samples. Figures 3-31 through 3-36 show the Day 15 high-flow fiberglass results.

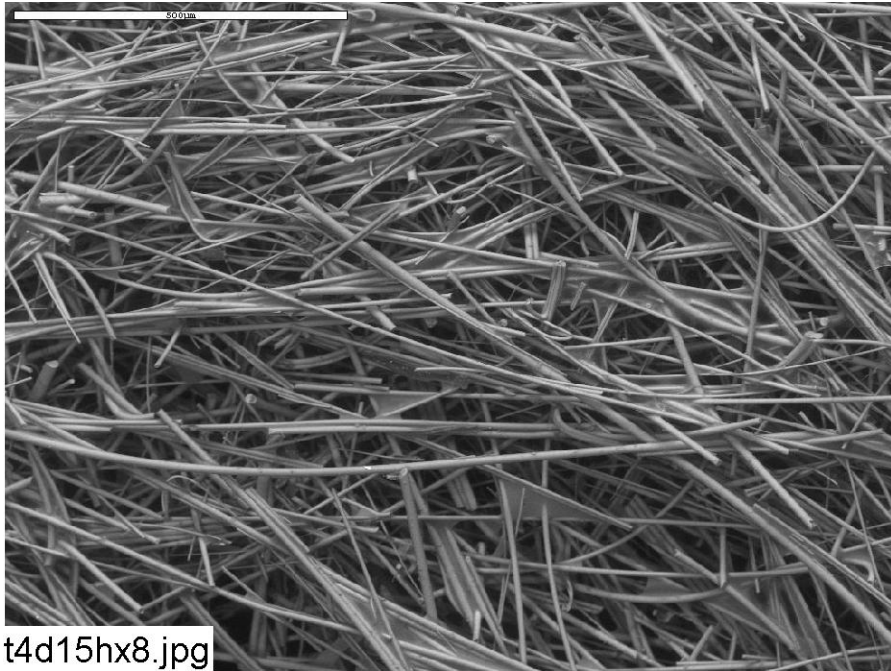


Figure 3-31. Environmental SEM image magnified 100 times for a Test #4 Day 15 exterior high-flow fiberglass sample. (t4d15hx8.jpg)

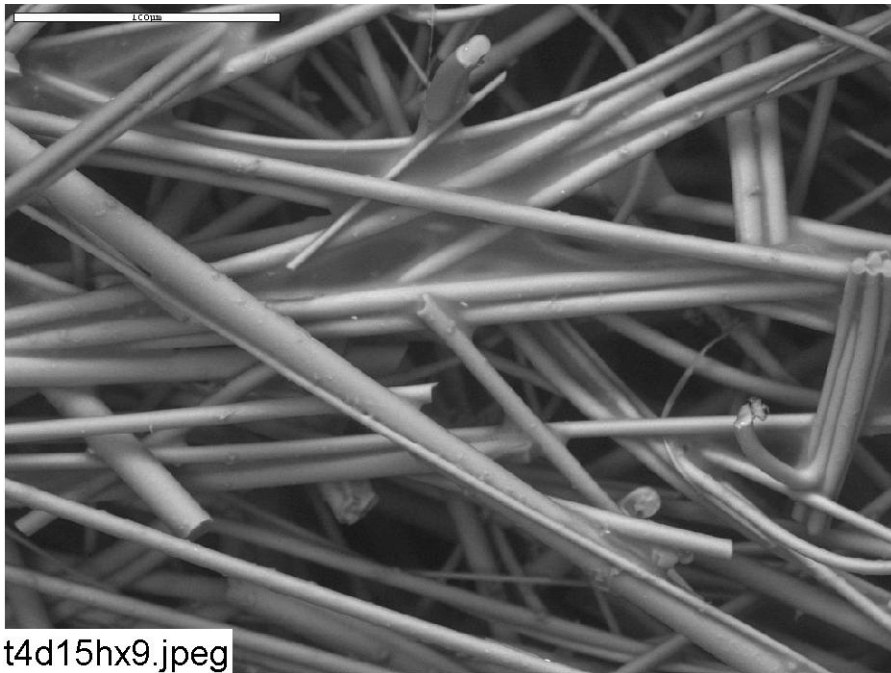


Figure 3-32. Environmental SEM image magnified 400 times for a Test #4 Day 15 exterior high-flow fiberglass sample. (t4d15hx9.jpeg)

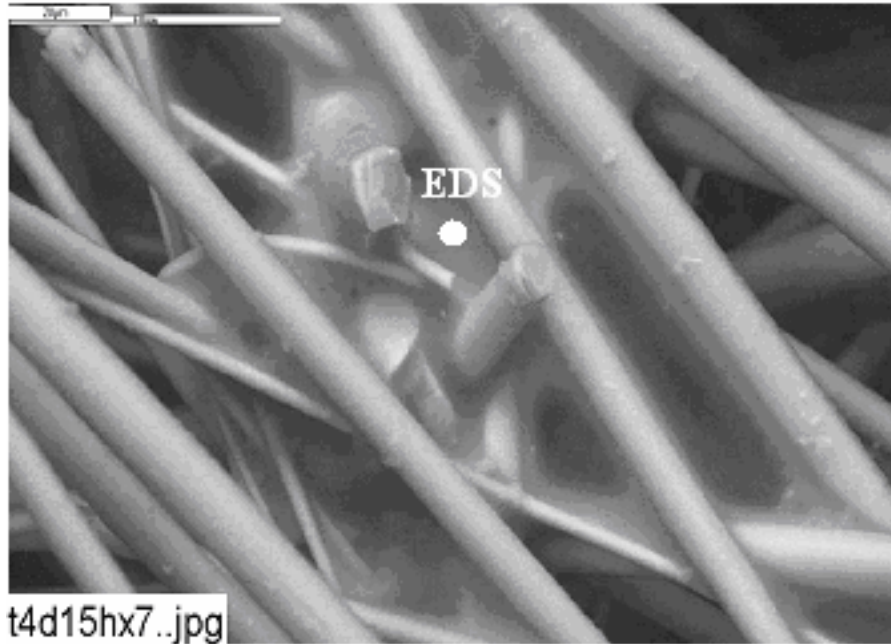


Figure 3-33. Environmental SEM image magnified 750 times for a Test #4 Day 15 exterior high-flow fiberglass sample. (t4d15hx7.jpg)

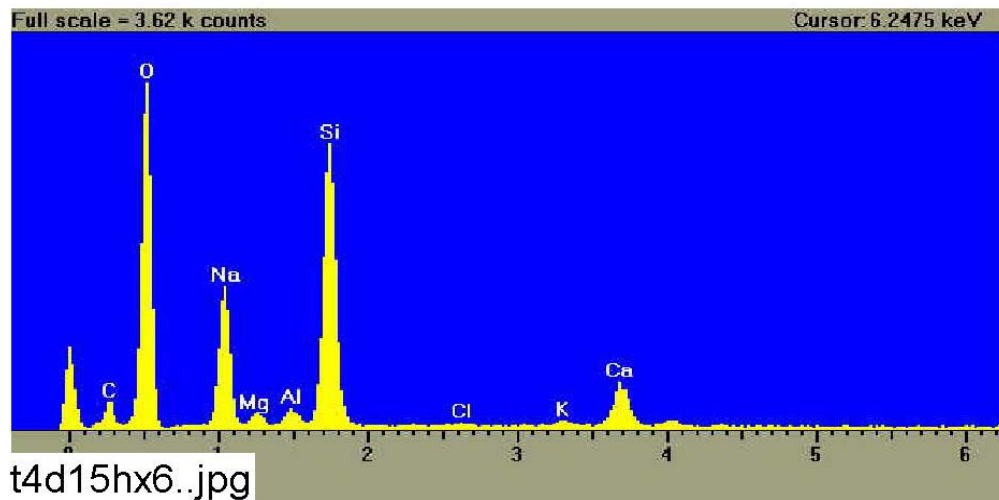


Figure 3-34. EDS counting spectrum for the spot on the film between the fibers shown in Figure 3-33. (t4d15hx6.jpg)

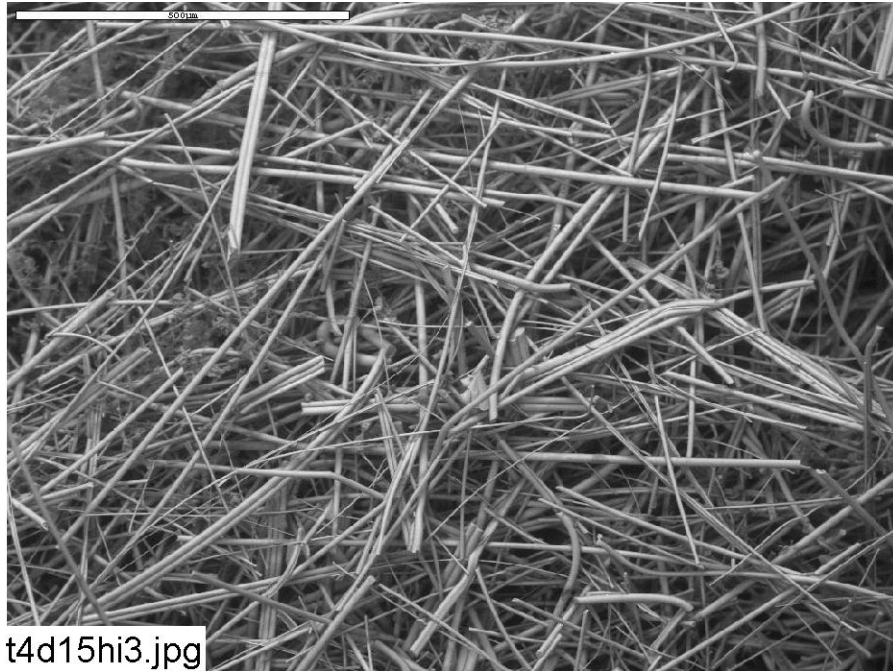


Figure 3-35. Environmental SEM image magnified 100 times for a Test #4 Day 15 interior high-flow fiberglass sample. (t4d15hi3.jpg)

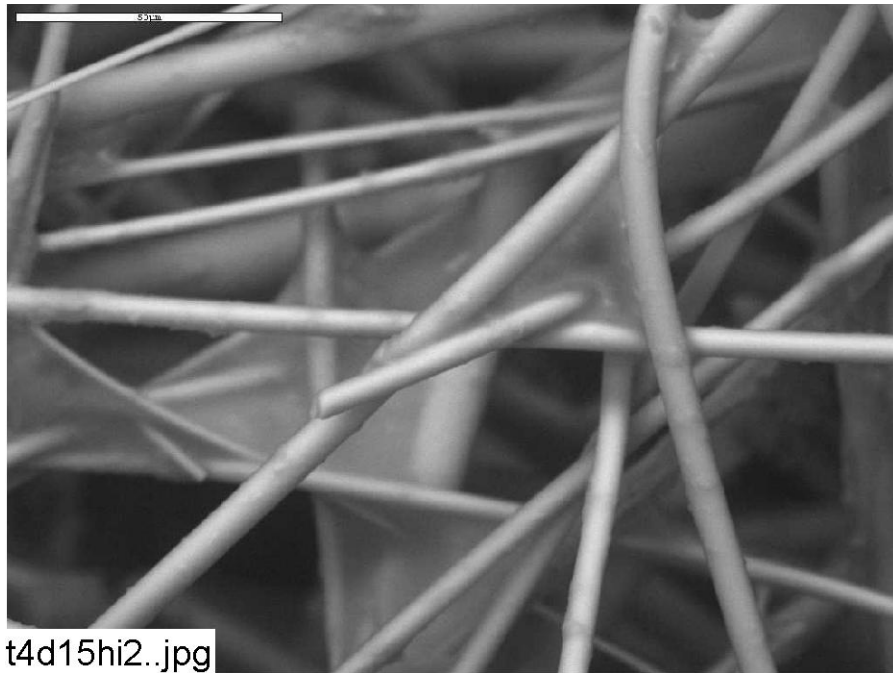


Figure 3-36. Environmental SEM image magnified 800 times for a Test #4 Day 15 interior high-flow fiberglass sample. (t4d15hi2.jpg)

3.3.1.4 Day 30 Low-Flow Fiberglass Samples

A similar amount and composition of the film deposits were found with Day 30 low-flow fiberglass samples compared to Day 5 and Day 15 low-flow fiberglass samples. No significant difference was found regarding the amount of the film deposits between the exterior and the interior Day 30 low-flow fiberglass samples. As with the Day 5 and 15 samples, the film was composed of O, Na, Ca, Mg, Al, C, K, and possibly Si. Besides the film, a coating was found on the glass fibers (see Figure 3-39). The coating was likely formed by chemical precipitation. EDS analysis shows the coating had the same composition as the film, suggesting both are likely of chemical origin. Figures 3-37 through 3-43 show the Day 30 low-flow fiberglass results.

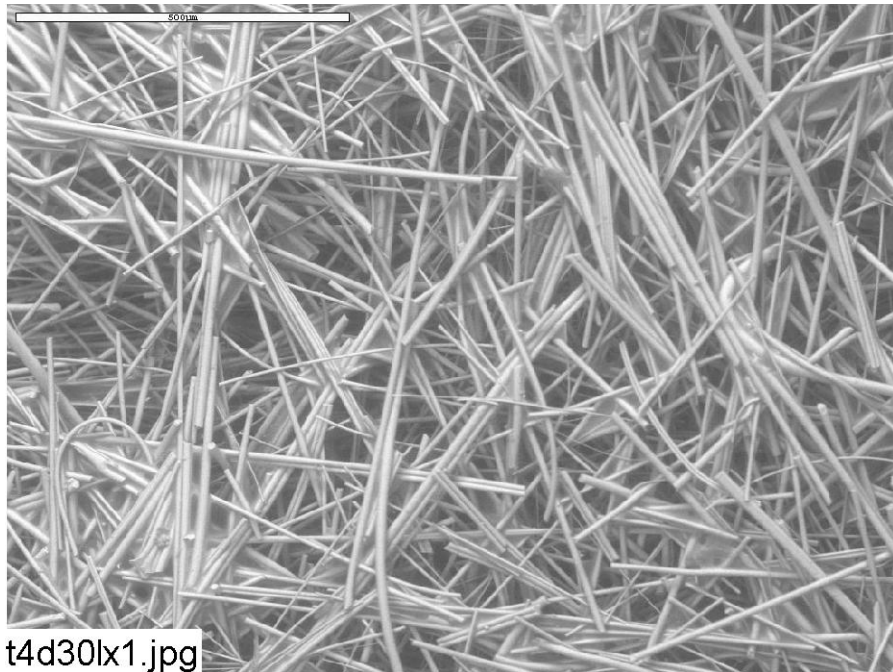


Figure 3-37. Environmental SEM image magnified 100 times for a Test #4 Day 30 exterior low-flow fiberglass sample. (t4d30lx1.jpg)

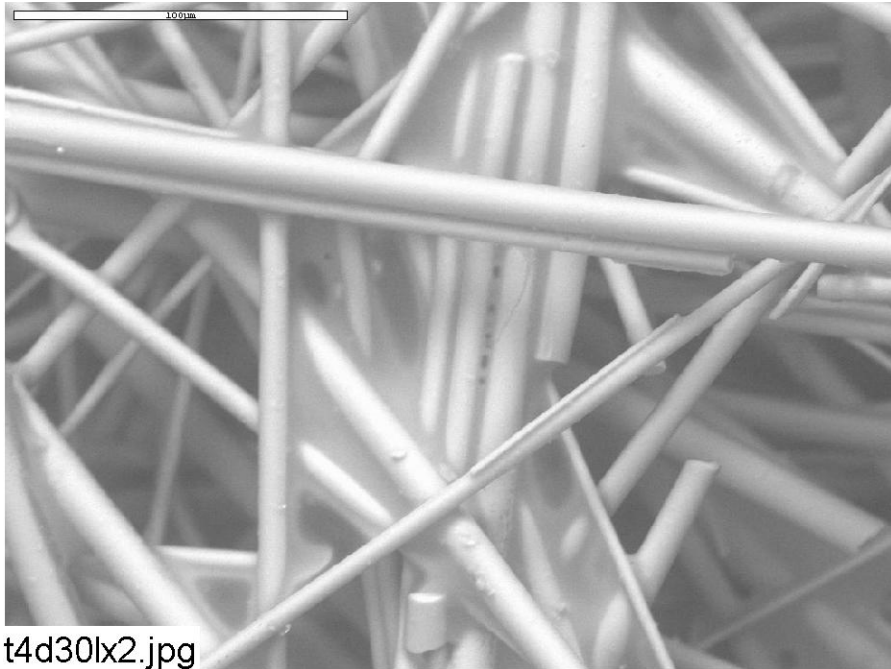


Figure 3-38. Environmental SEM image magnified 500 times for a Test #4 Day 30 exterior low-flow fiberglass sample. (t4d30lx2.jpg)

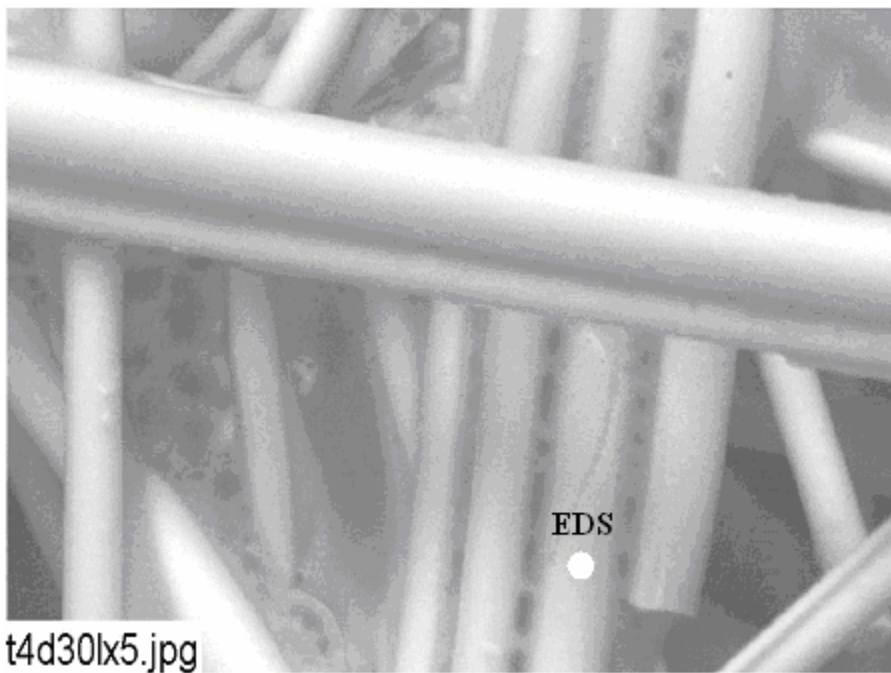


Figure 3-39. Environmental SEM image magnified 1000 times for a Test #4 Day 30 low-flow fiberglass sample. (t4d30lx5.jpg)

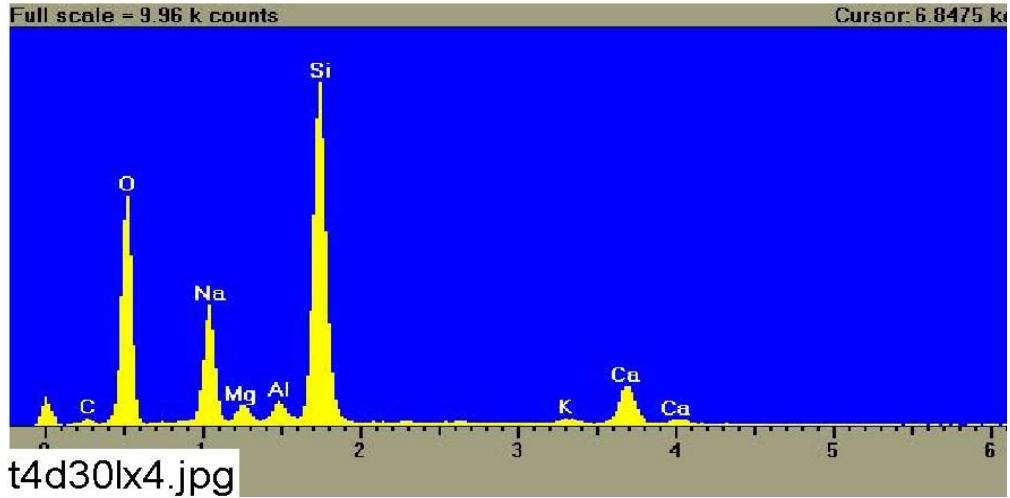


Figure 3-40. EDS counting spectrum for the spot of coating substance on the fiberglass shown in Figure 3-39. (t4d30lx4.jpg)

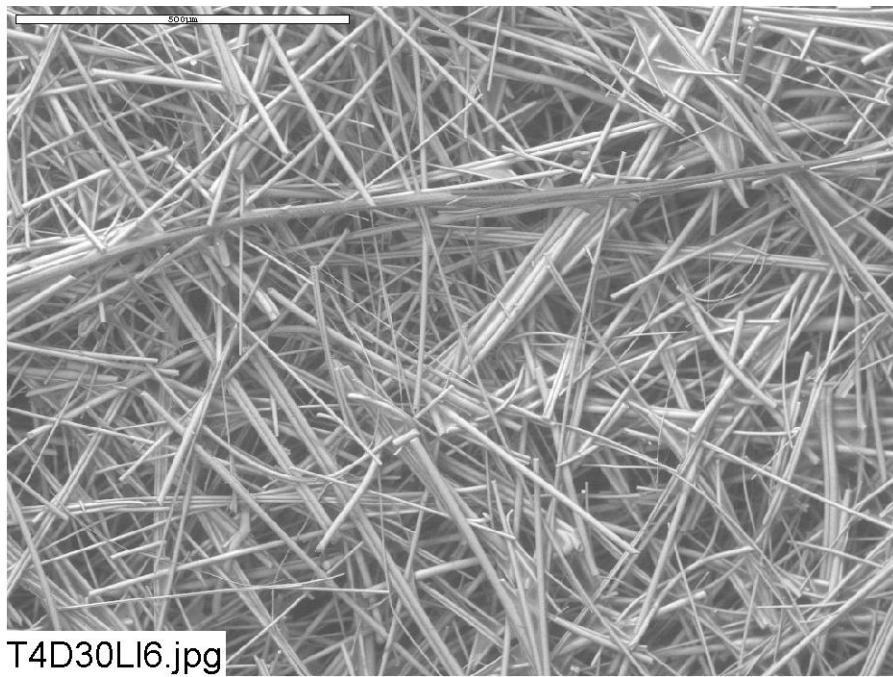


Figure 3-41. Environmental SEM image magnified 100 times for a Test #4 Day 30 interior low-flow fiberglass sample. (T4D30LI6.jpg)

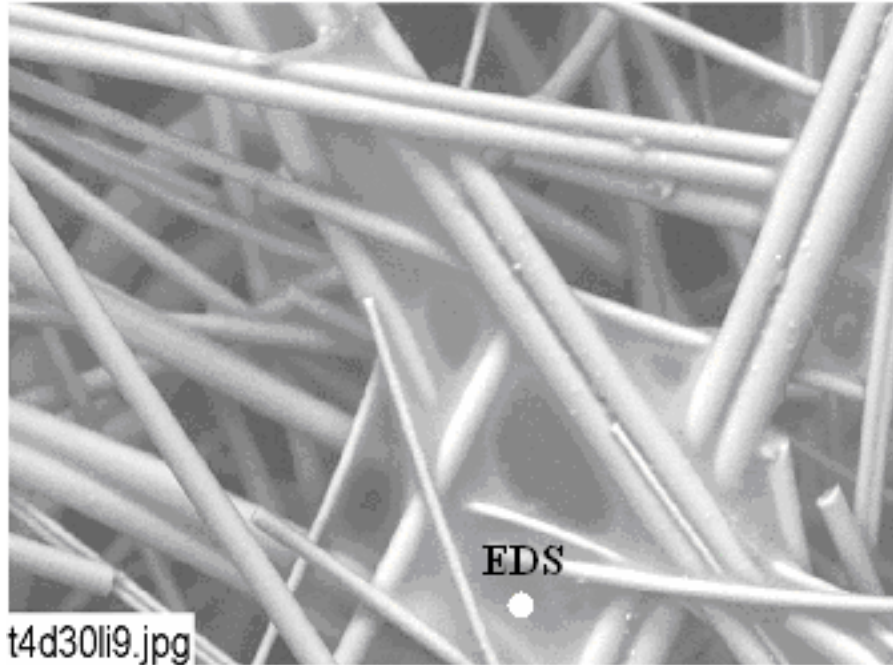


Figure 3-42. Environmental SEM image magnified 500 times for a Test #4 Day 30 interior low-flow fiberglass sample. (t4d30li9.jpg)

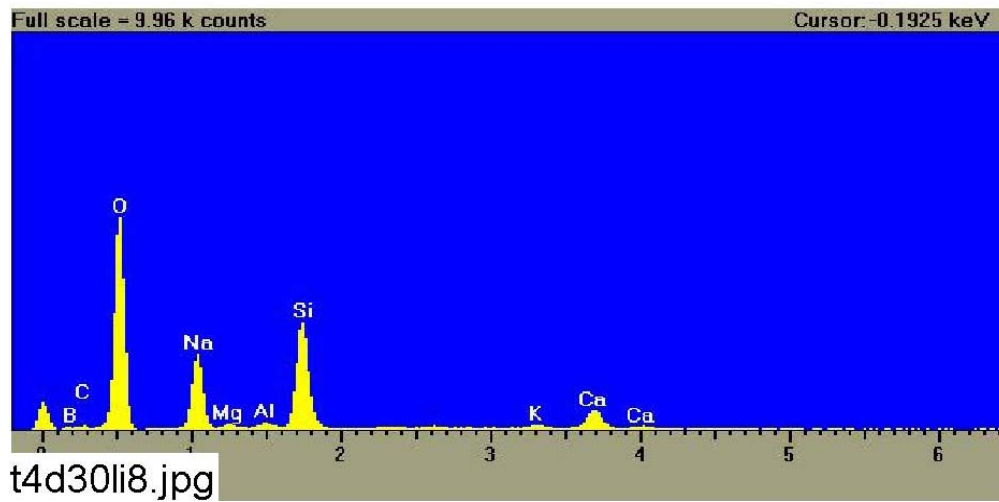


Figure 3-43. EDS counting spectrum for the film on the fiberglass shown in Figure 3-42. (t4d30li8.jpg)

3.3.1.5 Day 30 Fiberglass Inserted in Nylon Mesh in Low-Flow Zone

A 5 g fiberglass sample was enclosed in a nylon mesh and submerged in a low-flow zone of the tank on Day 3, to provide a comparison to all other fiberglass samples, which were enclosed in stainless steel mesh and placed in the tank on Day 0. The purpose of using a nylon mesh was to see if the mesh material (i.e., stainless steel or nylon) affects the deposits on the fiberglass samples. Comparing these results to Day 30 low-flow fiberglass samples, no significant difference was observed. The film was still the dominant deposit on both of the exterior and the interior samples. There were no particulate deposits found on the fiberglass. This result suggests that the mesh material did not significantly affect the deposits on fiberglass. In addition, ESEM images show that the nylon fiber was relatively clean and without significant deposits on it. The nylon mesh sample was put in the tank on Day 3, and no significant difference was found compared to the low-flow fiberglass samples put in the tank at the start of the test. Figures 3-44 through 3-49 show the Day 30 nylon-enclosed fiberglass results.

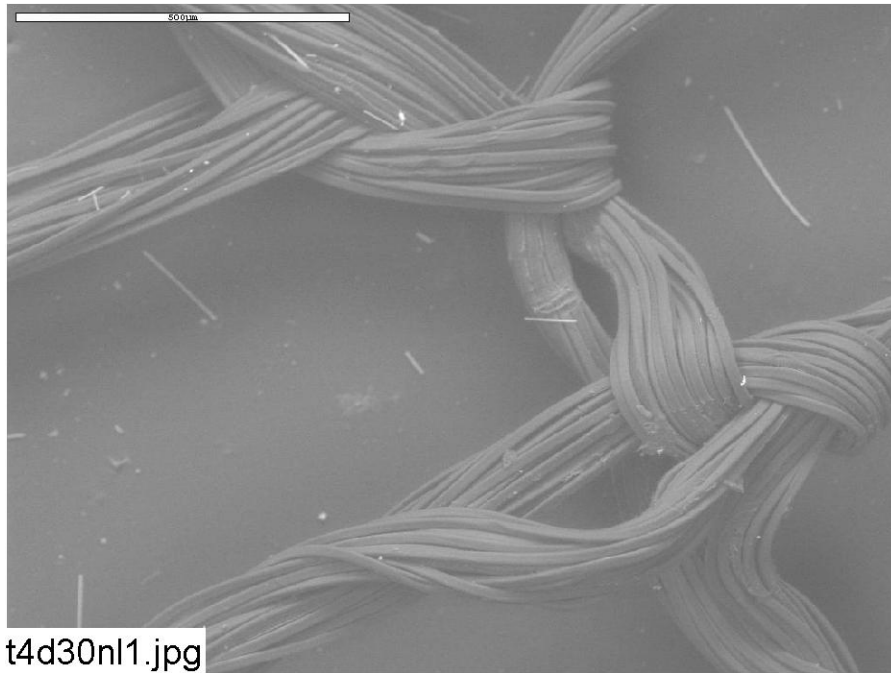


Figure 3-44. Environmental SEM image magnified 100 times for a Test #4 Day 30 nylon mesh submerged in low-flow area (inserted on Day 4). (t4d30nl1.jpg)

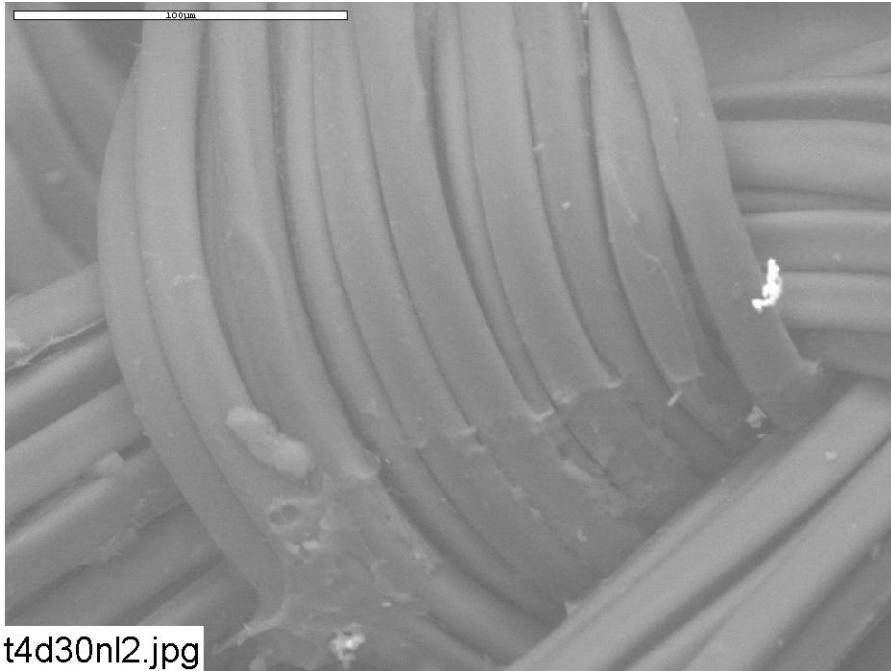


Figure 3-45. Environmental SEM image magnified 500 times for a Test #4 Day 30 nylon mesh submerged in low-flow area (inserted on Day 4). (t4d30nl2.jpg)

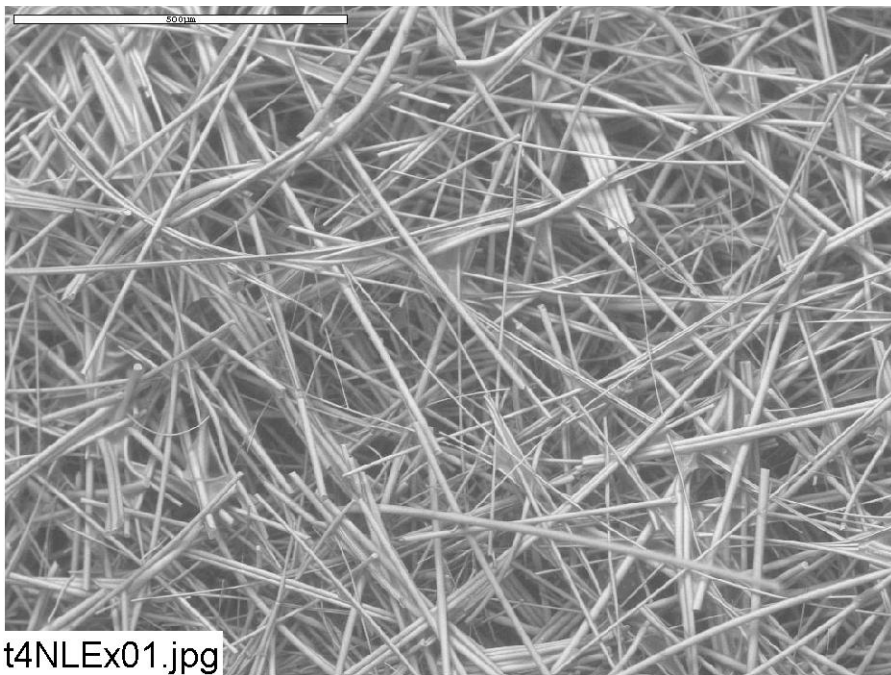


Figure 3-46. Environmental SEM image magnified 100 times for a Test #4 Day 30 exterior low-flow fiberglass sample contained in a nylon mesh (inserted on Day 4). (t4NLEx01.jpg)

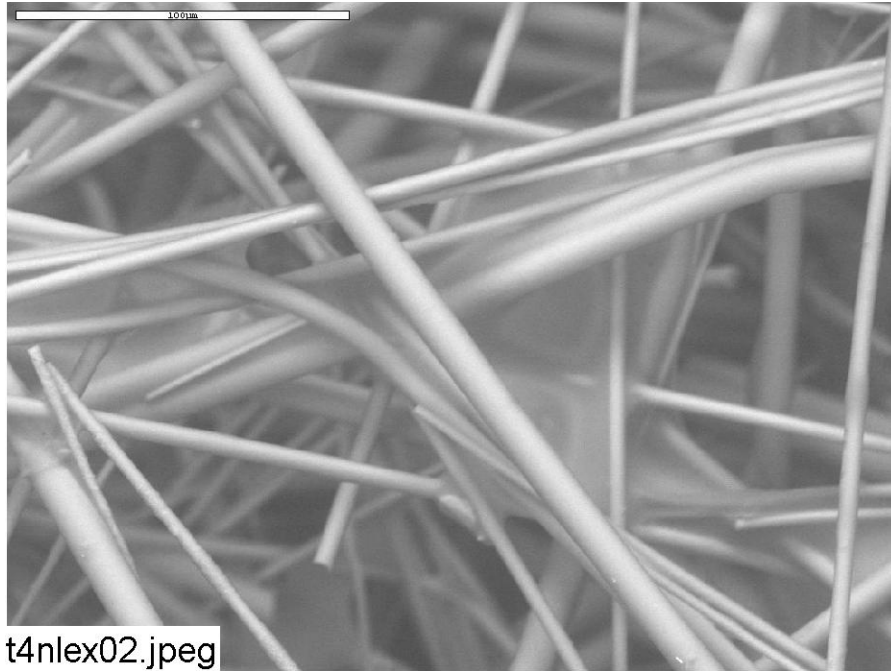


Figure 3-47. Environmental SEM image magnified 500 times for a Test #4 Day 30 exterior low-flow fiberglass sample contained in a nylon mesh (inserted on Day 4). (t4nlex02.jpeg)

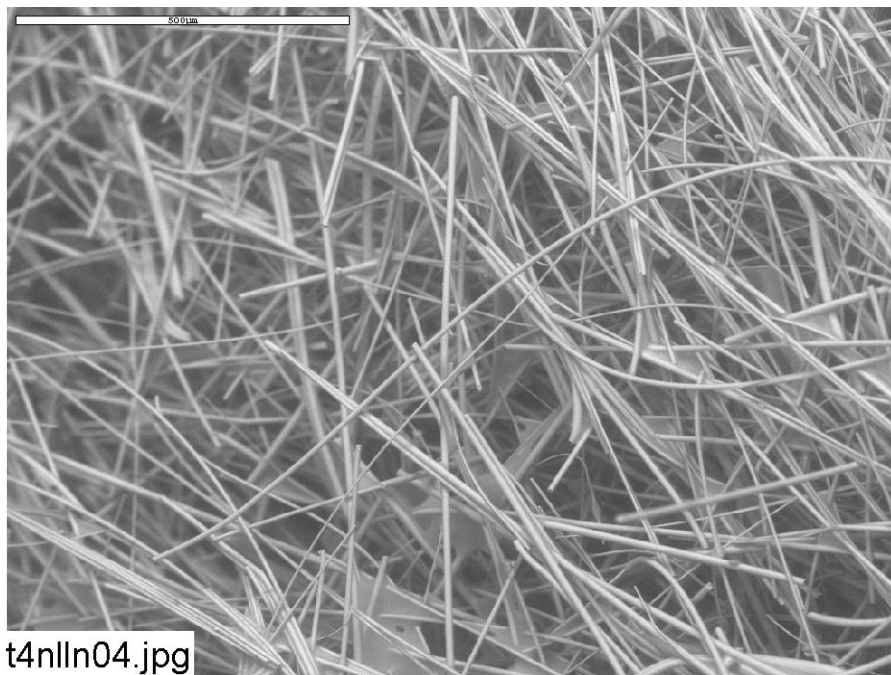


Figure 3-48. Environmental SEM image magnified 100 times for a Test #4 Day 30 interior low-flow fiberglass sample contained in a nylon mesh (inserted on Day 4). (t4nlln04.jpg)

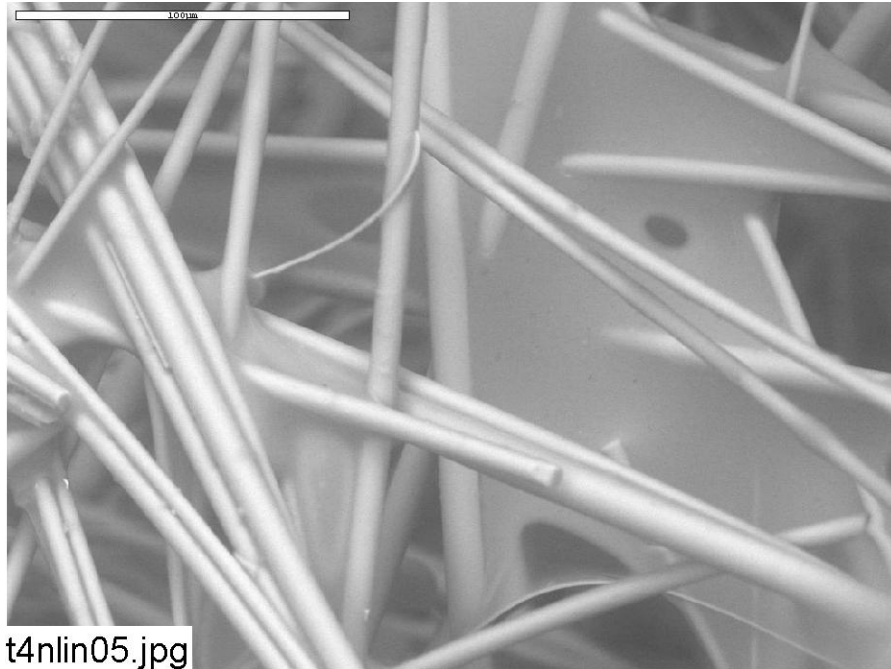


Figure 3-49. Environmental SEM image magnified 500 times for a Test #4 Day 30 interior low-flow fiberglass sample contained in a nylon mesh (inserted on Day 4). (t4nlin05.jpg)

3.3.1.6 Day 30 Low-Flow Fiberglass Samples in the Big Envelope

Compared to other Day 30 low-flow fiberglass samples, a significant amount of particulate deposits was observed on the exterior of the Day 30 low-flow samples in the big envelope. The big envelope sat on the tank bottom and was in contact with the test sediment on the bottom of the envelope. Figure 3-120 shows the sediment after the samples were lifted out of the tank. However, no particulate deposits were observed on the fiberglass interior. In addition, some large flat fibers were found on the exterior fiberglass samples (see Figure 3-51). These large flat fibers were likely from cal-sil (see Appendix D). It is possible that the particulate deposits and cal-sil fibers were physically attached/retained on the exterior of the fiberglass samples. Figures 3-50 through 3-53 show the results from the Day 30 low-flow fiberglass enclosed in the big envelope. In contrast to other samples, these samples were gently rinsed with RO water and no film was found on either the exterior or the interior of the fiberglass. The disappearance of the film is likely caused by the rinse of RO water to keep the sample moist before ESEM analysis. Based on the control experiment noted earlier (See Appendix C4), the film is soluble.



Figure 3-50. Environmental SEM image magnified 100 times for a Test #4 Day 30 exterior low-flow fiberglass sample in a big envelope. (t4evlx3.jpg).

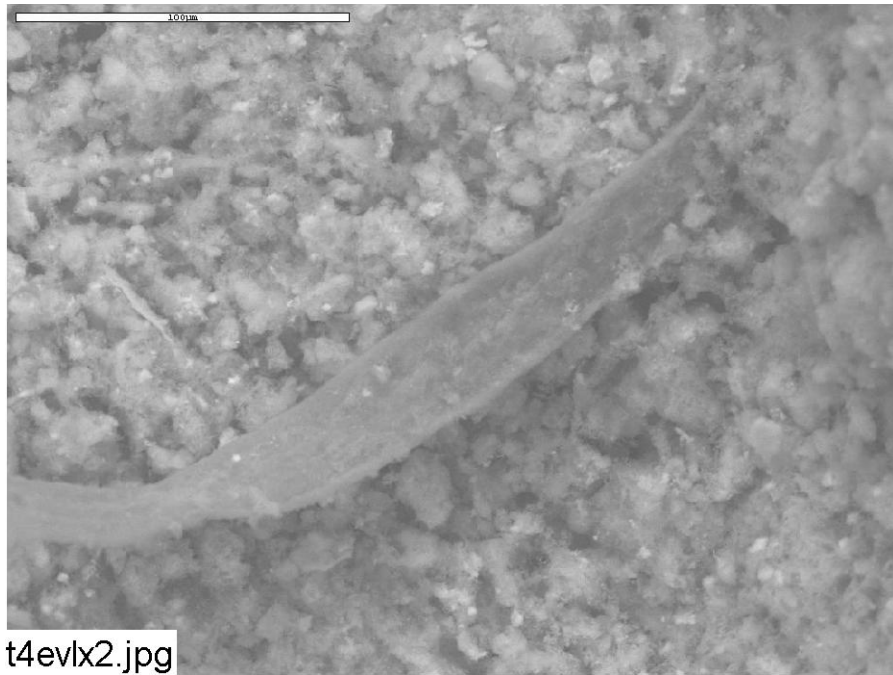


Figure 3-51. Environmental SEM image magnified 500 times for a Test #4 Day 30 exterior low-flow fiberglass sample in a big envelope. (t4evlx2.jpg)

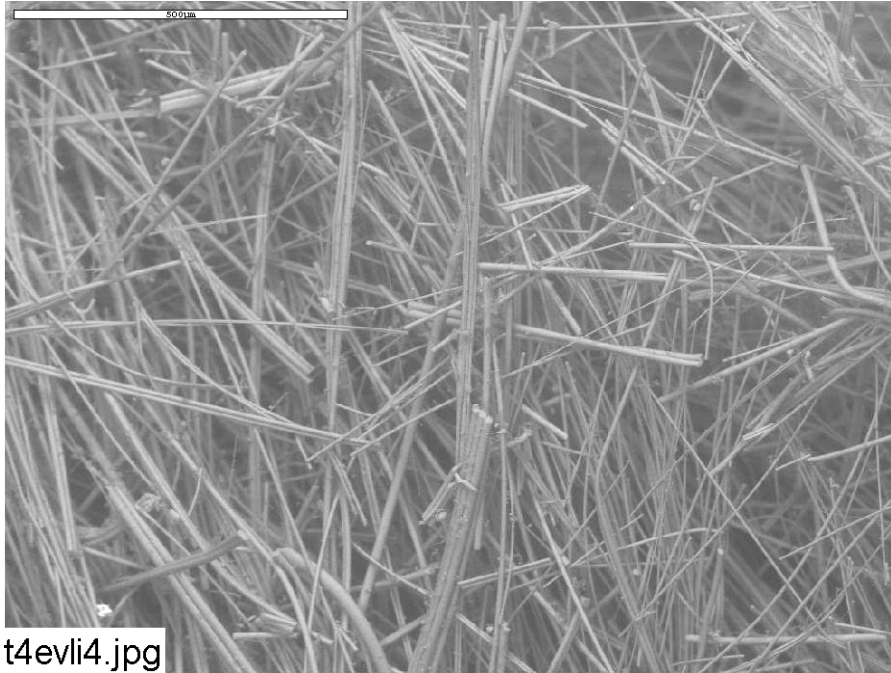


Figure 3-52. Environmental SEM image magnified 100 times for a Test #4 Day 30 interior low-flow fiberglass sample in a big envelope. (t4evli4.jpg)



Figure 3-53. Environmental SEM image magnified 500 times for a Test #4 Day 30 interior low-flow fiberglass sample in a big envelope. (t4evli7.jpg)

3.3.1.7 Day 30 High-Flow Fiberglass Samples

Compared to Day 30 low-flow fiberglass samples, a significant amount of particulate deposits and fiberglass debris were found on high-flow exterior samples. However, no particulate deposits were found on the interior. This result suggests that these particulate deposits were physically attached/retained on the fiberglass exterior. However, similar film deposits were found on both of the fiberglass exterior and the interior. The EDS result shows the film was composed of O, Na, Ca, C, Mg, Al, K, and possibly Si, which is similar to other EDS results. Figures 3-54 through 3-61 show the Day 30 high-flow fiberglass results. Figures 3-60 and 3-61 show fiberglass after it was rinsed with RO water.

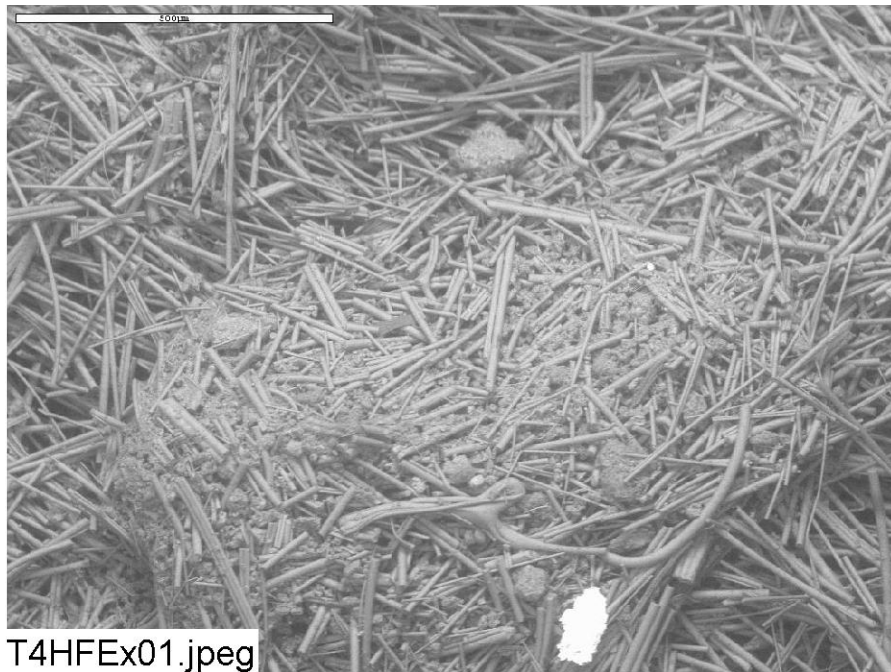


Figure 3-54. Environmental SEM image magnified 100 times for a Test #4 Day 30 exterior high-flow fiberglass sample. (T4HFEx01.jpg)

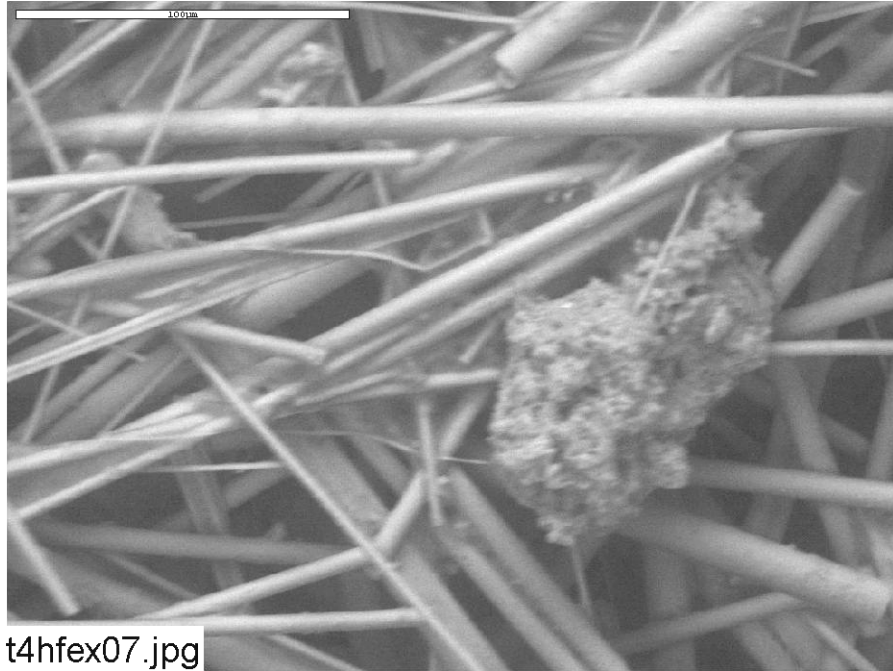


Figure 3-55. E Environmental SEM image magnified 500 times for a Test #4 Day 30 exterior high-flow fiberglass sample. (t4hfex07.jpg)

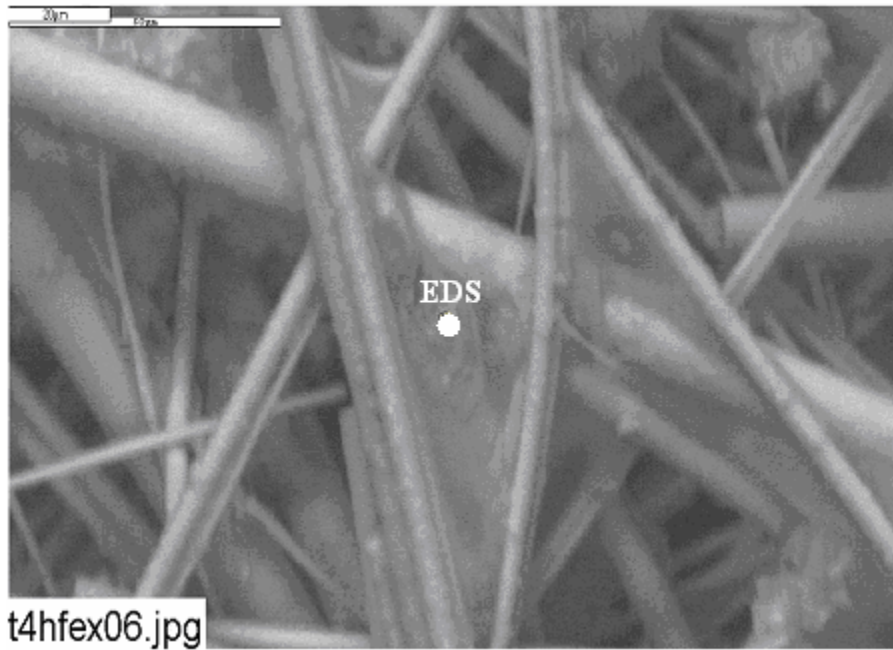


Figure 3-56. Environmental SEM image magnified 800 times for a Test #4 Day 30 exterior high-flow fiberglass sample. (t4hfex06.jpg)

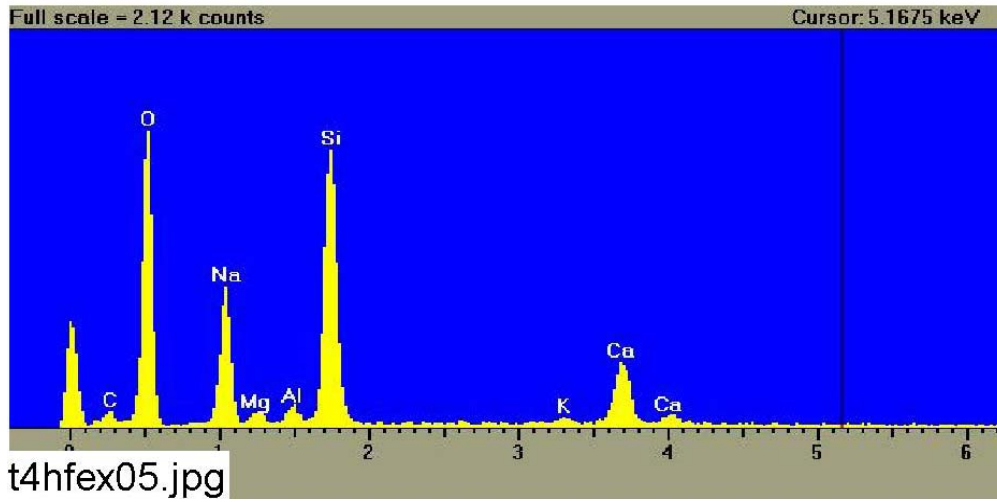


Figure 3-57. EDS counting spectrum for the spot of film on the fiberglass shown in Figure 3-56. (t4hfex05.jpg)

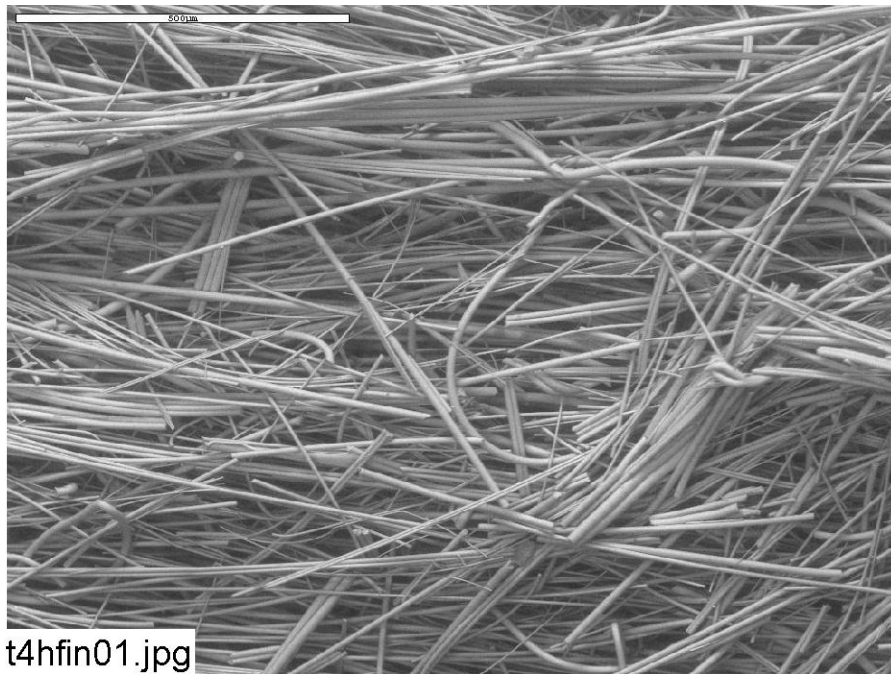


Figure 3-58. Environmental SEM image magnified 100 times for a Test #4 Day 30 interior high-flow fiberglass sample. (t4hfin01.jpg)

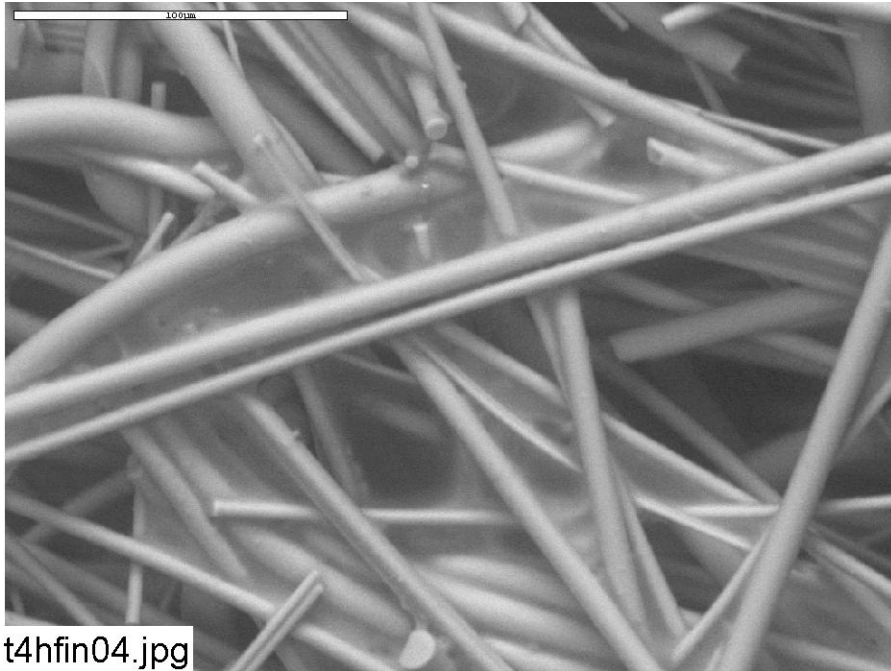


Figure 3-59. Environmental SEM image magnified 500 times for a Test #4 Day 30 interior high-flow fiberglass sample. (t4hfin04.jpg)

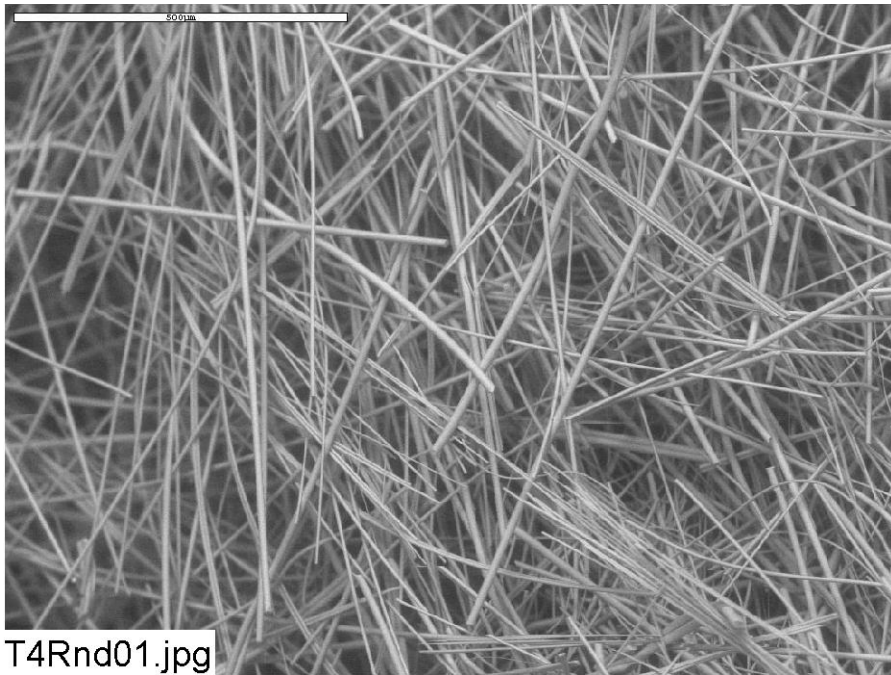


Figure 3-60. Environmental SEM image magnified 100 times for a Test #4 Day 30 interior high-flow fiberglass sample. The sample was gently pre-rinsed with RO water. (T4Rnd01.jpg)

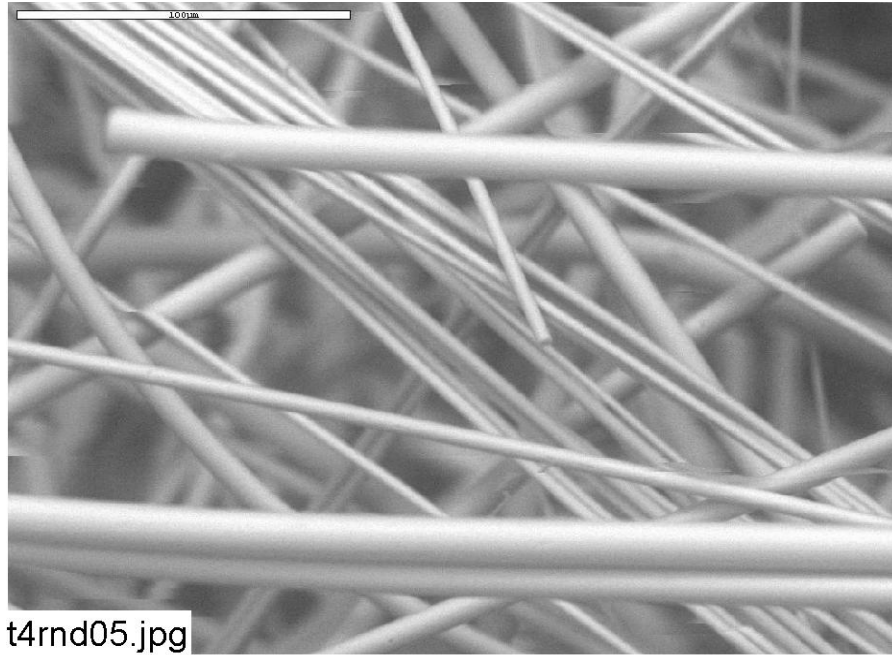


Figure 3-61. Environmental SEM image magnified 500 times for a Test #4 Day 30 interior high-flow fiberglass sample. The sample was gently pre-rinsed with RO water. (t4rnd05.jpg)

3.3.1.8 Day 30 High-Flow Fiberglass Samples in Front of a Header

The images of the fiberglass in front of a header are different from the conventional high-flow fiberglass samples in Section 3.3.1.7. The header sample was put in the tank on Day 2 to compare with samples placed in the tank on Day 0. Due to settling of suspended particles and decrease in turbidity during the first two days of the test, no significant particulate deposits were found on the header fiberglass exterior, as shown by ESEM images. This suggests that the deposits observed on the exterior of the high-flow samples put in the tank on Day 0 are due to the higher suspended solids and turbidity present in the system during the first several days. However, the coating and film deposits were found on both the exterior and the interior of the header samples. Consistent with earlier observations, the coating and the film were composed of O, Na, Ca, Mg, Al, C, K, and possibly Si. As mentioned before, coating and film deposits are likely caused by chemical precipitation when the samples were partially dehydrated. Figures 3-62 through 3-68 show the results from the Day 30 high-flow fiberglass in front of a header.

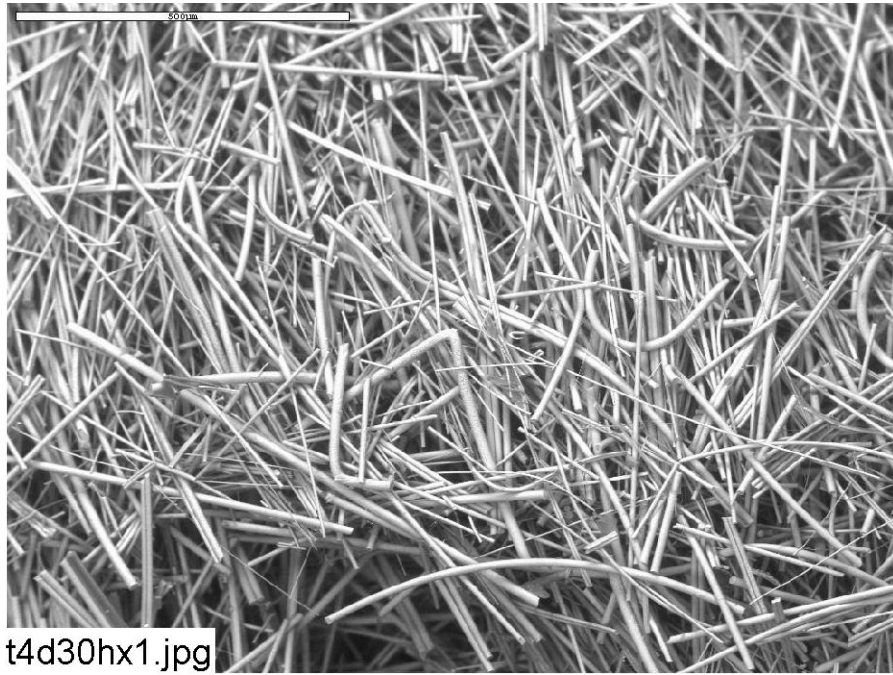


Figure 3-62: Environmental SEM image magnified 100 times for a Test #4 Day 30 exterior high-flow fiberglass sample in front of a header (inserted on Day 4). (t4d30hx1.jpg)

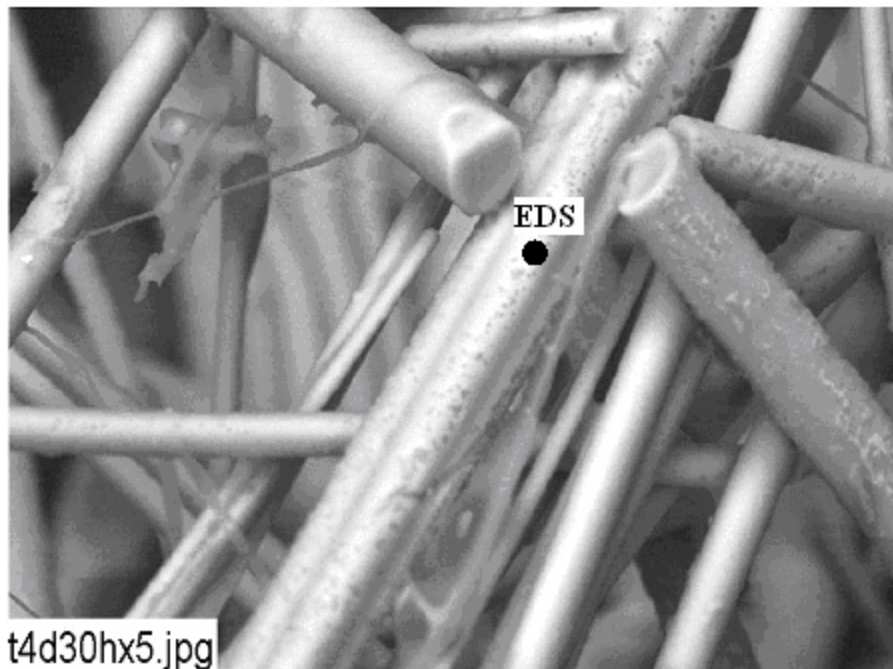


Figure 3-63: Environmental SEM image magnified 1000 times for a Test #4 Day 30 exterior high-flow fiberglass sample in front of a header (inserted on Day 4). (t4d30hx5.jpg)

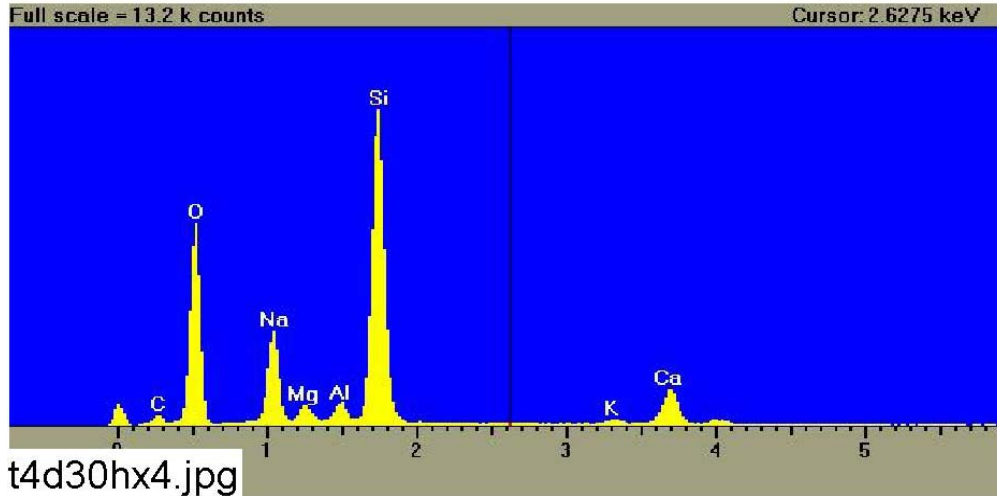


Figure 3-64: EDS counting spectrum for the spot of coating substance on fiberglass shown in Figure 3-63. (t4d30hx4.jpg)

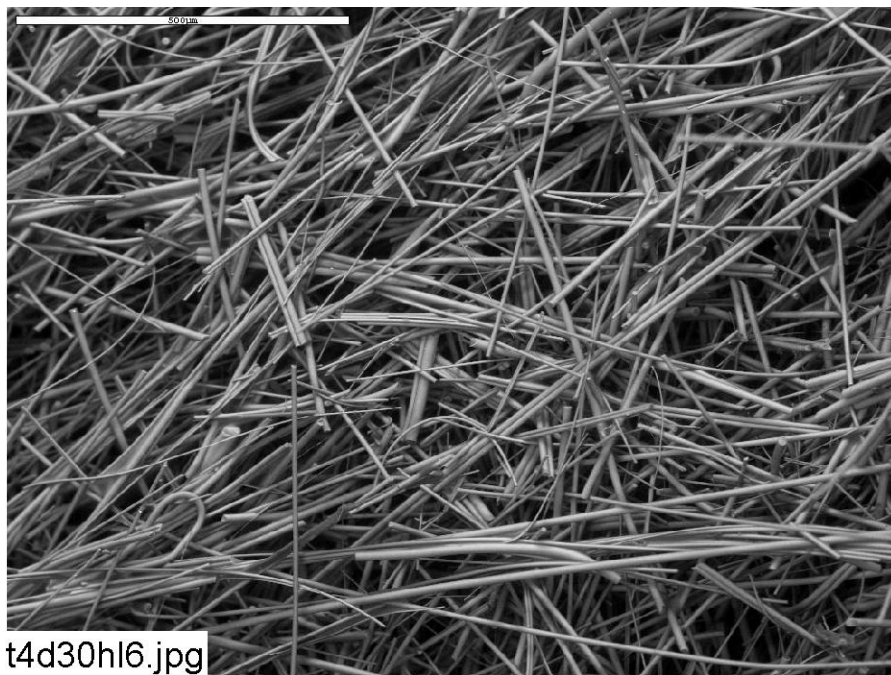


Figure 3-65: Environmental SEM image magnified 100 times for a Test #4 Day 30 interior high-flow fiberglass sample in front of a header (inserted on Day 4). (t4d30hI6.jpg)

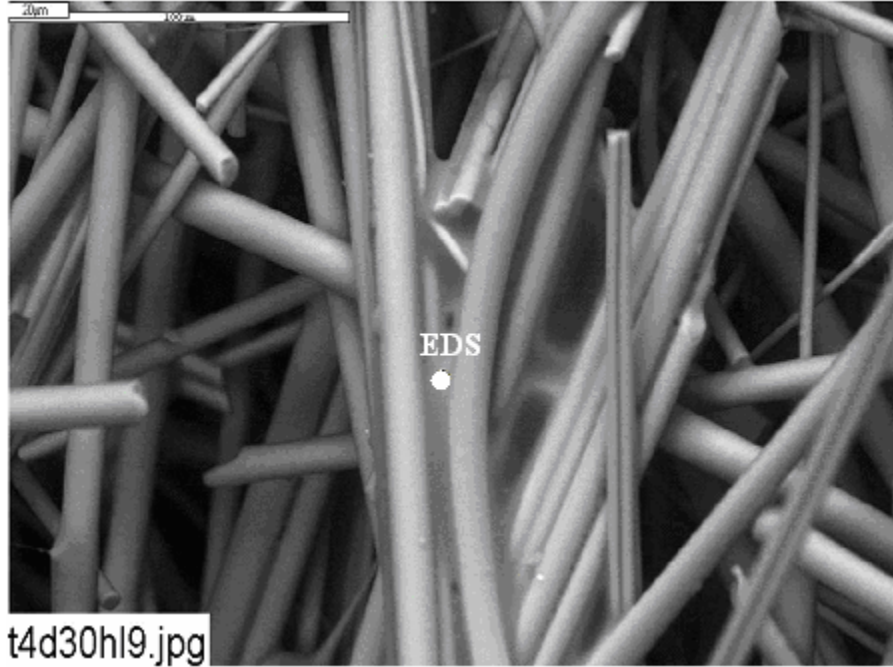


Figure 3-66: Environmental SEM image magnified 500 times for a Test #4 Day 30 interior high-flow fiberglass sample in front of a header (inserted on Day 4). (t4d30h19.jpg)

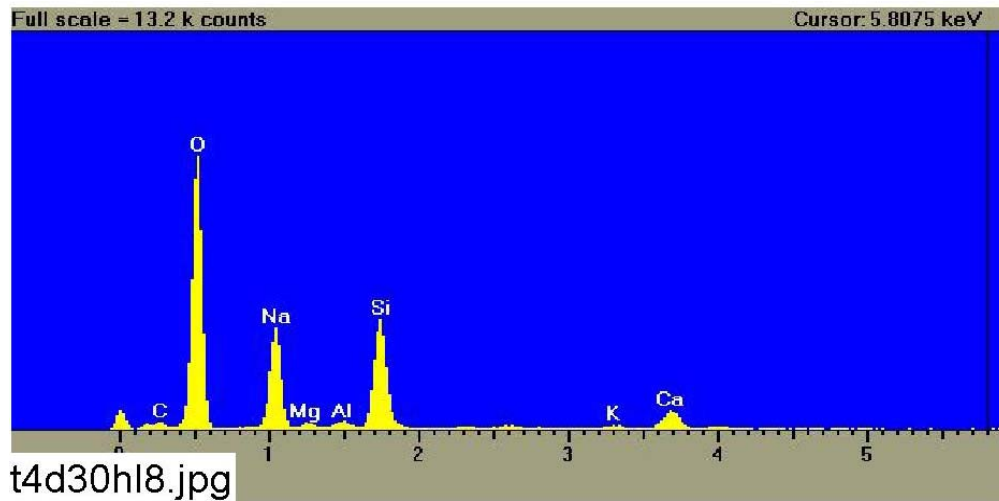


Figure 3-67: EDS counting spectrum for the spot of substance attached on fiberglass shown in Figure 3-66. (t4d30h18.jpg)

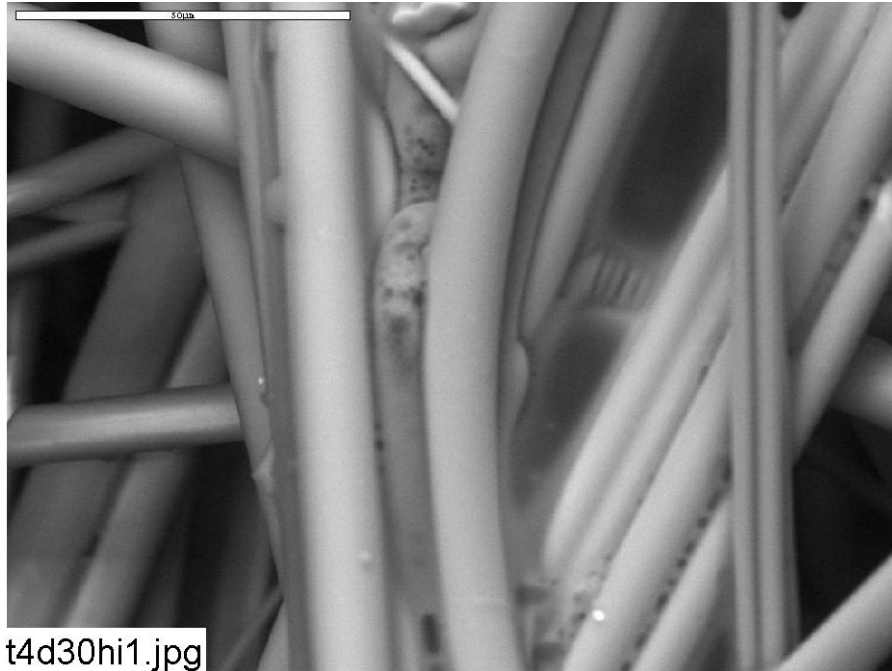


Figure 3-68: Environmental SEM image magnified 1000 times for a Test #4 Day 30 interior high-flow fiberglass sample in front of a header (inserted on Day 4). (t4d30hi1.jpg)

3.3.1.9 Day 30 Drain Collar Fiberglass Samples

When the tank was drained, the drain collar was totally surrounded by sediment. Figure 3-121 shows the drain collar after the tank was drained. Both the exterior fiberglass sample that was farthest from the drain screen and the exterior sample that was next to the drain screen have significant amounts of particulate deposits. Inspection revealed the development of a continuous coating on the drain collar exterior, including particulate deposits that were likely physically retained or attached. The amount of deposits on the drain collar exterior was greater than on high- and low-flow fiberglass samples. EDS results indicate that the particulate deposits were mainly composed of O, Si, Ca, Na, Al, and C, regardless of whether the drain collar exterior was farthest from the drain screen or next to the drain screen. The high content of Si and Ca in the particulate deposits suggests that they were probably from cal-sil debris. In contrast to the exterior, no significant particulate deposits were found in the drain collar interior sample, and only film-like deposits were found (see Figure 3-75). The drain collar interior appears similar to the other high- and low- flow fiberglass interior samples. This result suggests that almost all of the particulate deposits were physically retained at the fiberglass exterior, which is consistent with Day 30 high-flow fiberglass samples. Figures 3-69 through 3-79 show the drain collar fiberglass results.

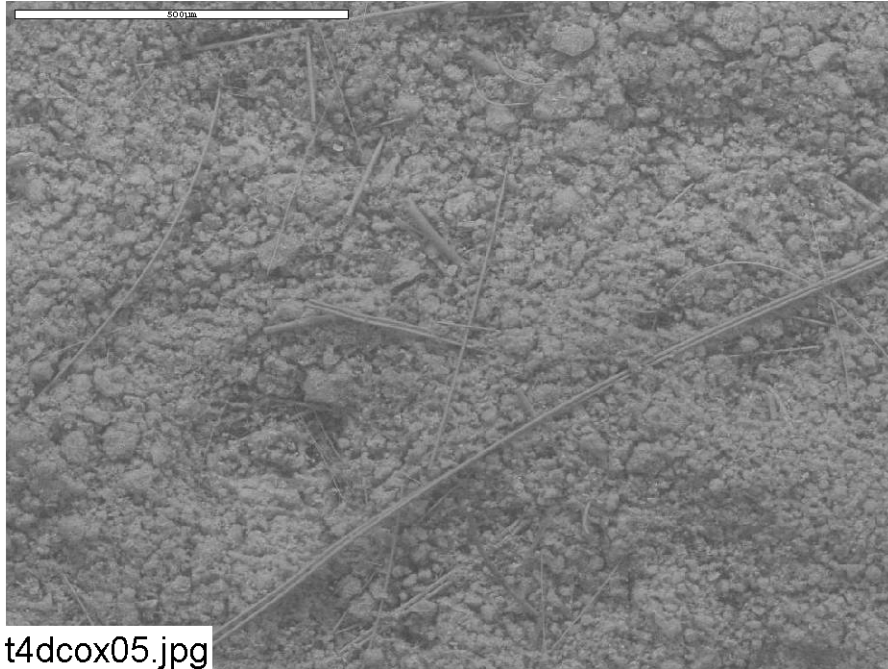


Figure 3-69: Environmental SEM image magnified 100 times for a Test #4 Day 30 exterior fiberglass sample on the drain collar (away from the drain screen). (t4dcox05.jpg)

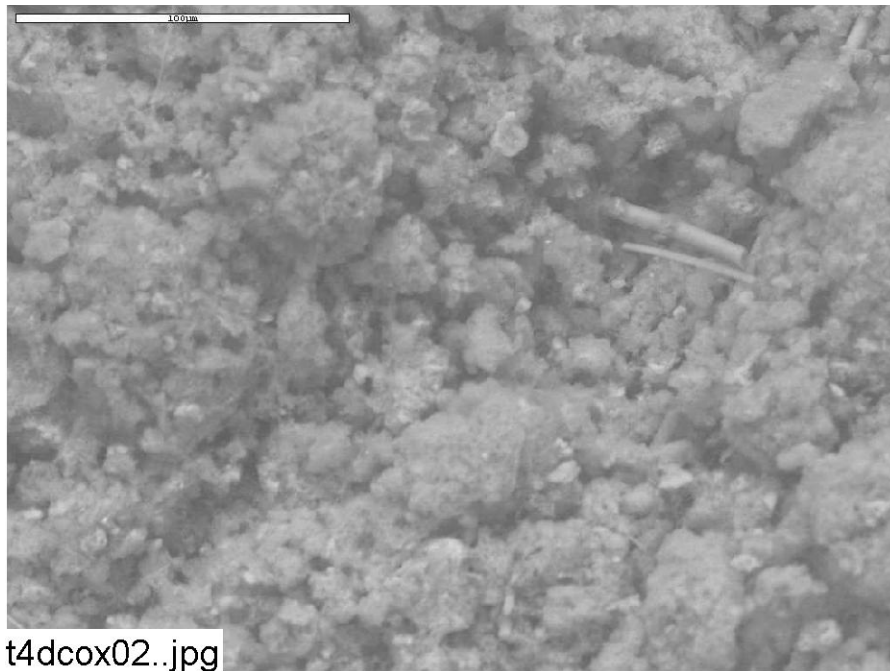


Figure 3-70: Environmental SEM image magnified 500 times for a Test #4 Day 30 exterior fiberglass sample on the drain collar (away from the drain screen). (t4dcox02.jpg)

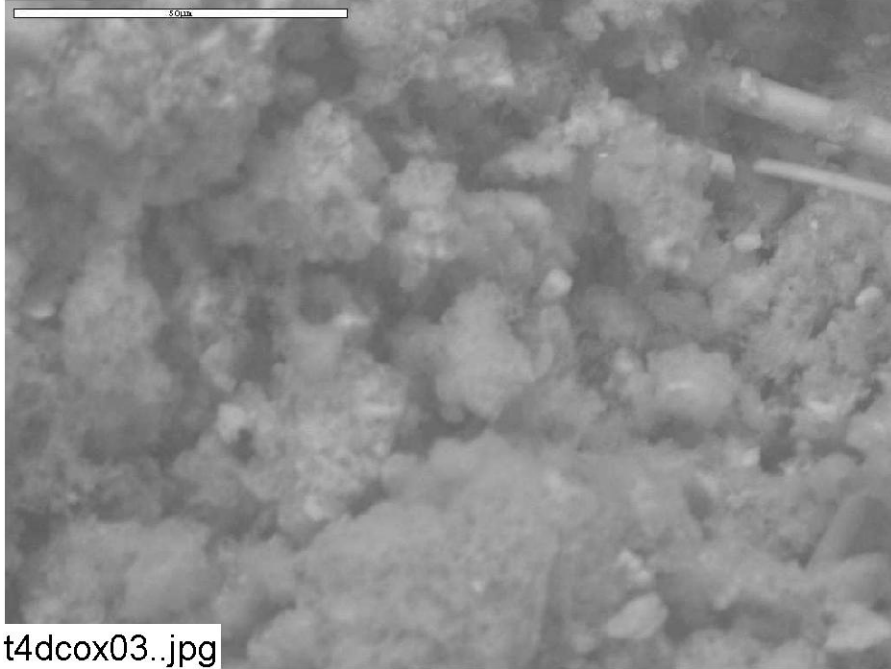


Figure 3-71: Environmental SEM image magnified 1000 times for a Test #4 Day 30 exterior fiberglass sample on the drain collar (away from the drain screen). (t4dcox03.jpg)

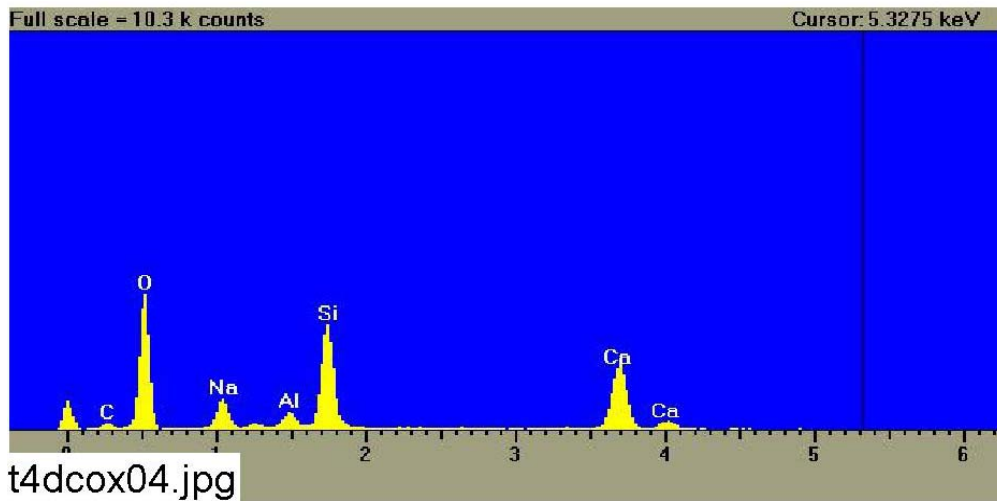


Figure 3-72: EDS counting spectrum for the large mass of particulate deposits on fiberglass shown in Figure 3-71. (t4dcox04.jpg)

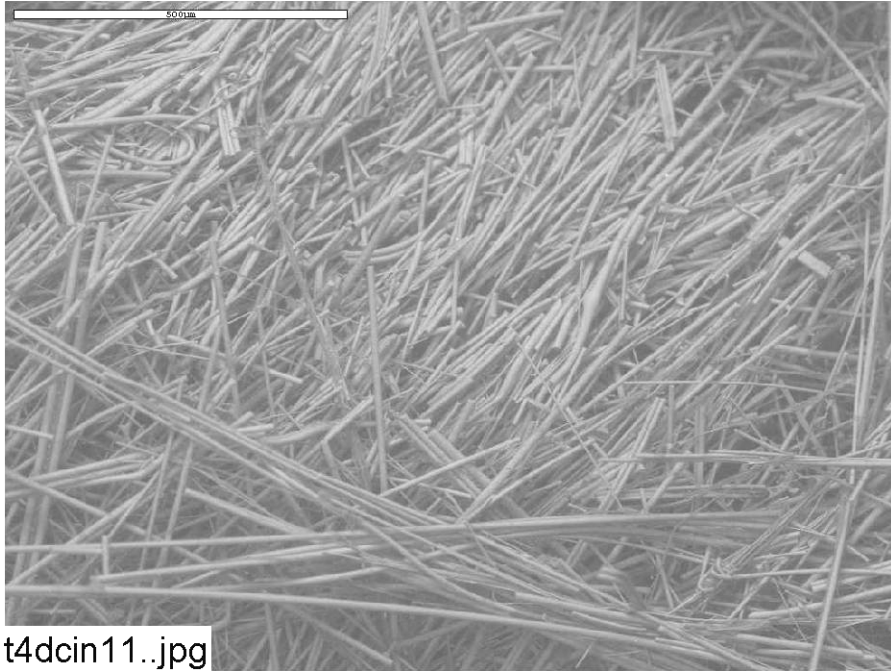


Figure 3-73: Environmental SEM image magnified 100 times for a Test #4 Day 30 interior fiberglass sample on the drain collar. (t4dcin11.jpg)

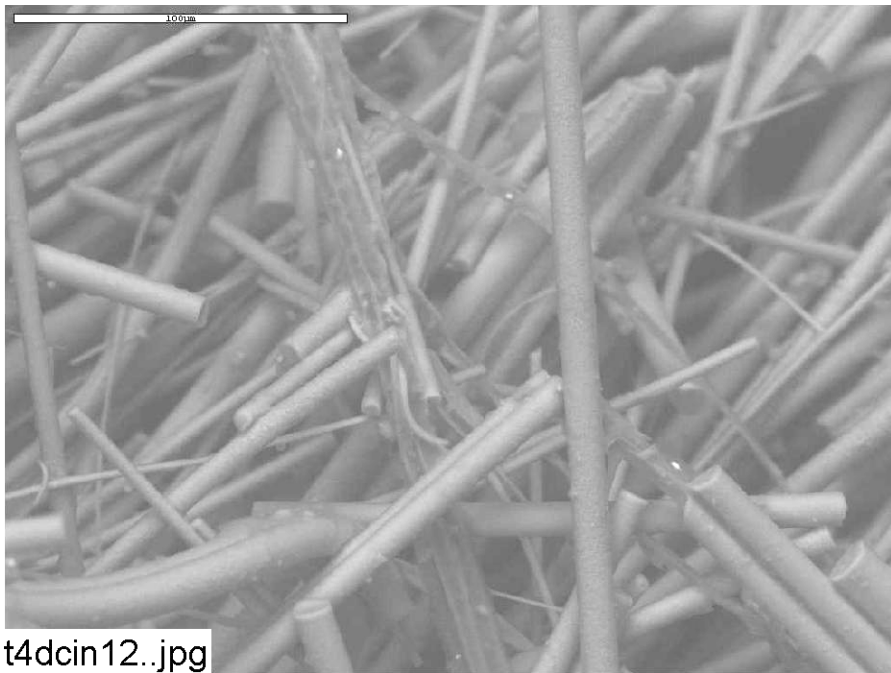


Figure 3-74: Environmental SEM image magnified 500 times for a Test #4 Day 30 interior fiberglass sample on the drain collar. (t4dcin12.jpg)

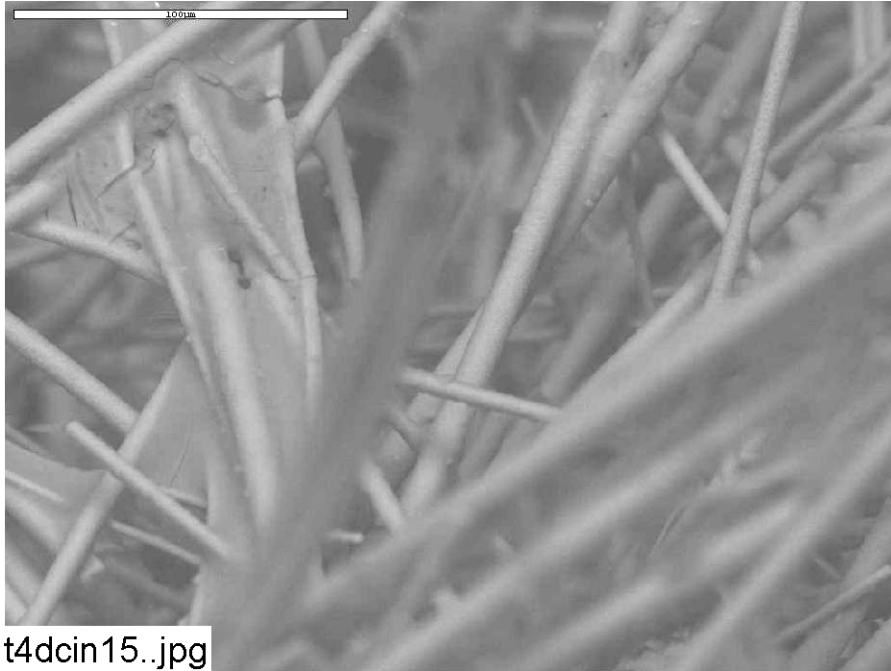


Figure 3-75: Environmental SEM image magnified 500 times for a Test #4 Day 30 interior fiberglass sample on the drain collar. (t4dcin15.jpg)

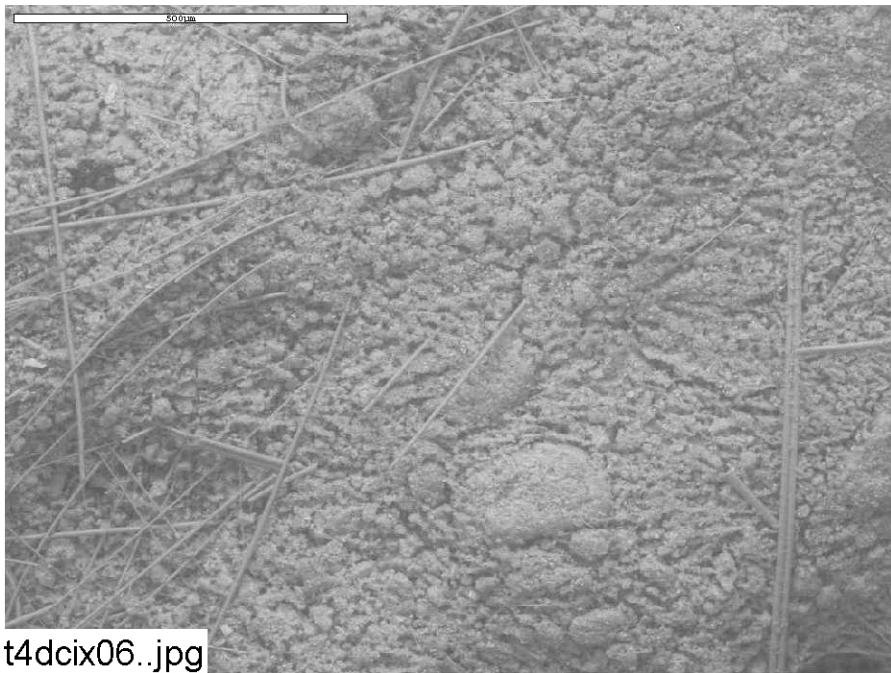


Figure 3-76: Environmental SEM image magnified 100 times for a Test #4 Day 30 exterior fiberglass sample on the drain collar (next to the drain screen). (t4dcix06.jpg)

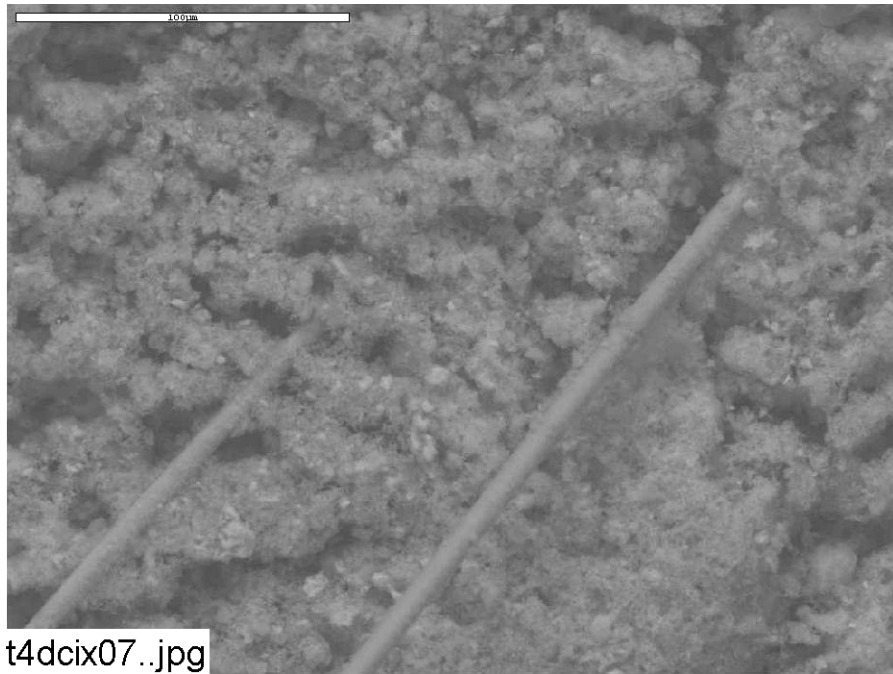


Figure 3-77: Environmental SEM image magnified 500 times for a Test #4 Day 30 exterior fiberglass sample on the drain collar (next to the drain screen). (t4dcix07.jpg)

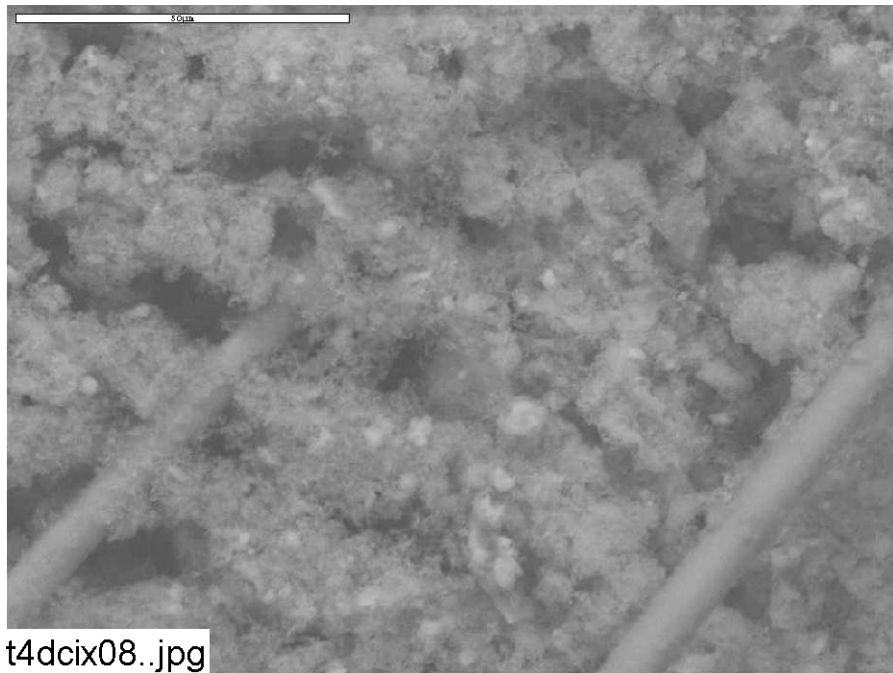


Figure 3-78: Environmental SEM image magnified 1000 times for a Test #4 Day 30 exterior fiberglass sample on the drain collar (next to the drain screen). (t4dcix08.jpg)

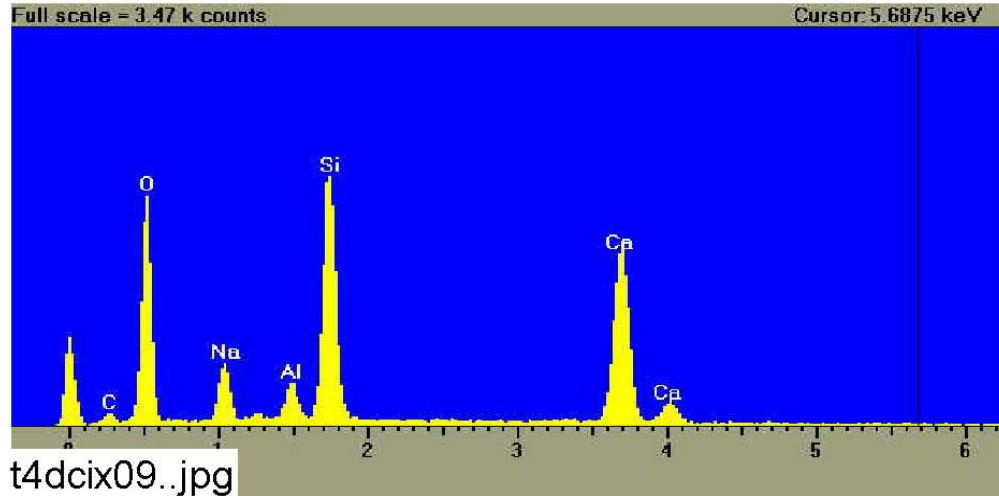


Figure 3-79: EDS counting spectrum for the large mass of particulate deposits on fiberglass shown in Figure 3-78. (t4dcix09.jpg)

3.3.1.10 Day 30 Fiberglass Sample within the Birdcage

For the Day 30 fiberglass sample within the birdcage, the SEM images indicate a significant amount of particulate deposits (see Figure 3-80) on the exterior of the fiberglass. The location of the birdcage was on top of a large cal-sil sample that sat on the bottom of the tank and was in direct contact with the sediment. The birdcage, however, was not in direct contact with the sediment. The amount of particulate deposits was greater than the amounts on the high- and low-flow fiberglass samples, but less than the drain collar exterior. The EDS result shows that the particulate deposits were composed of O, Si, Ca, Na, Al, and C, which is consistent with the drain collar exterior. Again, the high content of Si and Ca suggests these particulate deposits were from cal-sil debris. Compared to the exterior, the interior sample was relatively clean. Only film deposits were found. These film deposits were similar to the observed high- and low-flow fiberglass samples, which were likely caused by chemical precipitation during the drying process. Again, this result suggests that almost all of the particulate deposits were physically retained at the fiberglass exterior, consistent with Day 30 high-flow and drain collar fiberglass samples. Figures 3-80 through 3-85 show the birdcage fiberglass results.

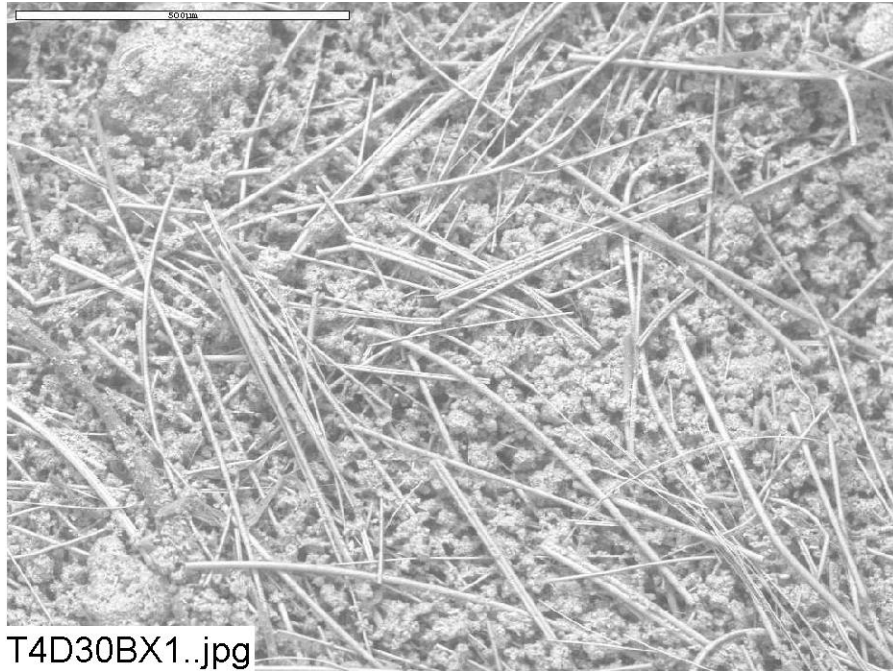


Figure 3-80: Environmental SEM image magnified 100 times for a Test #4 Day 30 exterior fiberglass sample within the birdcage. (T4D30BX1.jpg)

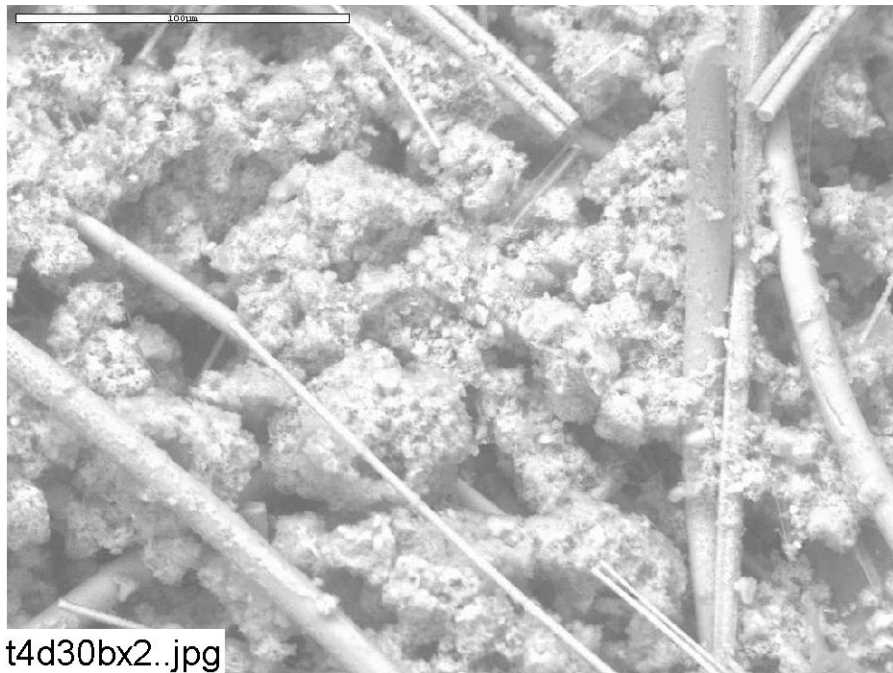


Figure 3-81: Environmental SEM image magnified 500 times for a Test #4 Day 30 exterior fiberglass sample within the birdcage. (T4D30bx2.jpg)

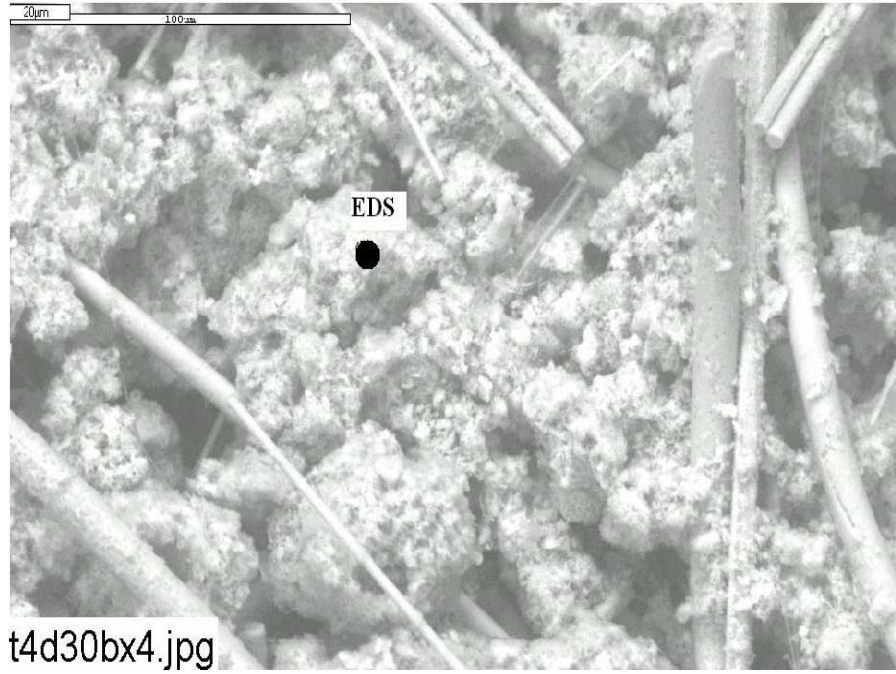


Figure 3-82: Annotated environmental SEM image magnified 500 times for a Test #4 Day 30 exterior fiberglass sample within the birdcage. (t4d30bx4.jpg)

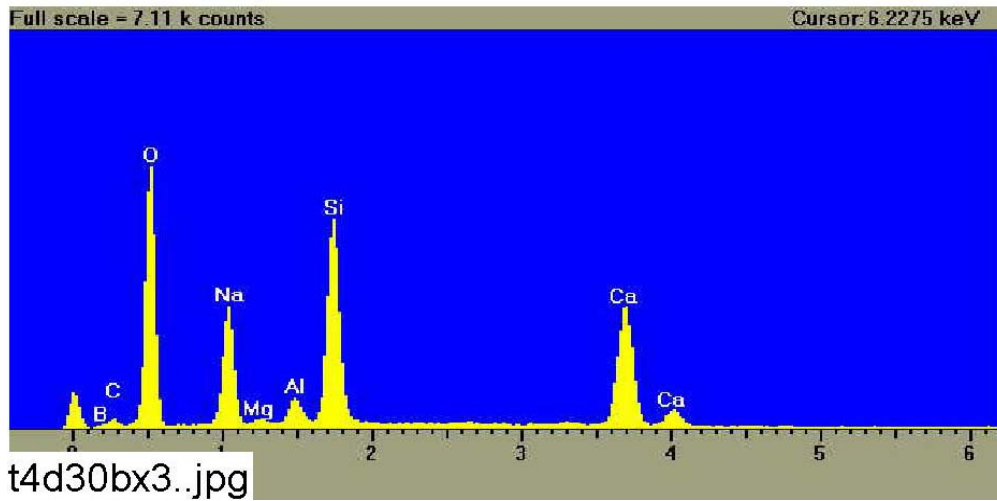


Figure 3-83: EDS counting spectrum for the particulate deposits on fiberglass shown in Figure 3-82. (T4D30bx3.jpg)

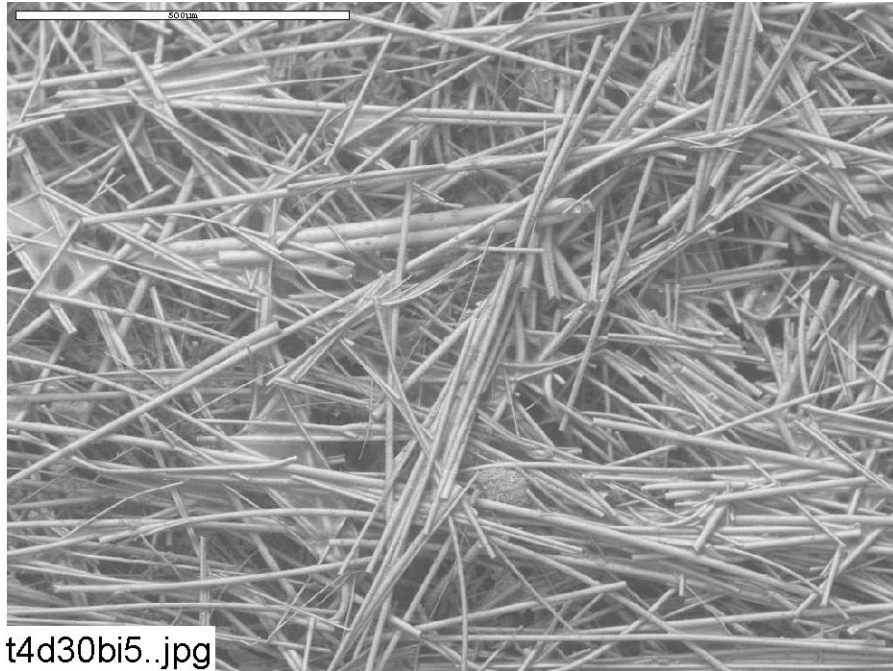


Figure 3-84: Environmental SEM image magnified 100 times for a Test #4 Day 30 interior fiberglass sample within the birdcage. (t4d30bi5.jpg)

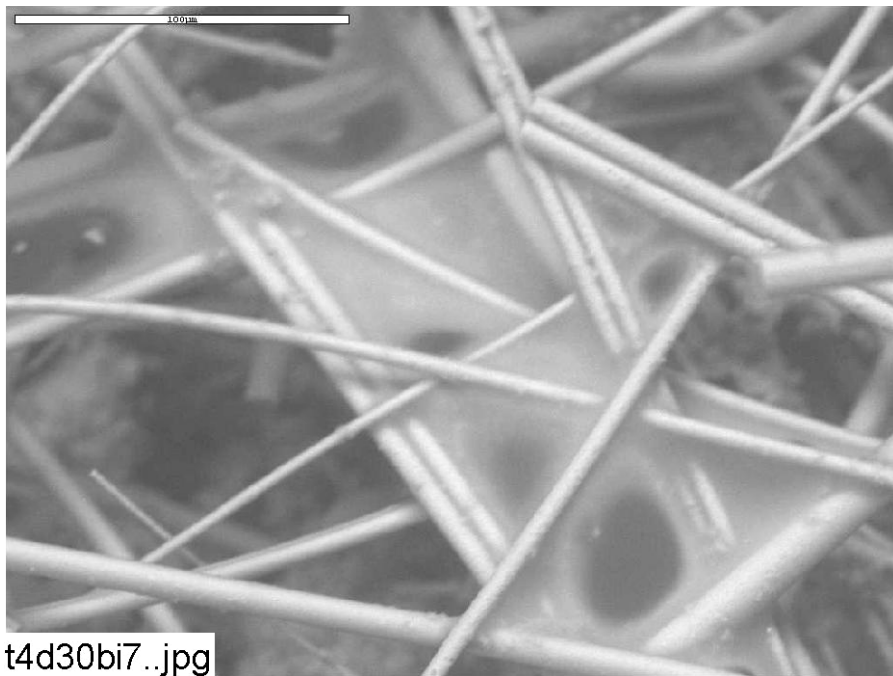


Figure 3-85: Environmental SEM image magnified 500 times for a Test #4 Day 30 interior fiberglass sample within the birdcage. (t4d30bi7.jpg)

3.3.2 Calcium Silicate Samples

ICET Test #4 was the second test that included cal-sil insulation samples in addition to fiberglass samples. XRD/XRF results show the crystal structure and the chemical composition of the unused raw and unused baked cal-sil samples. Based on XRD results, both unused raw and unused baked cal-sil samples contained crystalline substances of tobermorite ($\text{Ca}_{2.25}(\text{Si}_3\text{O}_{7.5}(\text{OH})_{1.5})(\text{H}_2\text{O})$) and calcite (CaCO_3). XRF results indicated that the dominant elemental compositions of cal-sil include Si and Ca and small amounts of Al, Fe, Na, and Mg. There was no significant difference in elemental composition between raw and baked unused cal-sil. After being baked in a laboratory oven at 260°C for 72 hours, the raw cal-sil color changed from yellow to pink. The possible property changes of cal-sil after being baked include loss of water and oxidation of reductive species such as organic carbon, Fe(0), and Fe(II), as well as possible mineral and crystal structural changes. Specifically, oxidation of Fe(0) and Fe(II) into Fe_2O_3 is likely responsible for the baked cal-sil's turning pink.

Both raw and baked cal-sil samples were submerged in the tank throughout the test. No significant differences were found between the raw and baked cal-sil, or between the exterior and the interior. EDS results show that both raw and baked cal-sil were composed primarily of O, Si, Ca, Na, Al, C, Mg, and Fe. Due to the granular shape of cal-sil particles, it is difficult to distinguish whether the particles are foreign deposits or they are the cal-sil particles themselves. Figures 3-86 through 3-97 show cal-sil results.

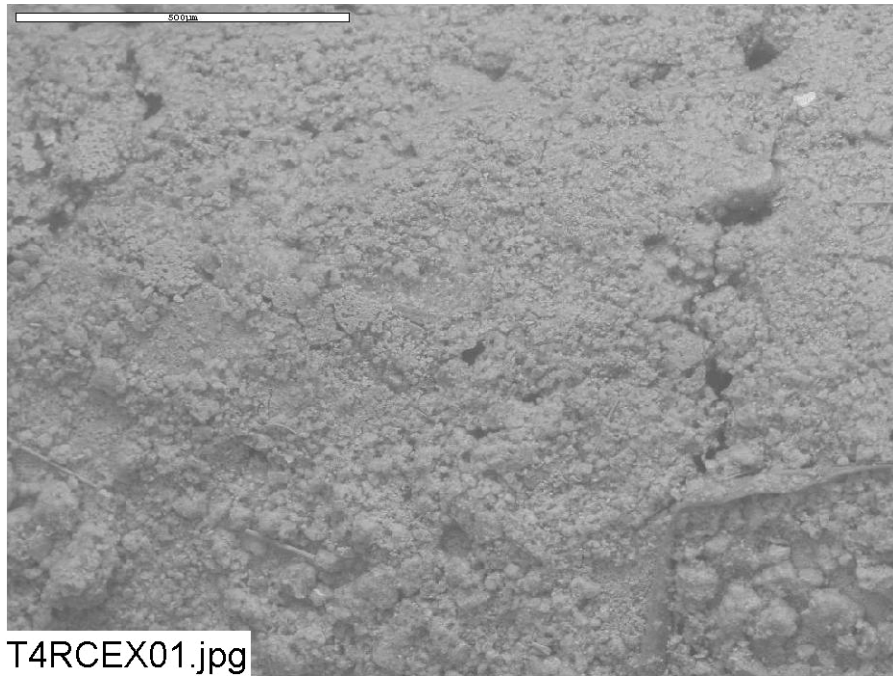


Figure 3-86: Environmental SEM image magnified 100 times for a Test #4 Day 30 low-flow exterior raw cal-sil sample. (T4RCEX01.jpg)

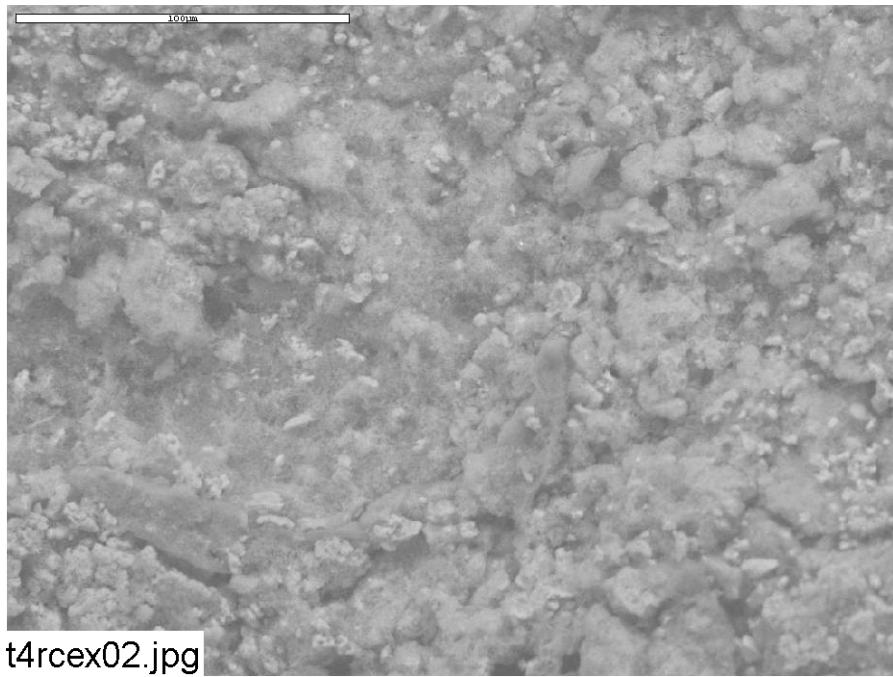


Figure 3-87: Environmental SEM image magnified 500 times for a Test #4 Day 30 low-flow exterior raw cal-sil sample. (t4rcex02.jpg)

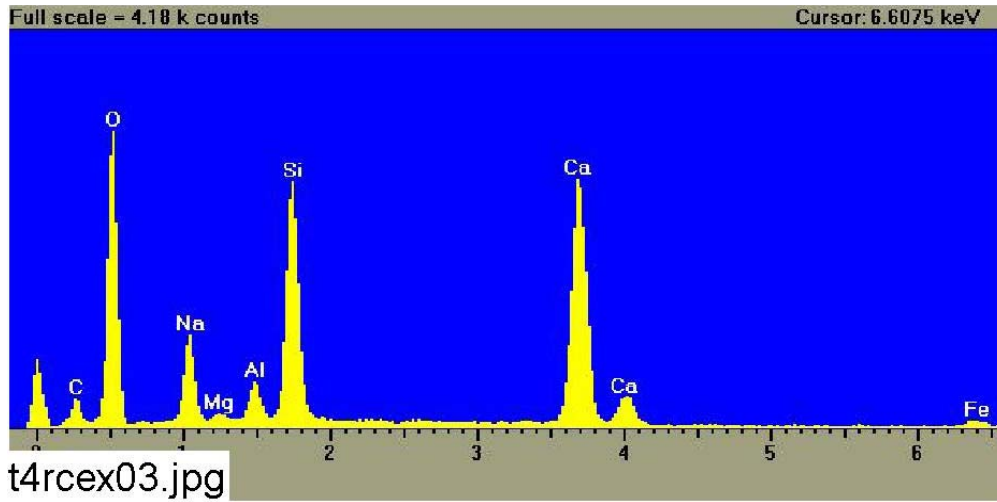


Figure 3-88: EDS counting spectrum for the whole image shown in Figure 3-87. (t4rcex03.jpg)

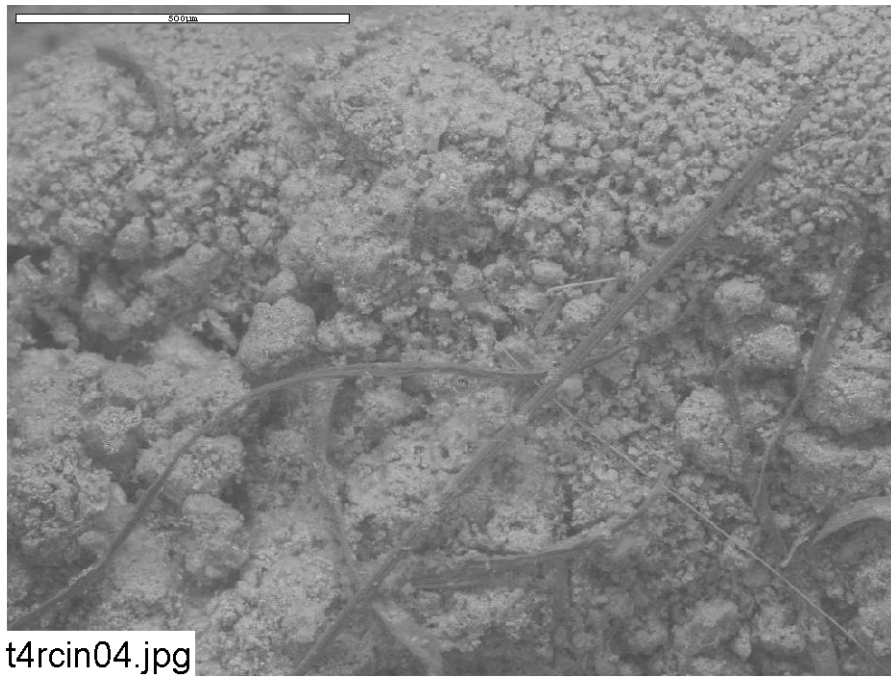


Figure 3-89: Environmental SEM image magnified 100 times for a Test #4 Day 30 low-flow interior raw cal-sil sample. (t4rcin04.jpg)

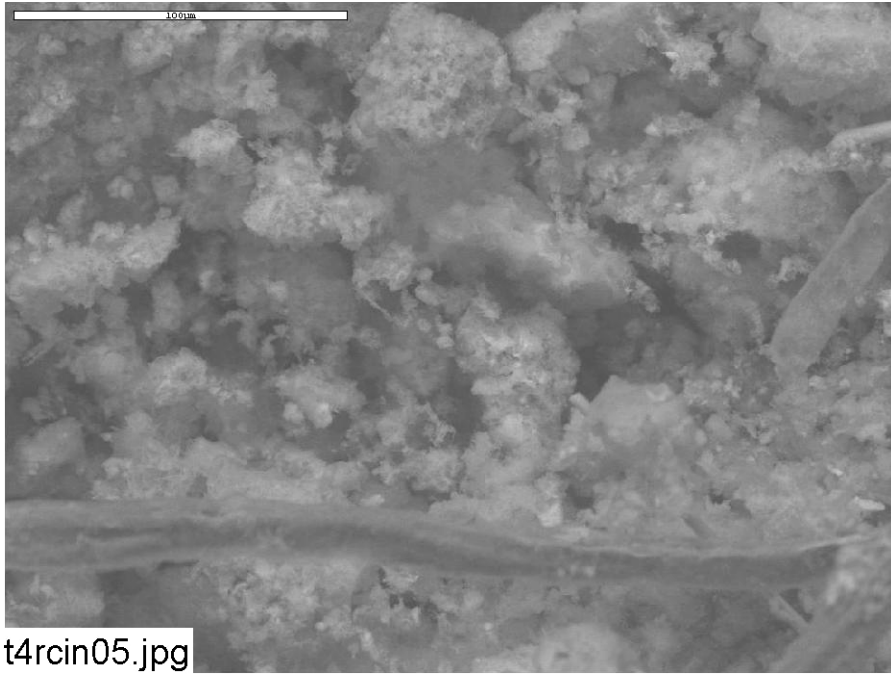


Figure 3-90: Environmental SEM image magnified 500 times for a Test #4 Day 30 low-flow interior raw cal-sil sample. (t4rcin05.jpg)

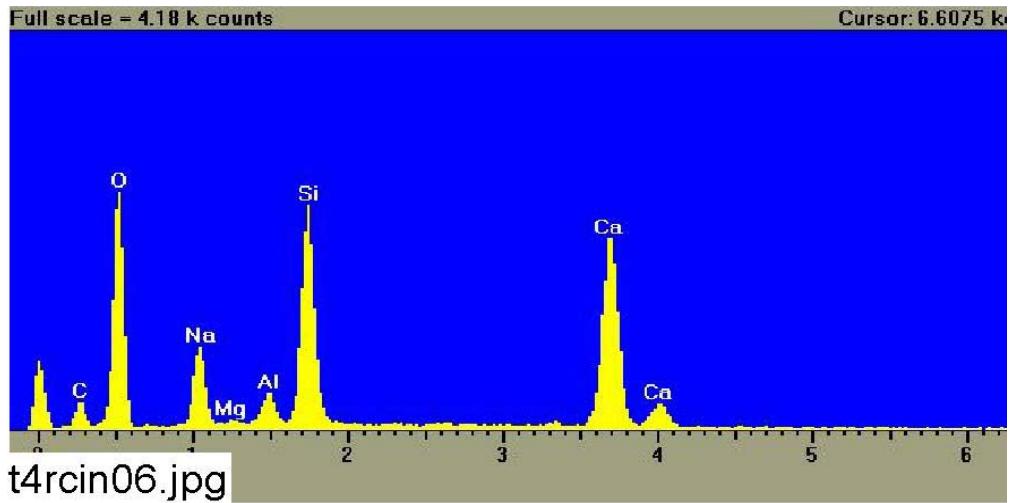


Figure 3-91: EDS counting spectrum for the whole image shown in Figure 3-90. (t4rcin06.jpg)

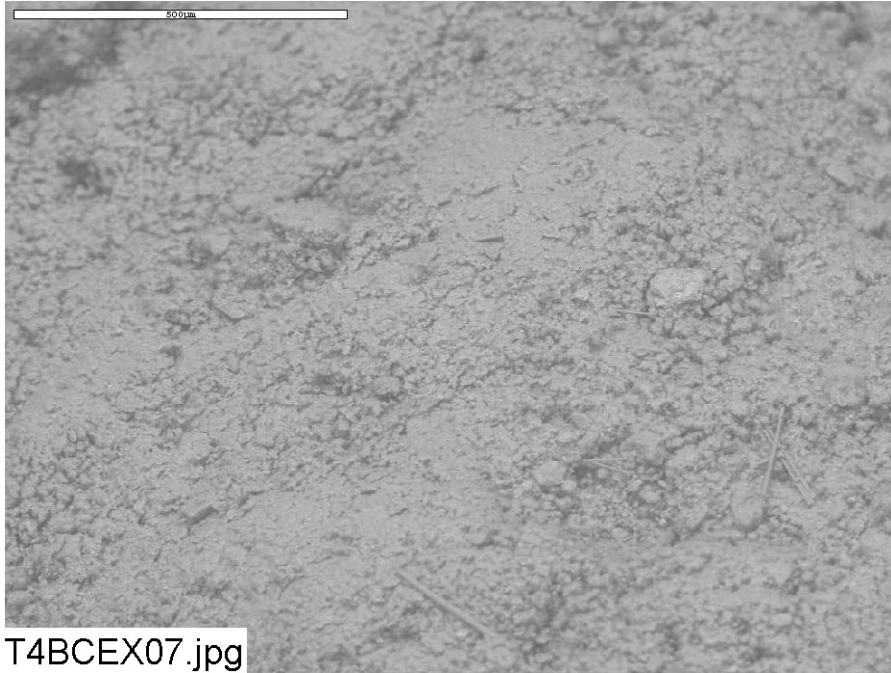


Figure 3-92: Environmental SEM image magnified 100 times for a Test #4 Day 30 low-flow exterior baked cal-sil sample. (T4BCEX07.jpg)

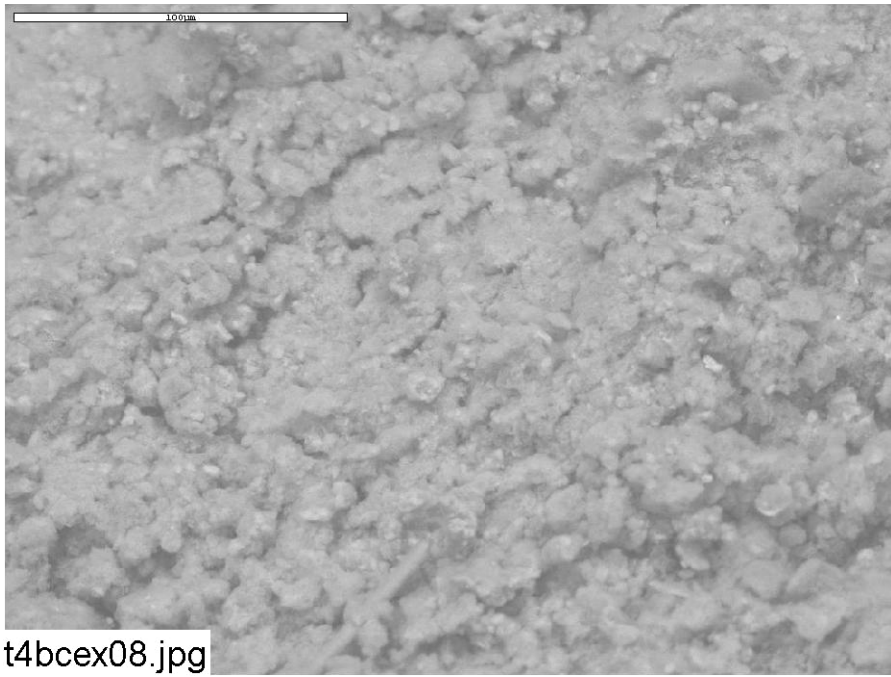


Figure 3-93: Environmental SEM image magnified 500 times for a Test #4 Day 30 low-flow exterior baked cal-sil sample. (t4bcex08.jpg)

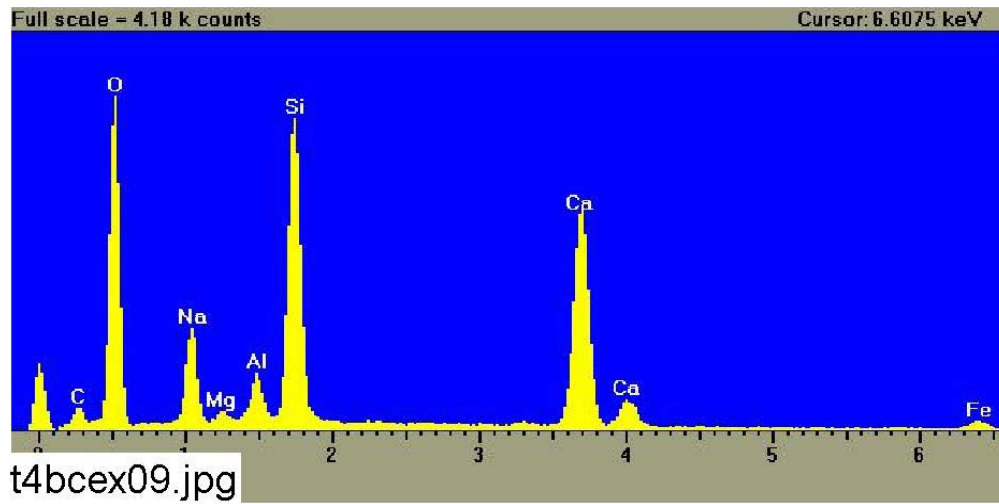


Figure 3-94: EDS counting spectrum for the whole image shown in Figure 3-93. (t4bcex09.jpg)

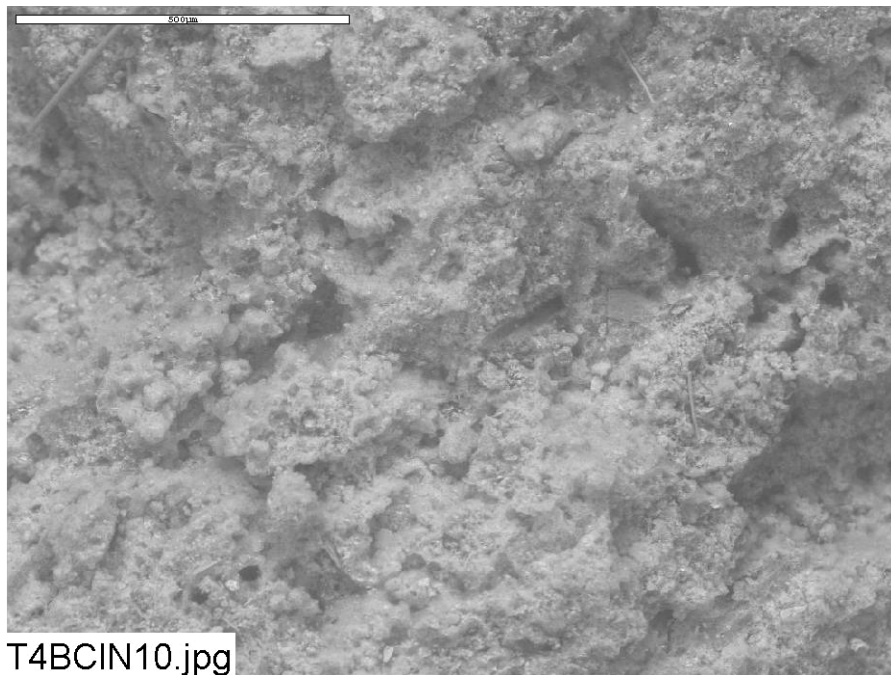


Figure 3-95: Environmental SEM image magnified 100 times for a Test #4 Day 30 low-flow interior baked cal-sil sample. (T4BCIN10.jpg)

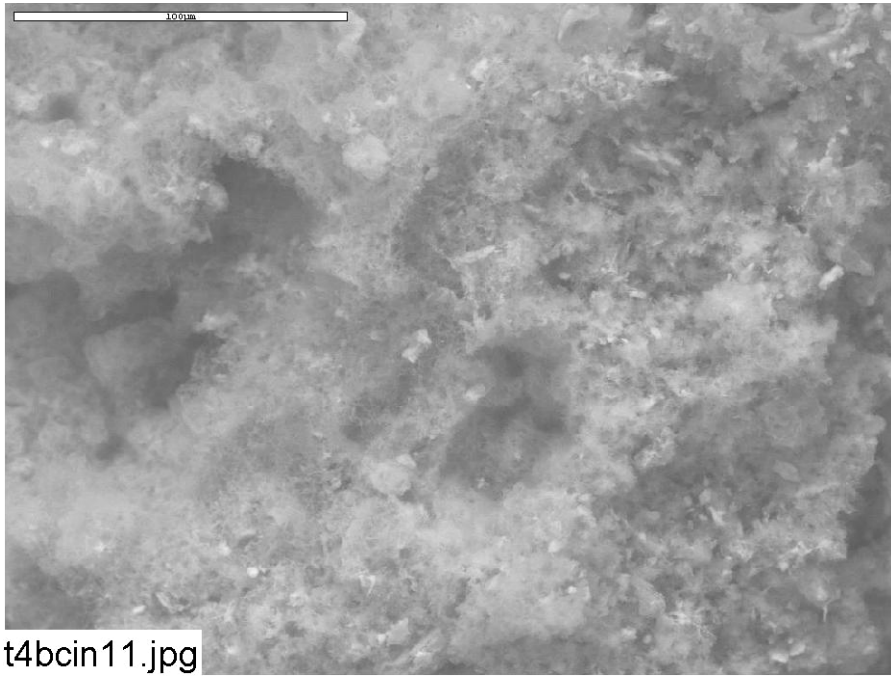


Figure 3-96: Environmental SEM image magnified 500 times for a Test #4 Day 30 low-flow interior baked cal-sil sample. (t4bcin11.jpg)

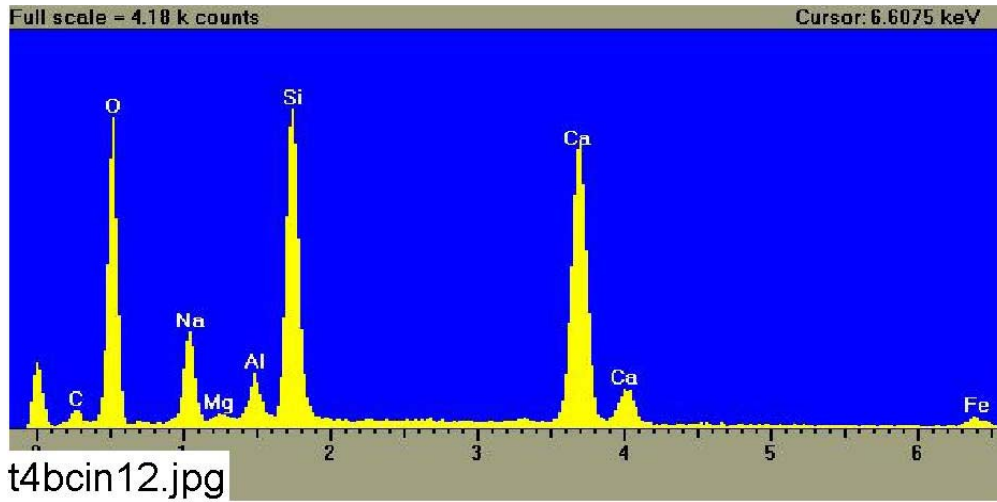


Figure 3-97: EDS counting spectrum for the whole image shown in Figure 3-95. (t4bcin12.jpg)

3.4 Metallic and Concrete Coupons

3.4.1 Weights and Visual Descriptions

3.4.1.1 Submerged Coupons

Examination of the 40 submerged coupons provides insights into the nature of the chemical kinetics that occurred during this 30-day test. The physical change that these coupons experienced is determined through both visual evidence and weight measurement of each coupon before and after the test. Pre-test pictures were taken of the coupons when they were received and prior to insertion in the racks. Post-test pictures were taken several days after the racks had been removed from the tank. All racks with coupons still inserted were staged to allow complete drying of the coupons prior to the post-test pictures. The coupons were placed in a low-humidity room and allowed to air dry. All coupons were also weighed before they were inserted into the tank and after the 30-day test was completed.

There are three submerged aluminum coupons in each test. Figures 3-98 through 3-100 display the pre- and post-test pictures of those coupons that were in Test #4. The relative locations of the aluminum coupons from east to west of the tank are: Al-239, Al-238, and Al-237. Al-239 and Al-238 were the two aluminum coupons that were isolated next to the concrete coupon. There were no visual differences between the three coupons after they were removed from the tank. The overall appearance of the aluminum coupons did not significantly change from their pre-test appearance. The post-test coupons appeared to have a light film on them and had lost their pre-test shiny appearance.



Figure 3-98: Al-237 submerged, pre-test (left) and post-test (right).



Figure 3-99: Al-238 submerged, pre-test (left) and post-test (right).



Figure 3-100: Al-239 submerged, pre-test (left) and post-test (right).

Figures 3-101 through 3-103 present the pre- and post-test pictures of three submerged galvanized steel coupons. The galvanized steel coupons did not experience any significant observable change. The coupons appeared to be relatively clean and the only noticeable marks of any sort are the circular marks caused by the racks that they are mounted in. GS-130 does appear to have some particle deposition that is concentrated mainly on the bottom corners and on the top where the coupon resides in the rack.



Figure 3-101: GS-130 submerged, pre-test (left) and post-test (right).



Figure 3-102: GS-132 submerged, pre-test (left) and post-test (right).



Figure 3-103: GS-134 submerged, pre-test (left) and post-test (right).

Figures 3-104 and 3-105 present the pre- and post-test pictures of two submerged inorganic zinc (IOZ) coated steel coupons. Both submerged IOZ coated steel coupons have similar, light particle depositions. There is a small accumulation of a white precipitate that originates mostly from the points of contact with the racks. However on IOZ-233, the particles seem to be distributed over the majority of the surface of the coupon. This coupon was the westernmost IOZ coupon in the rack in relation to the others.



Figure 3-104: IOZ-233 submerged, pre-test (left) and post-test (right).



Figure 3-105: IOZ-234 submerged, pre-test (left) and post-test (right).

Figures 3-106 and 3-107 present the pre- and post-test pictures of two submerged copper coupons. The copper coupons were mainly unchanged. Like the other coupons, there is a very light concentration of particulate deposits in the areas where the coupons contact the rack.



Figure 3-106: CU-548 submerged, pre-test (left) and post-test (right).



Figure 3-107: CU-572 submerged, pre-test (left) and post-test (right).

Figure 3-108 presents the pre- and post-test pictures of the submerged carbon steel coupon. Other than some discoloration, there was no change. There was a small amount of rust on the bottom corners.



Figure 3-108: US-17 submerged, pre-test (left) and post-test (right).

Figure 3-109 presents the pre- and post-test pictures of the submerged concrete coupon. The post-test concrete coupon exhibits a brownish color.



Figure 3-109: Conc-004 submerged, pre-test (left) and post-test (right).

Table 3-2 presents the pre- and post-test weight data for each representative submerged coupon.

Table 3-2: Weight Data for Submerged Coupons

Type	Coupon No.	Pre-Test Wt. (g)	Post-Test Wt. (g)	Net Gain/Loss
Al	237	392.1	391.9	-0.2
Al	238	393.1	393.3	0.2
Al	239	392.8	392.8	0.0
GS	130	1042.9	1042.9	0.0
GS	132	1062.1	1062.3	0.2
GS	134	1028.5	1029.0	0.5
IOZ	233	1610.9	1612.6	1.7
IOZ	234	1635.7	1637.9	2.2
CU	548	1300.7	1300.9	0.2
CU	572	1316.7	1316.9	0.2
US	17	1017.4	1017.6	0.2
Conc	04	7950.7	8190.3	239.6

The aluminum coupons average weight differential was zero. This supports the observation that there was little particle deposition. The galvanized steel coupons gained an average of 0.23 g, and the coated steel coupons gained an average of 2.0 g. Both representative copper coupons gained 0.2 g, and the carbon steel coupon also gained 0.2 g. The concrete coupon gained 239.6 g, a gain of 3% of its original weight. The concrete coupon was weighed after sitting in an air environment for one week.

3.4.1.2 Unsubmerged Coupons

Figures 3-110 and 3-111 show the pre- and post-test pictures of two unsubmerged aluminum coupons. Each unsubmerged aluminum coupon accumulated a white particle deposition along with some areas of a brownish color. This coating caused the surface of the aluminum coupons to become coarse and rough. The photo of Al-229 shows that most of the surface is coated with the particle deposition, however, in the upper right hand corner the surface is relatively smooth with a color change observable. This is likely caused by uneven spray on the coupons. Even though the four spray nozzles were set to spray uniformly across their spray radius, the spray was not a perfect mist. There were some non-uniform areas, and the positions of the six coupon racks also interfered with the sprays. Al-003 was loaded in Rack 2 (bottom tier, southernmost) and Al-229 was loaded in Rack 7 (upper tier, northernmost)



Figure 3-110: Al-003 unsubmerged, pre-test (left) and post-test (right).



Figure 3-111: Al-229 unsubmerged, pre-test (left) and post-test (right).

Figures 3-112 and 3-113 show the pre- and post-test pictures of two unsubmerged galvanized steel coupons. There was some white deposition on the surface of these coupons although it was in small amounts. The post-test coupons were relatively clean,

with little change. GS-33 was mounted in Rack 3 (bottom tier, middle rack) and GS-91 was mounted in Rack 6 (upper tier, middle rack).



Figure 3-112: GS-33 unsubmerged, pre-test (left) and post-test (right).



Figure 3-113: GS-91 unsubmerged, pre-test (left) and post-test (right).

Figures 3-114 and 3-115 present the pre- and post-test pictures of two unsubmerged copper coupons. All of the copper coupons had vertical water marks that were caused by water flowing downward on the coupon surface during the spray portion of the test. The copper coupons did not appear to accumulate any particle deposition. CU-536 was mounted in Rack 2 (bottom tier, southernmost) and CU-584 was mounted in Rack 7 (upper tier, northernmost).



Figure 3-114: CU-536 unsubmerged, pre-test (left) and post-test (right).

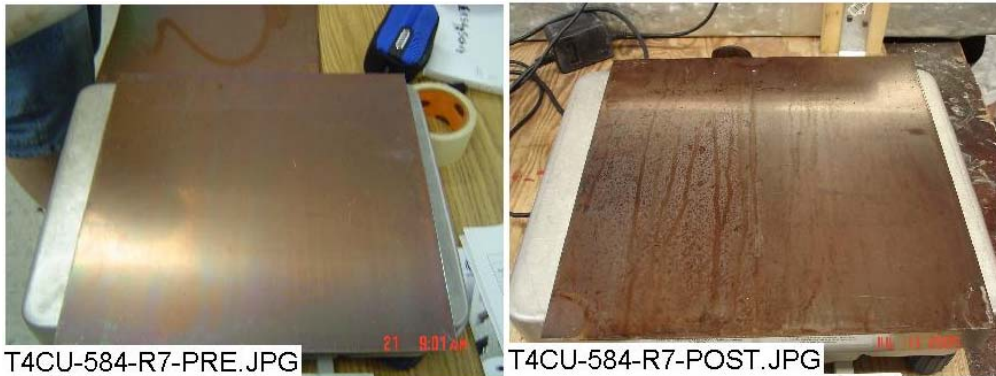


Figure 3-115: CU-584 unsubmerged, pre-test (left) and post-test (right).

Figures 3-116 and 3-117 present the pre- and post-test pictures of two unsubmerged inorganic zinc coated steel coupons. IOZ-263 was mounted in Rack 4 (bottom tier, northernmost) and IOZ-275 was mounted in Rack 5 (upper tier, northernmost).



Figure 3-116: IOZ-263 unsubmerged, pre-test (left) and post-test (left).



Figure 3-117: IOZ-275 unsubmerged, pre-test (left) and post-test (right).

Figure 3-118 presents the pre- and post-test pictures of one unsubmerged carbon steel coupon. US-16 was mounted in Rack 6 (upper tier, middle rack).



Figure 3-118: US-16 unsubmerged, pre-test (left) and post-test (right).

Table 3-3 presents the pre- and post-test weight data for each representative unsubmerged coupon.

Table 3-3: Weight Data for Unsubmerged Coupons

Type	Coupon No.	Pre-Test Wt. (g)	Post-Test Wt. (g)	Net Gain/Loss
Al	003	391.2	391.7	0.5
Al	229	392.8	394.5	1.7
GS	33	1046.6	1046.6	0.0
GS	91	1030.8	1030.6	-0.2
IOZ	263	1662.0	1662.7	0.7
IOZ	275	1655.0	1657.0	2.0
CU	536	1319.2	1319.3	0.1
CU	584	1334.2	1333.7	-0.5
US	16	1024.1	1023.7	-0.4

The aluminum coupons gained an average of 1.1 g, and the galvanized steel coupons lost an average of 0.1 g. The coated steel coupons average weight gain was 1.4 g, and the copper coupons average weight difference was -0.2 g. The carbon steel coupon lost 0.4 g.

Table 3-4 displays the mean weight gain/loss summary in grams for all of the submerged coupons. Table 3-5 displays the mean weight gain/loss summary in grams for all of the unsubmerged coupons by rack.

Table 3-4: Mean Gain/Loss Data for All Submerged Coupons (g)

Coupon Type	Mean Gain - Loss (g)
AL	0.0
GS	0.3
CU	0.2
IOZ	2.3
US	0.2
Concrete	239.6

Table 3-5: Mean Gain/Loss Data for All Unsubmerged Coupons (g)

Mean Gain-Loss Per Coupon Type (g)					
Rack No.	AL	GS	CU	IOZ	US
2	-0.3	0.8	-0.4	0.8	n/a
3	0.2	1.1	0.2	0.3	n/a
4	-0.4	0.9	-0.2	0.7	-0.8
5	0.1	2.0	<0.1	1.9	n/a
6	-0.5	0.7	-0.4	0.9	-0.4
7	-0.3	0.9	-0.3	1.7	n/a
Overall	0.6	0.2	0.3	1.1	-0.4

3.4.2 SEM Analyses

3.4.2.1 Submerged Coupons

During the ICET tests, trace metal cations may be released from the submerged metal coupon surfaces due to corrosion effects. Subsequently, the released metal cations may complex with the anions from the solution through electrostatic interactions with anions such as OH^- , SiO_3^{2-} , and CO_3^{2-} . More complicated, the complexed anions may attract other cations from the solution, such as Ca^{2+} , Mg^{2+} , Al^{3+} , Cu^{2+} , Zn^{2+} , and H^+ . As a result, corrosion products (deposits) are formed and may continuously grow on the metal coupon surfaces. The thickness of the deposits were observed to be in the range of

millimeters. The adherence between the metal coupons and the deposits is through chemical bonds, which are much stronger than van der Waals forces. Due to the vertical orientation of the metal coupons in the tank (with a small horizontal cross-sectional area), the deposits on the metal coupon surface are likely of chemical origin, rather than being the result of particles settling on the surface.

According to SEM/EDS results, the dominant corrosion products on the submerged Al coupons are likely aluminum hydroxide with other substances containing Si, Ca, O, and C. For submerged Cu coupons, the possible corrosion products include CuO, $\text{Cu}_2(\text{CO}_3)(\text{OH})_2$, and substances containing Ca, Si, Al, and O. For the submerged galvanized steel coupons, the possible corrosion products are oxides, hydroxides, silicate, and carbonate compounds of Zn, Ca, and Al. For the submerged steel coupon, the possible corrosion products include oxide, hydroxide, silicate, and carbonate compounds of Fe and Ca and compounds composed of Fe, Si, Ca, O, and Al.

3.4.2.2 Unsubmerged Coupons

The unsubmerged coupons were affected by the testing solution only during the 4-hour spray phase on the first day of the test and, following that, were affected by water vapor throughout the test.

According to SEM/EDS results, the dominant corrosion products on the unsubmerged Al coupons are likely aluminum hydroxide and/or aluminum oxide, and other corrosion products containing Si, Ca, O, and C. For unsubmerged Cu, the corrosion products on the coupon surface are likely CuO. The corrosion products were composed of C, O, Ca, Si, and Cl on the unsubmerged galvanized steel coupon surface. For the unsubmerged steel coupon, the likely corrosion products are Fe_2O_3 , $\text{Fe}(\text{OH})_3$, and $\text{Fe}_2(\text{CO}_3)_3$.

Appendix F contains the SEM data for the coupons.

3.5 Sedimentation

Sediment was collected from the tank bottom after the test solution was drained. It consisted of a particulate sediment that covered the entire tank bottom. Figure 3-119 shows some of this sediment. In addition, Figure 3-120 shows the tank bottom with the sediment, after the samples were removed. Figure 3-121 shows the top of the drain screen with the drain collar surrounded by sediment, and Figure 3-122 shows the drain screen and drain collar after removal from the tank. Figure 3-123 shows the birdcage sitting on top of a basket of cal-sil after the tank was drained. The cal-sil baskets sat on top of the sediment, and thus, the birdcage was not in direct contact with the sediment.

The SEM/EDS and XRD/XRF analyses provided information on the morphology and composition of Test #4 sediment. EDS results show that more than 84% of the sediment was composed of Si, Ca, and O. Consistently, XRF result shows that Si, Ca, and O are

the major elements in the composition of the sediment, plus small amounts of Na, Al, Fe, and Mg.

Based on XRD results, the sediment sample contained crystalline substances of tobermorite ($\text{Ca}_{2.25}(\text{Si}_3\text{O}_{7.5}(\text{OH})_{1.5})(\text{H}_2\text{O})$) and $\text{Ca}_4(\text{Si}_6\text{O}_{15}(\text{OH})_2)(\text{H}_2\text{O})_5$) as well as calcite (CaCO_3), which are the same as unused raw or unused baked cal-sil samples. Considering the collective evidence from the EDS, XRF, and XRD analyses, it is likely that the sediment was composed of a significant amount of cal-sil debris, including both raw and baked cal-sil. It should be noted that other deposits such as fiberglass debris and corrosion products may also contribute to the sediments and can not be ruled out.

Figures 3-124 through 3-129 and Table 3-6 provide ESEM/EDS and XRD/XRF analysis results. The complete Day 30 sediment analyses are given in Appendix G.



Figure 3-119. Sediment removed from the tank.



Figure 3-120. Sediment on the tank bottom.



Figure 3-121. Drain collar surrounded by sediment on the tank bottom.



Figure 3-122. Drain collar and drain screen removed from the tank.



Figure 3-123. Birdcage and cal-sil baskets after the tank was drained.

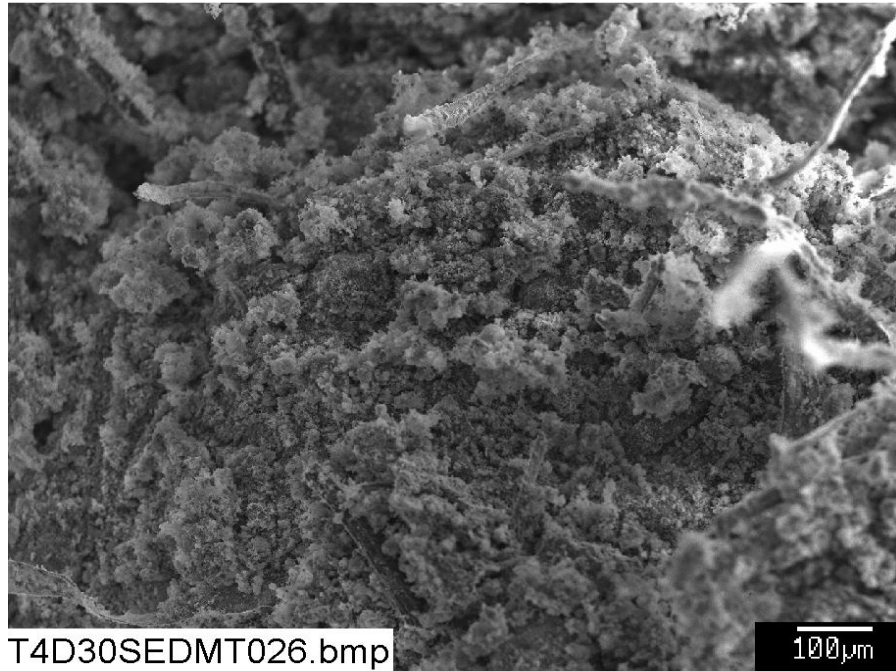


Figure 3-124: SEM image magnified 100 times for a Test #4 Day 30 sediment sample at the bottom of the tank. (T4D30SEDMT026.bmp)

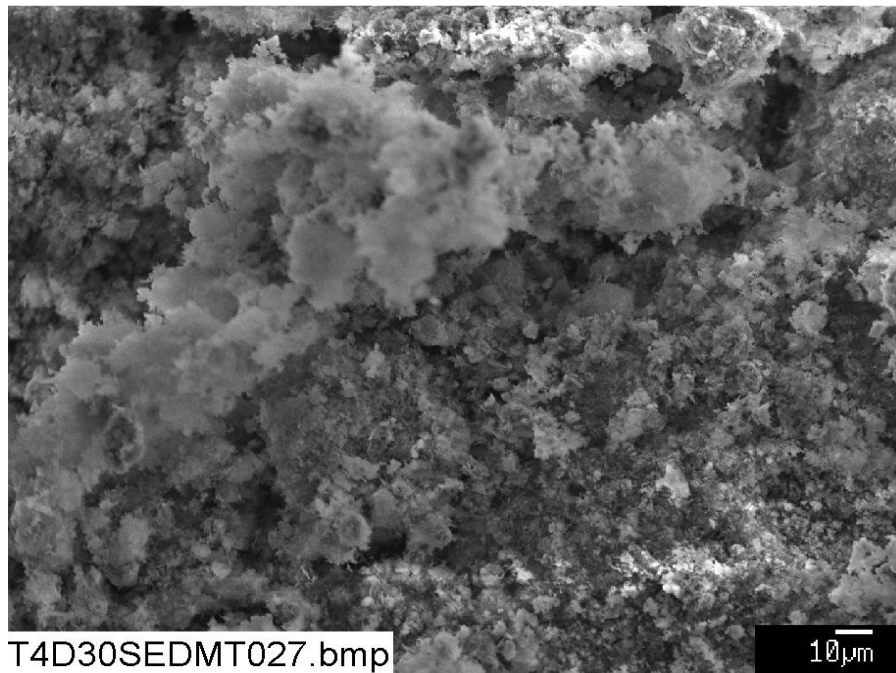


Figure 3-125: SEM image magnified 500 times for a Test #4 Day 30 sediment sample at the bottom of the tank. (T4D30SEDMT027.bmp)

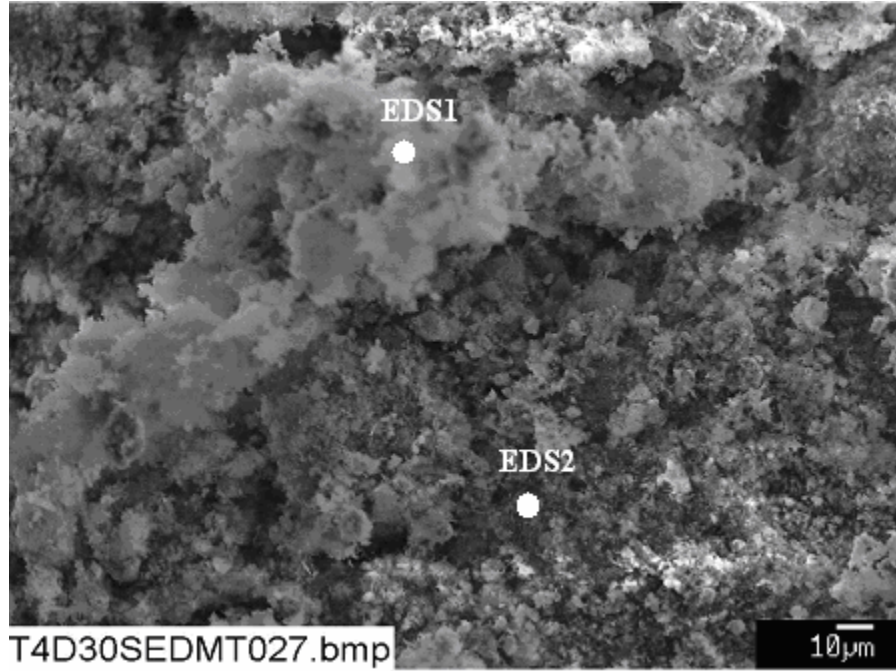


Figure 3-126: Annotated SEM image magnified 500 times for a Test #4 Day 30 sediment sample at the bottom of the tank. (T4D30SEDMT027.bmp)

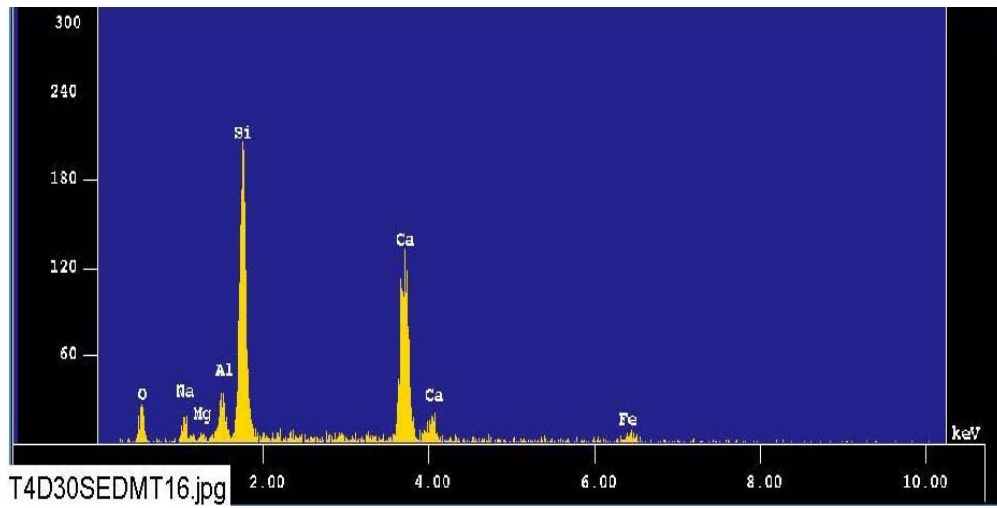


Figure 3-127: EDS counting spectrum for the white snow like deposits (EDS1) shown in Figure 3-126. (T4D30SEDMT16.jpg)

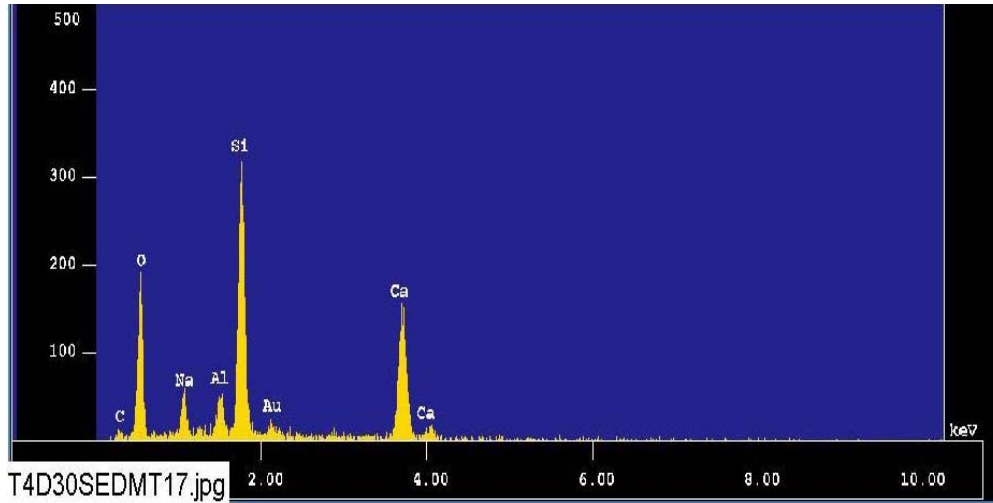


Figure 3-128: EDS counting spectrum for the dark deposits (EDS2) shown in Figure 3-126. (T4D30SEDMT17.jpg)

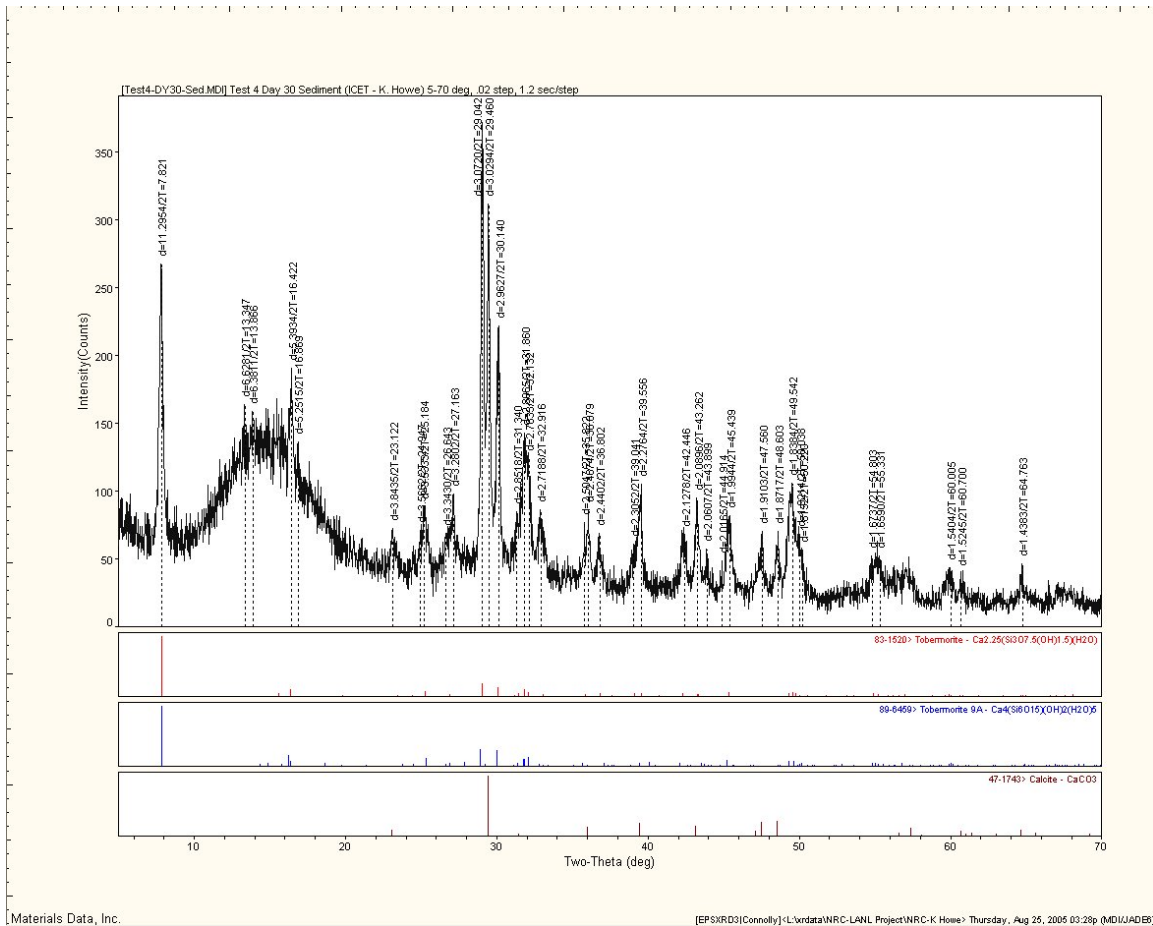


Figure 3-129: XRD result of the possible matching crystalline substances in Test #4 Day 30 sediment.

Table 3-6. Dry Mass Composition of Test #4 Day 30 Sediment by XRF Analysis

First row is chemical component; second row is mass composition (%).

SiO ₂	TiO ₂	Al ₂ O ₃	Fe ₂ O ₃	FeO	MnO	MgO	CaO	Na ₂ O	K ₂ O	H ₂ O(-)	H ₂ O(+) CO ₂	P ₂ O ₅	Total
34.20	0.18	4.78	2.18	0.00	0.06	0.66	28.58	5.05	0.24	1.25	23.55	0.15	100.88

3.6 Precipitates

Test #4 was markedly different from Test #1 in that no precipitate was found in the test solution, even after it cooled to room temperature. Based on a series of bench-top controlled experiments, the white precipitate observed in Test #1 contained a significant amount of aluminum. The aluminum concentration of the Test #1 solution was as high as 350 mg/L. However, the aluminum in the Test #4 solution occurred only in trace amounts for 2 days and then was below its detection limit.

3.7 Deposition Products

The deposition of debris/corrosion products in the tank after it was drained was observed on the submerged objects in the tank. These corrosion/deposition products, which looked like a fine powder, were collected for analysis. Those collected were from the submerged CPVC coupon rack. SEM/ EDS results indicated that these fine powders were mainly composed of O, Ca, Si, Na, Al, and C. The high content of Ca and Si suggests that the powders were likely from cal-sil and fiberglass debris.

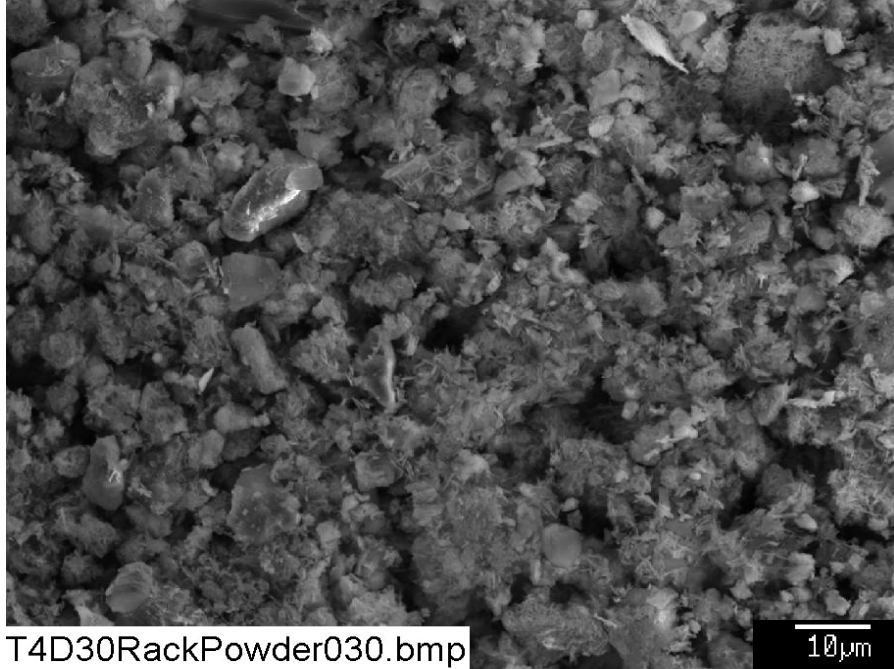


Figure 3-130: SEM image magnified 1000 times for a Test #4 Day 30 fine powder on the submerged rack. (T4D30RackPowder030.bmp)

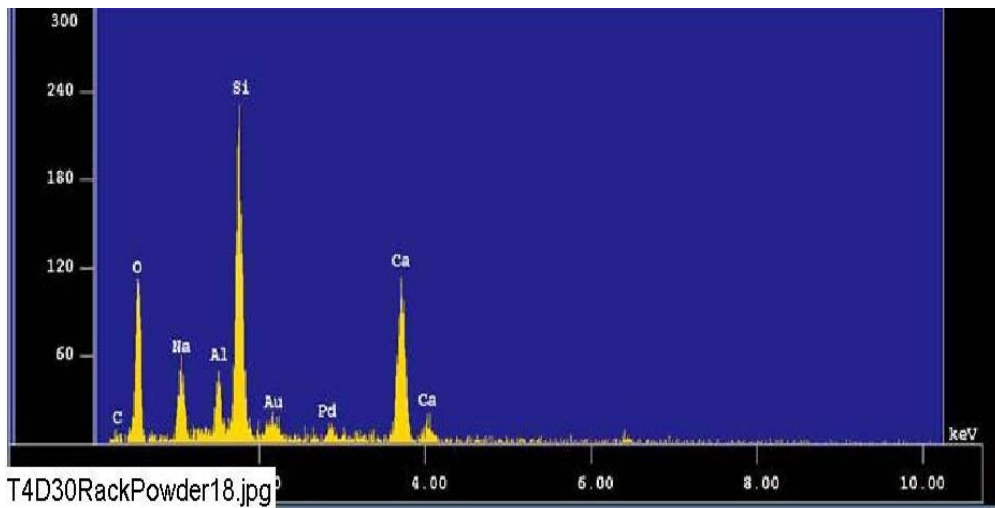


Figure 3-131: EDS counting spectrum for the particles (whole image) shown in Figure 3-130. (T4D30Rackpowder18.jpg)

3.8 Gel Analysis

In ICET Test #3, one significant phenomenon was the presence of white gel-like precipitates in the test solution, especially during and after the injection of TSP on the first day of the test. When Test #3 was shut down, deposits of the pinkish-white gel-like precipitates were observed on the top of the birdcage and on other objects on the tank's bottom. Test #4 had cal-sil and fiberglass samples as did Test #3, however, Test #4 used NaOH instead of TSP. No gel-like material was observed in Test #4.

4 SUMMARY OF KEY OBSERVATIONS

ICET Test #4 ran for 30 days, and all conditions were maintained within the accepted flow and temperature ranges, with two exceptions. On Day 11, a power outage occurred which caused a recirculation pump trip. Recirculation flow was re-established 2 hours and 15 minutes later. During that time, the maximum solution temperature rose to 62.4°C, which is 0.4°C above the target maximum. The maximum temperature was above 62.0°C for approximately one hour. The test solution pH varied from 9.5 to 9.8 over the first two days, rose to 9.9 on Day 8, and then stayed between 9.7 and 9.9 for the remainder of the test. The test solution turbidity decreased to less than 3 NTU after 24 hours. The turbidity continued to decrease and averaged 0.5 NTU over the last three weeks of the test.

Samples of the solution were taken daily. The chemical elements present were calcium, silica, and sodium. Aluminum was present for only the first 24 hours and then only at trace amounts. Strain-rate viscosity measurements indicated that the solution remained Newtonian throughout the test. No precipitates were observed in the solution, even after it had cooled to room temperature.

The submerged metal coupons were relatively unchanged, with light deposits and color changes observed. The IOZ-coated steel coupons had an average weight gain of 2.3 g, and the other metal coupons weight gains were less than 1 g. According to SEM/EDS results, the dominant corrosion products on the submerged Al coupons are likely aluminum hydroxide with other substances containing Si, Ca, O, and C. The other submerged coupons were covered with oxides, hydroxides, and other unidentified compounds. The unsubmerged coupons exhibited some vertical streaking and color changes. The IOZ-coated steel coupons had an average weight gain of 1.1 g, and the other metal coupons weight gains were less than 1 g.

Deposits on the fiberglass samples increased over time, and the deposits appeared to be chemically originated for the samples not lying on the tank bottom. These deposits covered individual fiberglass strands and in some cases formed webs between strands. The deposits did not significantly increase with time in the test solution. It is likely that these deposits were caused by chemical precipitation, since they appear to be soluble. Particulate deposits were evident on samples that were sitting on the tank bottom

In general, particulate deposits were found only on the exterior of the fiberglass. This result suggests that almost all of the particulate deposits were physically retained or attached on the fiberglass exterior. The amount of particulate deposits increases from Day 15 low- and high-flow to the Day 30 high-flow samples. EDS results show that these particulate deposits contain significant amounts of Si and Ca, suggesting they were from cal-sil debris.

Sediment on the tank bottom was prevalent, accumulating to depths of over 8 in. The sediment contained crystalline substances and calcite, making it primarily cal-sil, although some fugitive fiberglass was also present.

REFERENCES

1. "Test Plan: Characterization of Chemical and Corrosion Effects Potentially Occurring Inside a PWR Containment Following a LOCA, Rev. 12c," March 30, 2005.
2. J. Dallman, J. Garcia, B. Letellier, and K. Howe, "Integrated Chemical Effects Tests: Data Compilation for Test 1," LA-UR-05-0124, July 2005.
3. "Pre-Test Operations, Test #4," ICET-PI-015, Rev. 0, May 23, 2005.
4. "Test Operations, Test #4 (cal-sil and fiberglass, and NaOH at pH 10)," ICET-PI-016, Rev. 0, May 23, 2005.
5. "Post-Test Operations, Test #3," ICET-PI-008, Rev. 3, May 2, 2005.